SAND2014-4674P

Ignition and Reaction Behavior of Gasless Reactive Materials

Robert V. Reeves

Sandia National Laboratories
4 June 2014

Sandia National Laboratories is a multi-program laboratory managed and operated by Sandia Corporation, a wholly owned subsidiary of Lockheed Martin Corporation, for the U.S. Department of Energy's National Nuclear Security Administration under contract DE-AC04-94AL85000.

Background and definitions

- "Gasless" Reactive Systems
  - Can produce novel materials
    - Combustion synthesis [a,b]
  - Reactants contained in initial mixture
  - Reactions progress without evolution of gases
  - High heat release
- High heat release and reaction persistence allows many uses:
  - Used for joining, brazing [Tim Weihs- JHU, Indium Corp.]

Reactants	-Q, [J/g]	T_{ad}, [K]
Co+Al	1280[c]	1911[c]
Ni+Al	1380[c]	1911[c]
Ti+2B	5520[c]	3498[c]
Ni+Ti	640[d]	1583[d]
$Fe+KClO_4$	920-1250 (84-88 wt% Fe)[e]	1570-1650[f]

a. A.G. Merzhanov, Ceramics International **21**, 371 (1995)
b. Varma, A. S. Rogachev, A. Mukasyan, and S. Hwang, *Combustion Synthesis of Advanced Materials: Principles and Applications* (1998)
c. Fischer, S.H., Grubelich, M.C., SAND98-1176C
d. F.R. de Boer,,R. Boom, W.C.M.Mattens, A.R. Miedema, A.K.Niessen, *Cohesion in Metals Transition Metal Alloys*. 1989
e. Guidotti, R.A., SAND2001-2191
f. Calculated in CHEETAH 6.0 thermochemical program

Gasless Systems – Limiting Factors

- Typically, mixture of micron-scale metal powders are used
- Thermally initiated reactions limited by heat conduction and mass diffusion (Mukasyan, 2008)
  - Propagation rates up to a few cm/s (Barzykin, 1992)
  - Melting required for bulk reaction (Varma 1998)
  - Requires high heat flows for initiation (Merzhanov, 1975; Barzykin, 1992)

- Changing material form alters reaction behavior
  - Particle size – Nanopowders
  - Mechanical alteration – Ball-milling
  - Deposited structures – Nanolaminates
- Mechanical initiation could increase rates by coupling reaction to stress wave passage

A. S. Mukasyan, and A. S. Rogachev, Progress in Energy and Combustion Science **34**, 377 (2008)
A. Varma, A. S. Rogachev, A. Mukasyan, and S. Hwang, *Combustion Synthesis of Advanced Materials: Principles and Applications* (1998)
A. G. Merzhanov and I. P. Borovinskaya, Combustion Science and Technology **10**, 195 (1975)
V. V. Barzykin, Pure and Applied Chemistry **64**(7) 909, (1992)

Ball Milled Powders

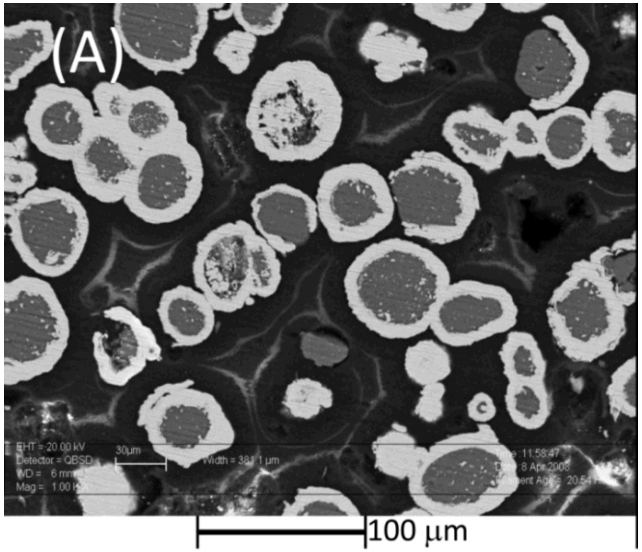

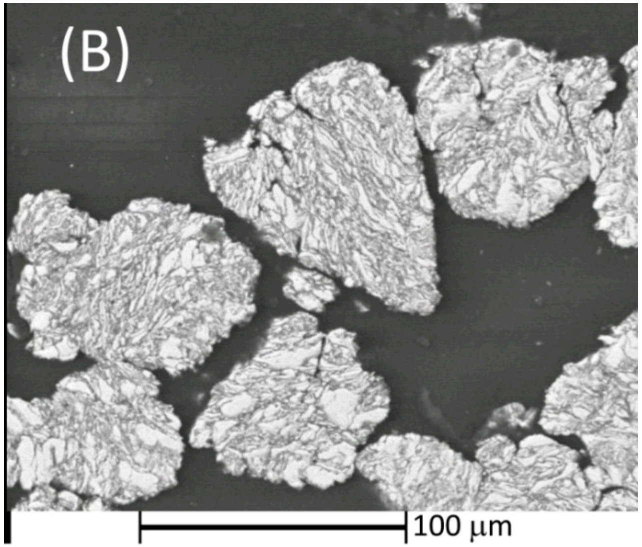

A) Section of baseline clad material

B) Cross section of aggregates, post-milling

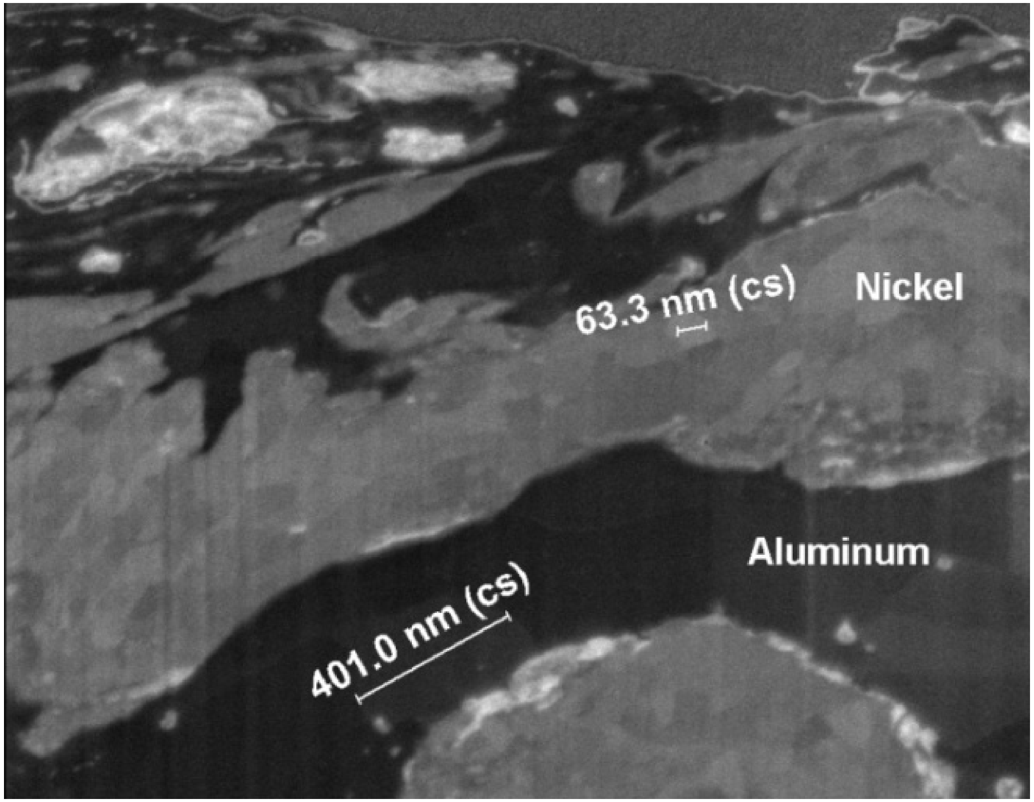

Material thicknesses reduced from 20-30 μm to 100's of nm

DTA Results

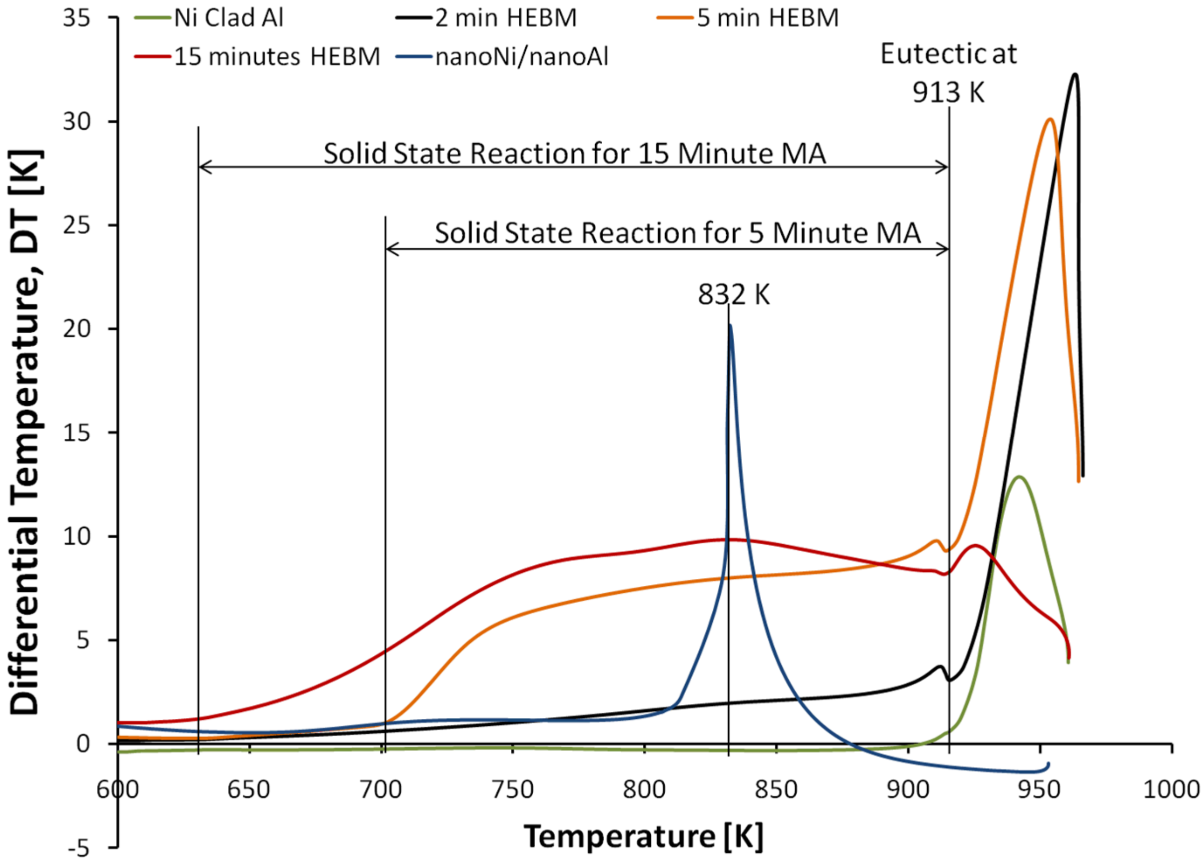

- Reaction onset at eutectic (913 K) for unmilled and lightly milled materials
- Nano material has narrow peak ΔT at lower temperature (832 K).
- Milled material exhibits solid state reaction with small heat release at eutectic

Thermal Explosion - Ignition Temp.

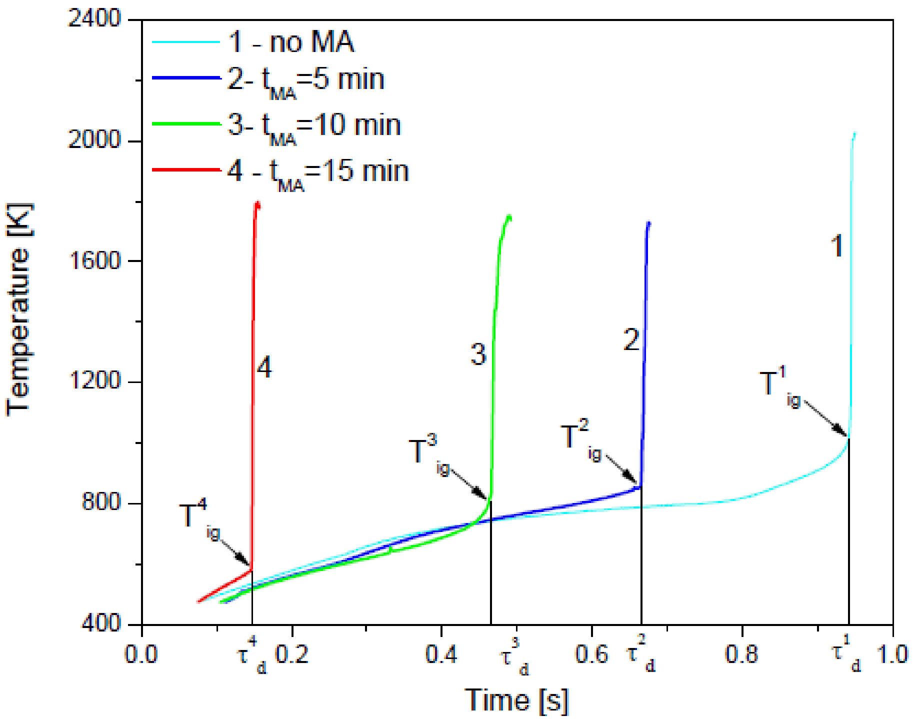

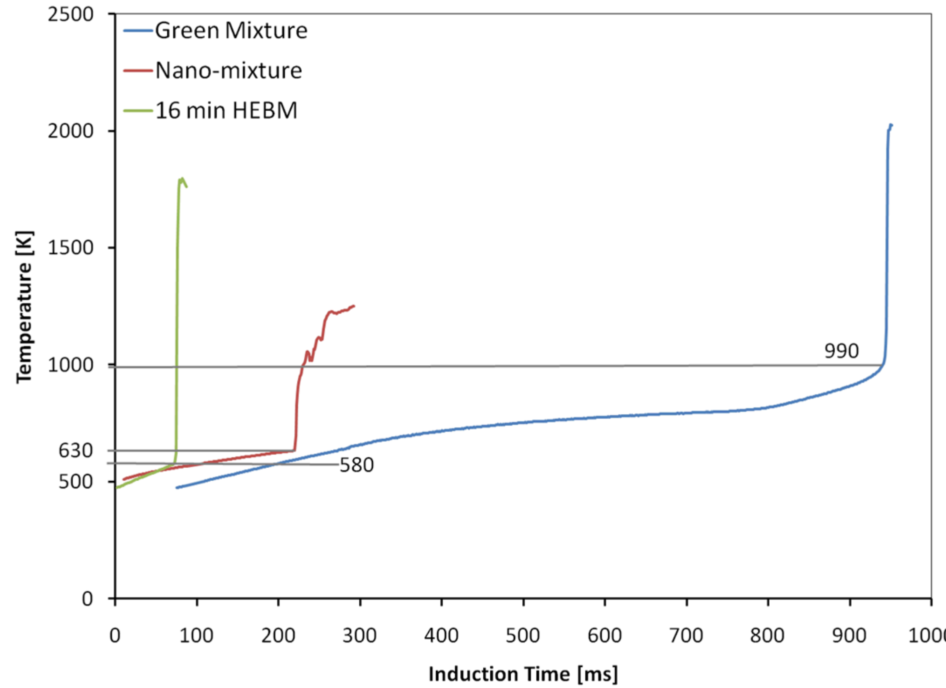

- Ignition by high rate Joule heating (1000's K/s)
- Clear relationship between milling time and ignition temperature
- Increased milling time reduced ignition temperature
- Greater refinement causes greater specific interfacial area
- Nanopowder mixture shows similar reduction in ignition temperature

Nanolaminates

- $Zr + 2Al \rightarrow ZrAl_2; \Delta H_{exp} = -46 \frac{kJ}{mol_{atoms}}$

(de Boer, Boom, Mattens, Miedema, Niessen, *Cohesion in Metals*, 1988)

- Typical design of sputtered reactive foils
  - Used extensively by Weihs, Adams, Rogachev, others
  - Macroscale stacks of nanometric metal layers
  - Clean interfaces, high purity materials

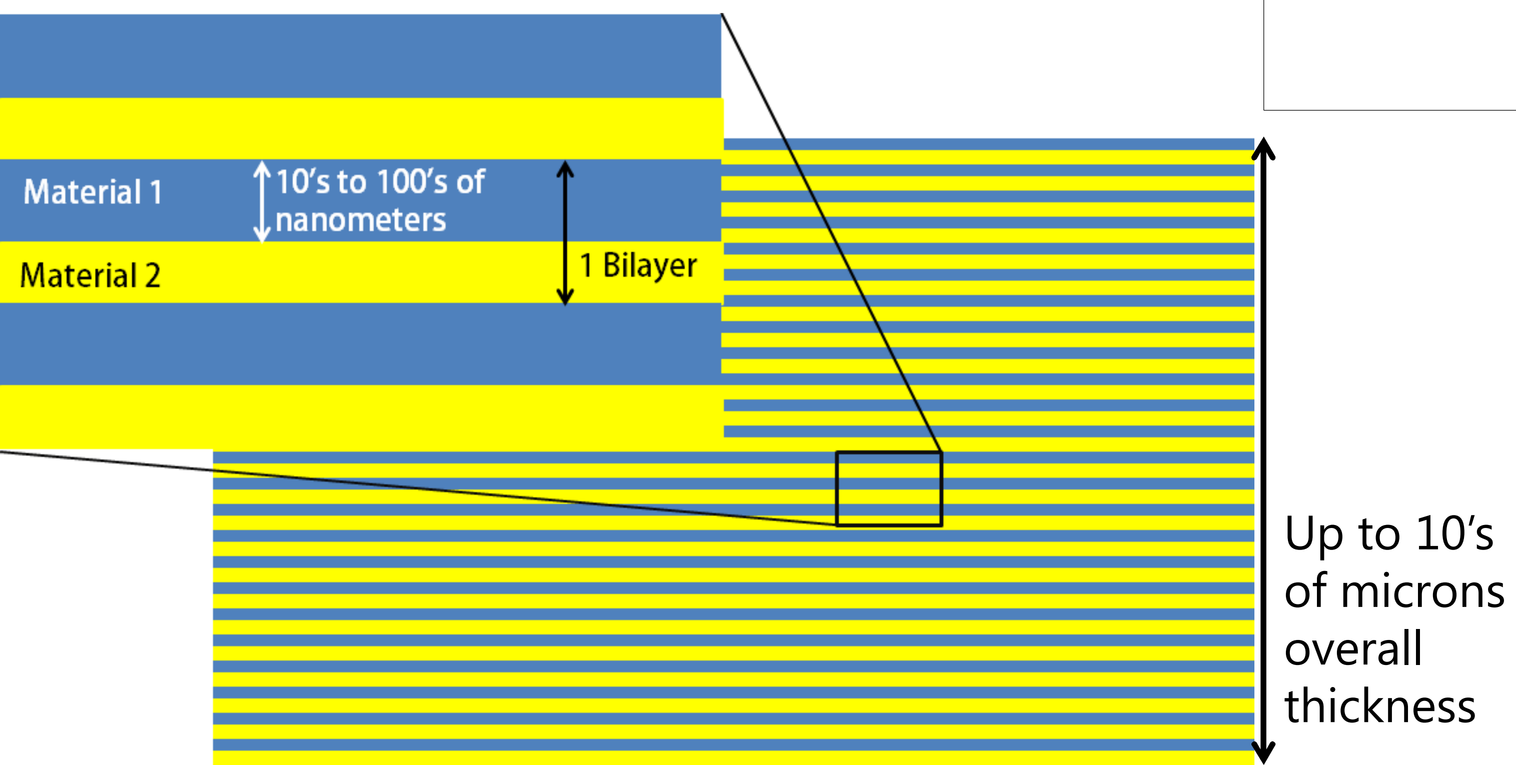

DSC of Nanolaminates

Heat Release Characteristics (Co/Al)

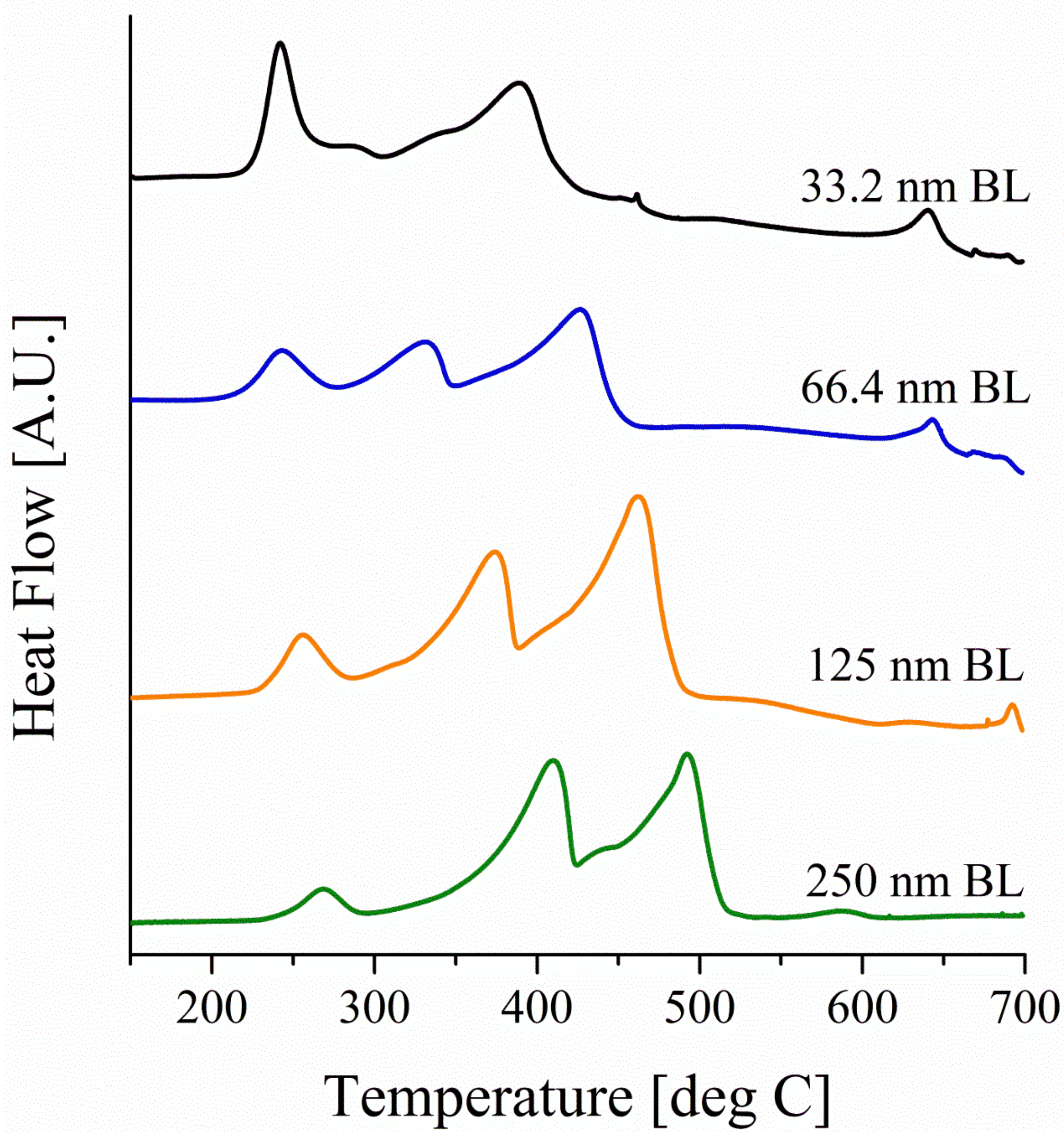

- Reaction onset significantly below eutectic (659 ^{o}C)
- Solid state reactions dominate

Ball-Milling and Nanolaminates

- Increased interfacial area and smaller diffusion distances than mixed powders
  - Lower onset temperature
  - Higher reaction propagation rates
- Both allow for tailored reaction characteristics by controlling reactant periodicity

Thin Films with 2-D Periodicity

- Use semiconductor fab to produce thin Si with patterned porosity
- Backfill to make reactive pair through chemical vapor deposition (ALD)
- Should improve
  - Mechanical properties
  - Scalability
  - Customization of reaction behavior
  - Direct view of chemical kinetics - DTEM

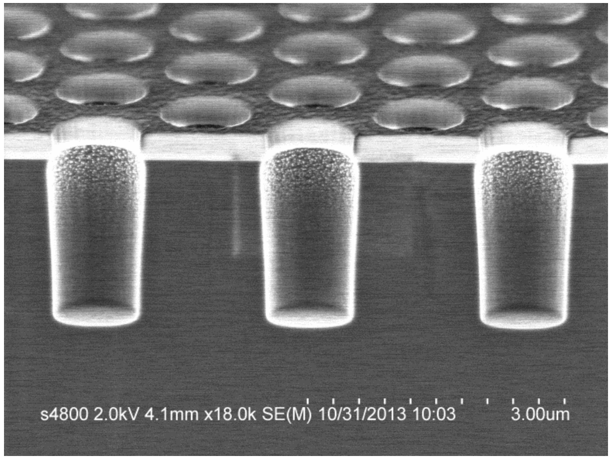

Cross Section showing partially etched holes
Ø = 1μm

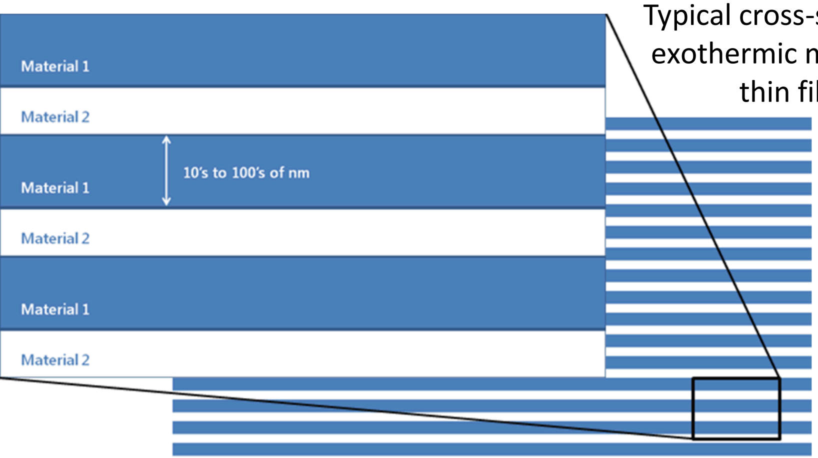

Typical cross-section of exothermic multilayer thin film

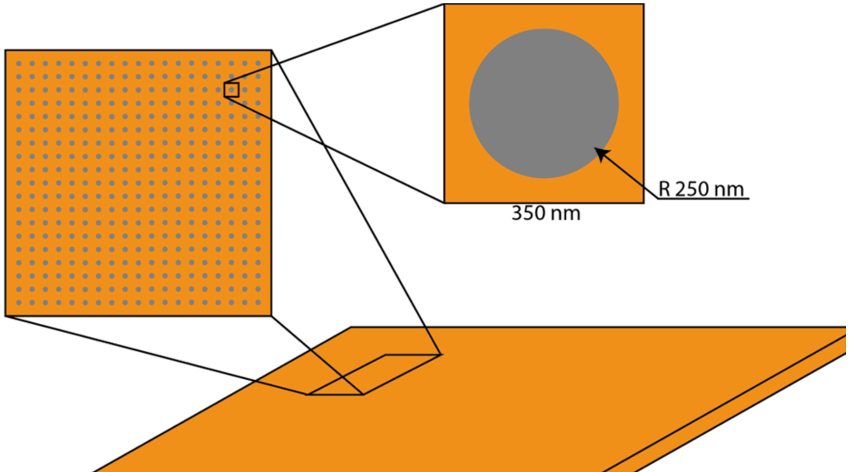

Thin Films with 2-D Periodicity

- Periodicity orientation provides easily viewable interfaces
- Ideal for study with dynamic TEM
  - ns temporal resolution and sub-μm spatial resolution
- Previous work with Tom LaGrange on Ti-B and Co-Al

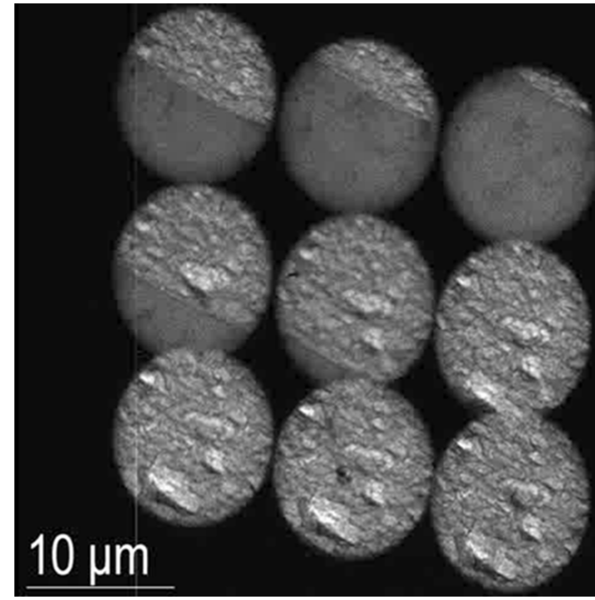

Propagating front seen by DTEM.
220 ns between frames.

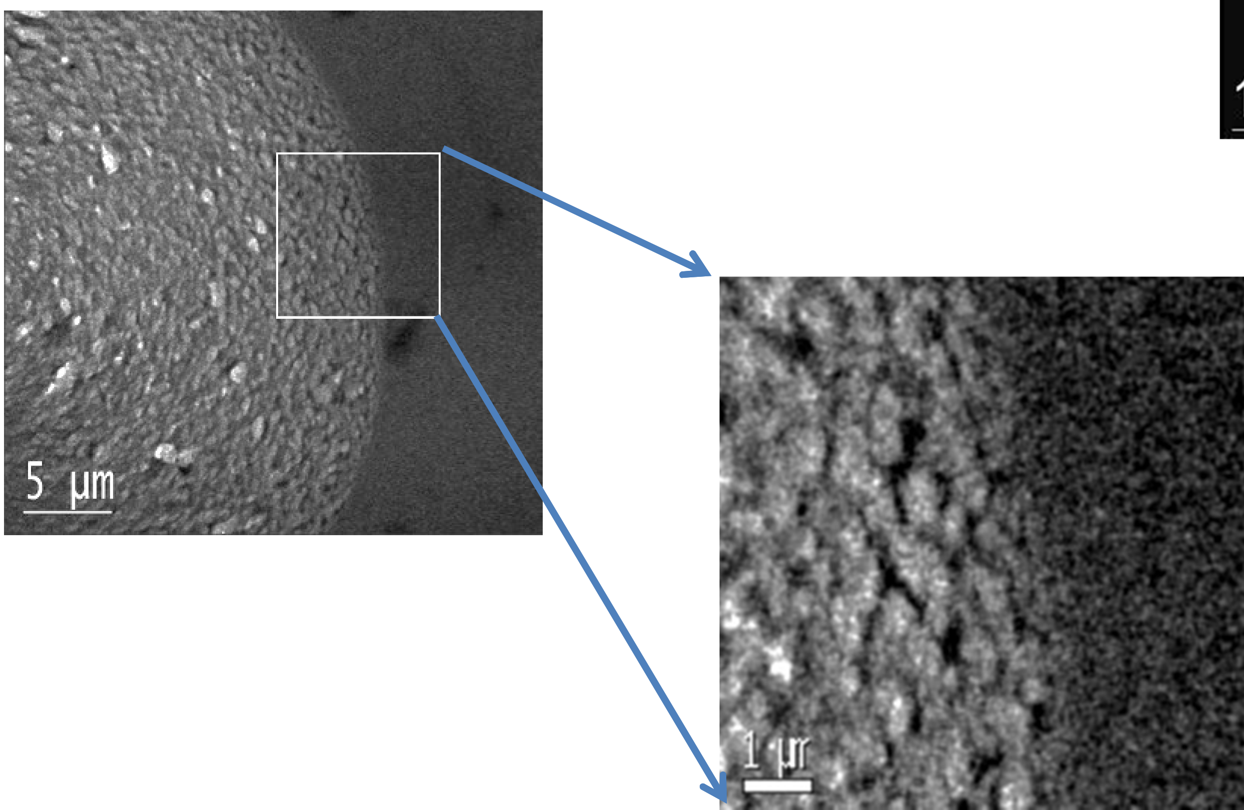

Applications

- Heat source
  - Reduced volume of pyrotechnic
  - Faster turn-on
- Functional energetics for safety
  - Optical Switch (transmissive to absorbing)
  - Magnetic switch (Ferro- to paramagnetic)
  - Electronic switch (conductive to insulative)

- High heat loss conditions must be managed
  - Instabilities can reduce performance or cause failure

Experimental Material

Co/Al Nanolaminates

Foils with 33.2 nm BL and thinner have stable reaction fronts

Total duration 3.125 ms

8.96mm window

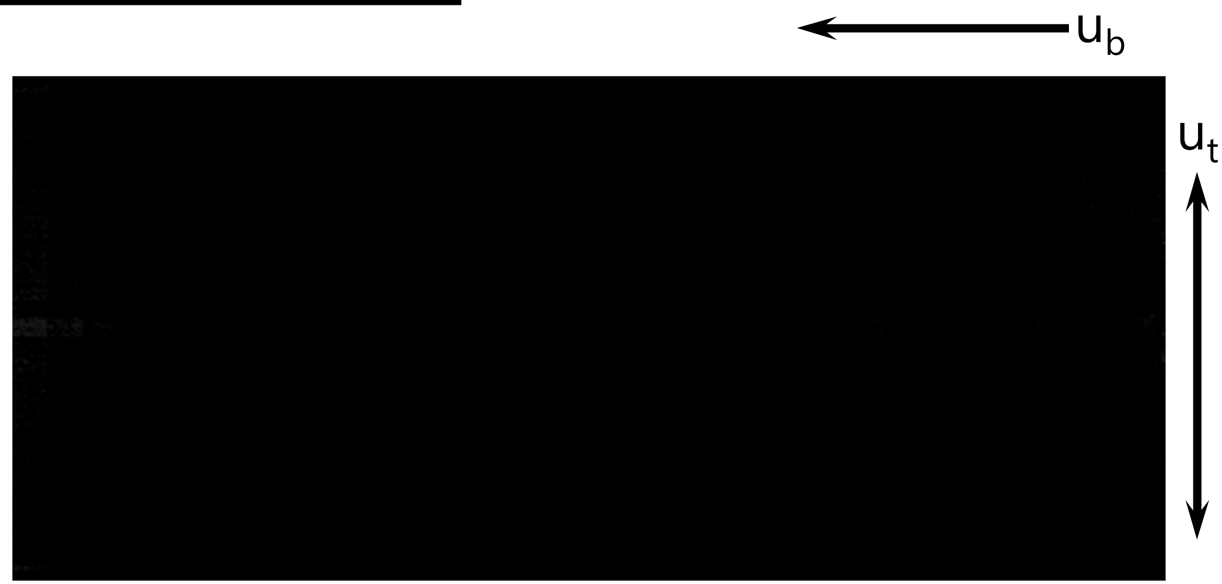

Foils with 66.4 nm BL and thicker have unstable reaction fronts

Total duration 11.7 ms

8.96 mm window

Experimental Motivation
Understanding and Controlling Stability

- Instabilities can be detrimental in typical application (joining)
- What are effects of initial temperature on reaction behavior?
- What does temp. dependent behavior inform us about local reaction kinetics/instability microstructure?

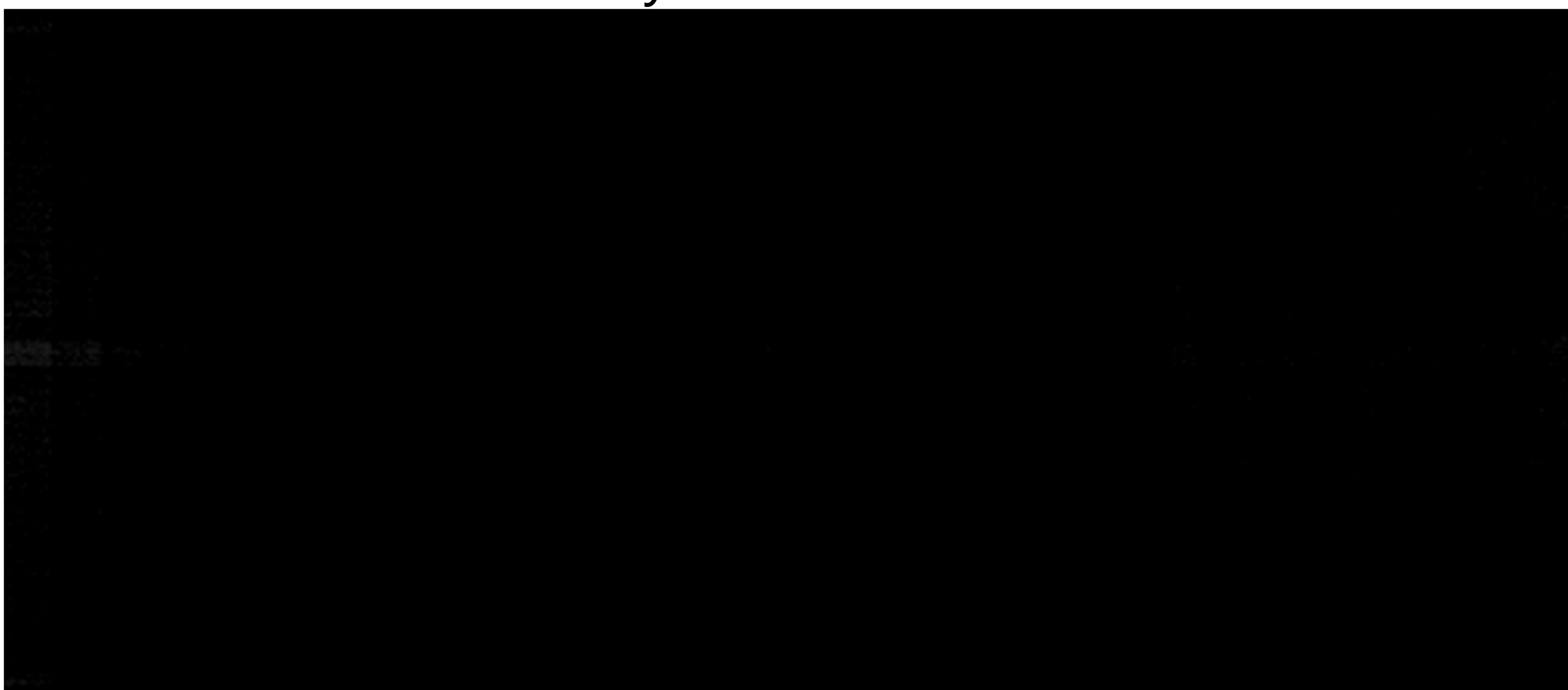

BL Dependent Behavior
Heat Release Characteristics

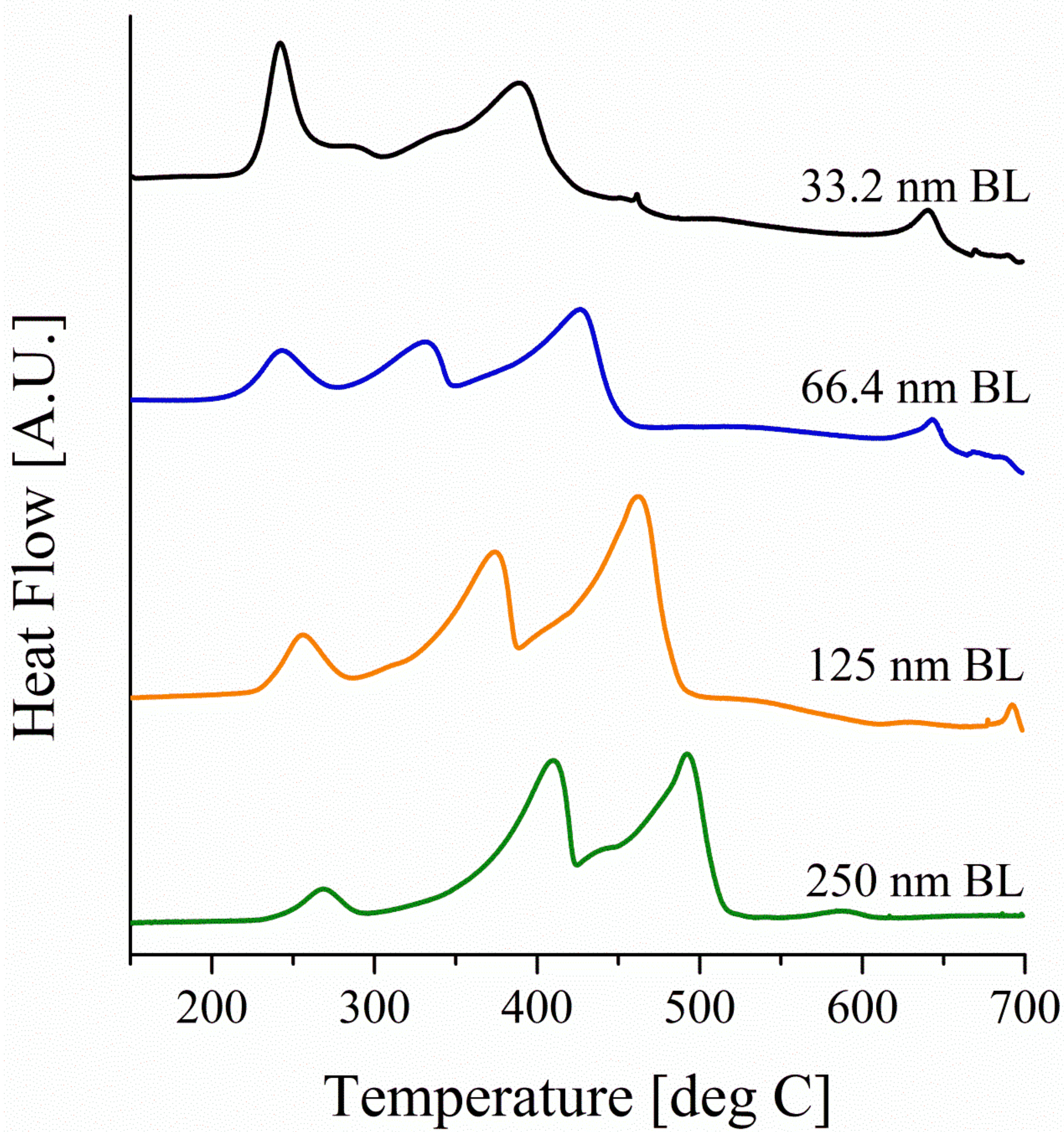

- Reaction progression changes with BL thickness during DSC heating
- Common to heterogeneous reactive materials
- Additional exotherm occurs in foils with BLs 66.4 nm and larger
- DSC heating not equivalent to self-propagating reaction

Quenched Samples – Phase ID

		Co	Al	Co_2Al_9	Co_4Al_{13}	Co_2Al_5	CoAl
BL ≤ 33.2 nm	Initial	x	x				
	Exotherm 1	x		x	o	o	
	Exotherm 2						x
BL ≥ 66.4 nm	Initial	x	x				
	Exotherm 1	x	x	x	o	o	
	Exotherm 2	x		o	o	o	
	Exotherm 3						x

- Initial exotherm results in ~10 nm Co diffusion

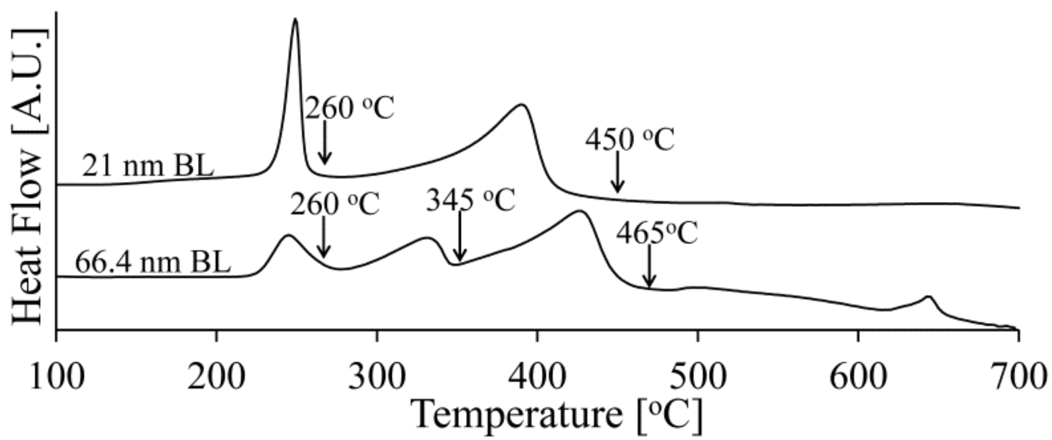

Propagating Reaction Test Setup
Simultaneous IR and Visible Light Imaging

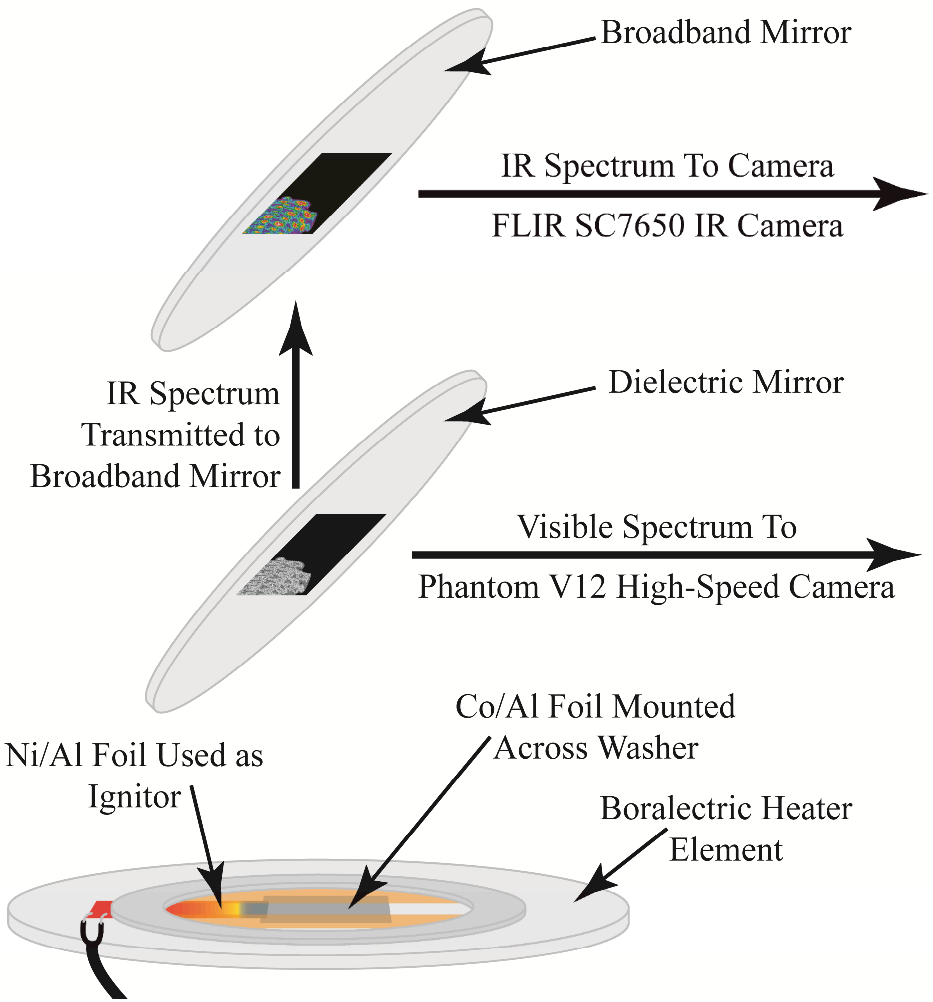

- Heater element allows temperature control of foil
- Dielectric mirror separates emitted IR and visible spectra
- Gathered data gives temperature/spatial data wrt time

Effects of Preheating
Heat Release Characteristics

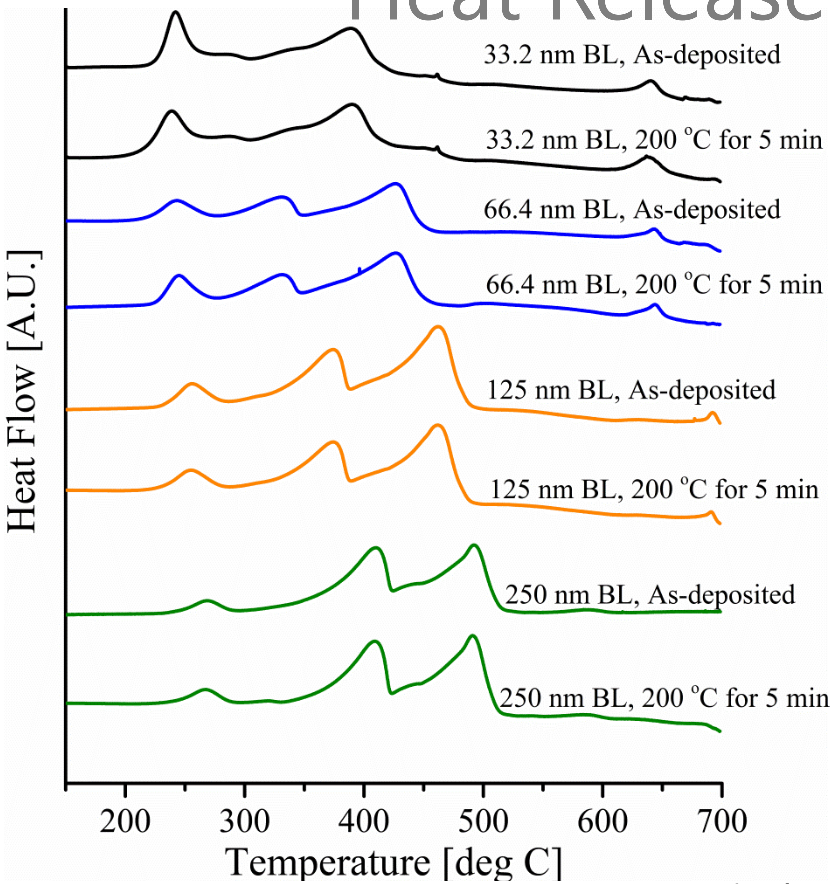

- Material held at 200 °C for 5 minutes
- Short times at elevated temperatures (below onset temp) have no effect on evolved heat
- E_a decreased for thick BLs
  – Possible grain coarsening

Bilayer Thickness	As-Deposited Foils: Total ΔH_f [kJ/mol$_{atoms}$]	As-Deposited Foils: E_a [kJ/mol$_{atoms}$]	After 5 min hold at 200 °C: Total ΔH_f [kJ/mol$_{atoms}$]	After 5 min hold at 200 °C: E_a [kJ/mol$_{atoms}$]
21 nm	-40.5 ± 1.0	27.5 ±0.1	-39.2 ± 0.9	28.9 ± 0.4
33.2 nm	-39.1 ± 1.5	28.2 ± 0.3	-44.6 ± 2.9	22.9 ± 5.3
66.4 nm	-45.7 ± 1.4	22.8 ± 5.2	-46.6 ± 1.6	27.9 ± 4.7
125 nm	-45.2 ± 1.9	30.8 ± 6.6	-45.7 ± 1.8	20.2 ± 7.1
250 nm	-46.2 ± 0.8	33.1 ± 6.5	-44.6 ± 1.8	14.2 ± 0.7

Stability is affected by BL thickness, initial Temperature

- 66.4, 75, 87.5 nm BLs transitioned to stability at elevated T_o

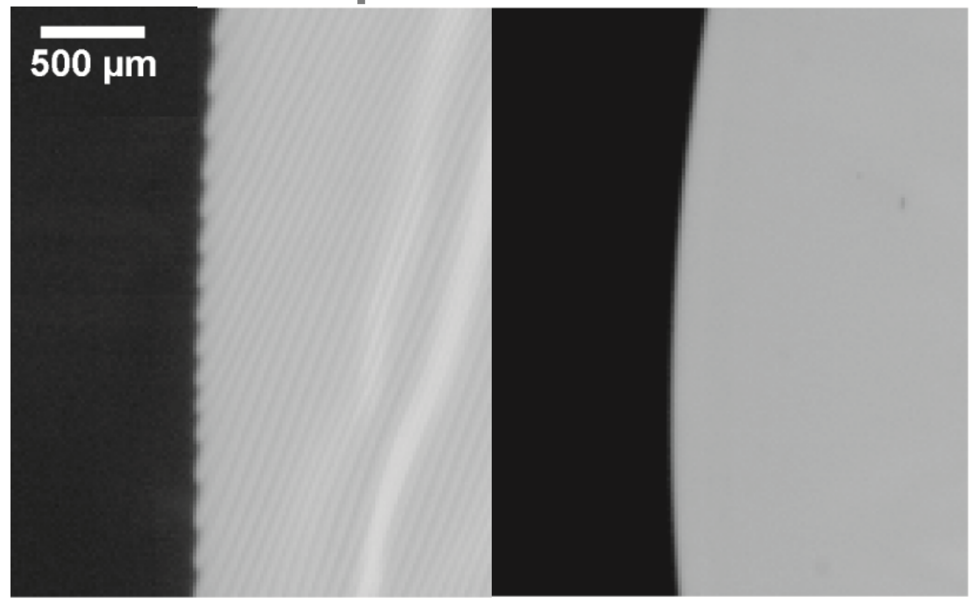

75 nm BL, T_o=25 °C

75 nm BL, T_o=150 °C

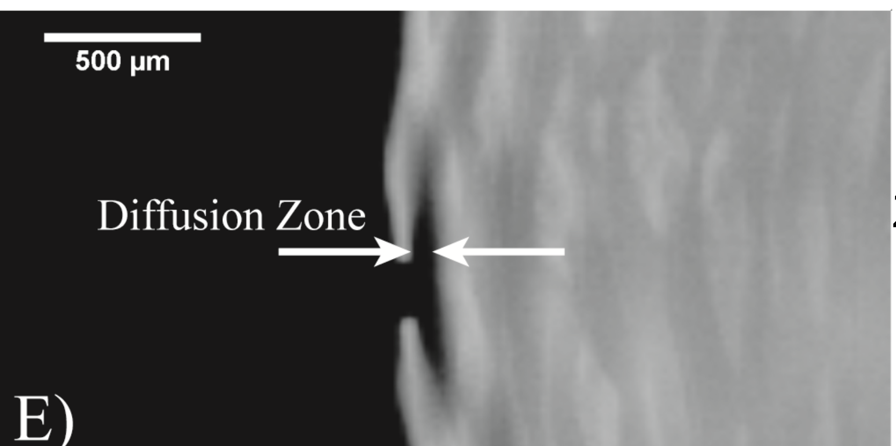

250 nm BL, T_o=25 °C

- Larger BLs unstable for all investigated T_o

Macroscale Reaction Behavior
Temperature and BL Dependence

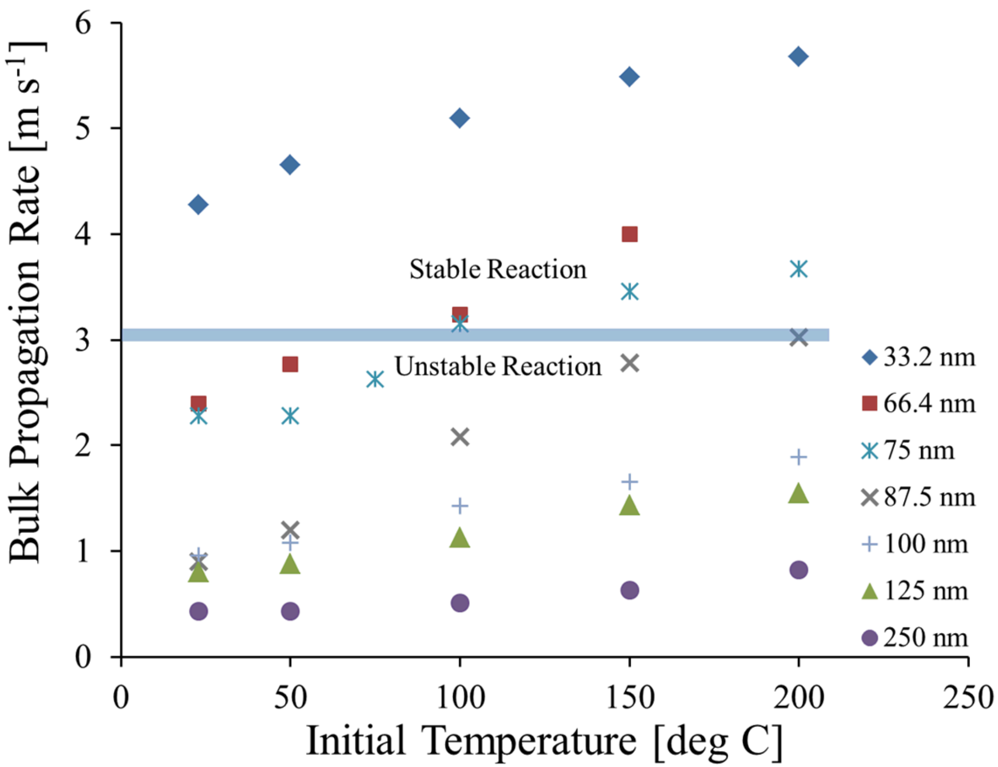

- Transition to stability takes place at $u_b \approx 3$ m/s for all BL designs
- Suggests a heat release rate for stability – system dependent, not BL dependent

Simultaneous IR/Visible Light Imaging

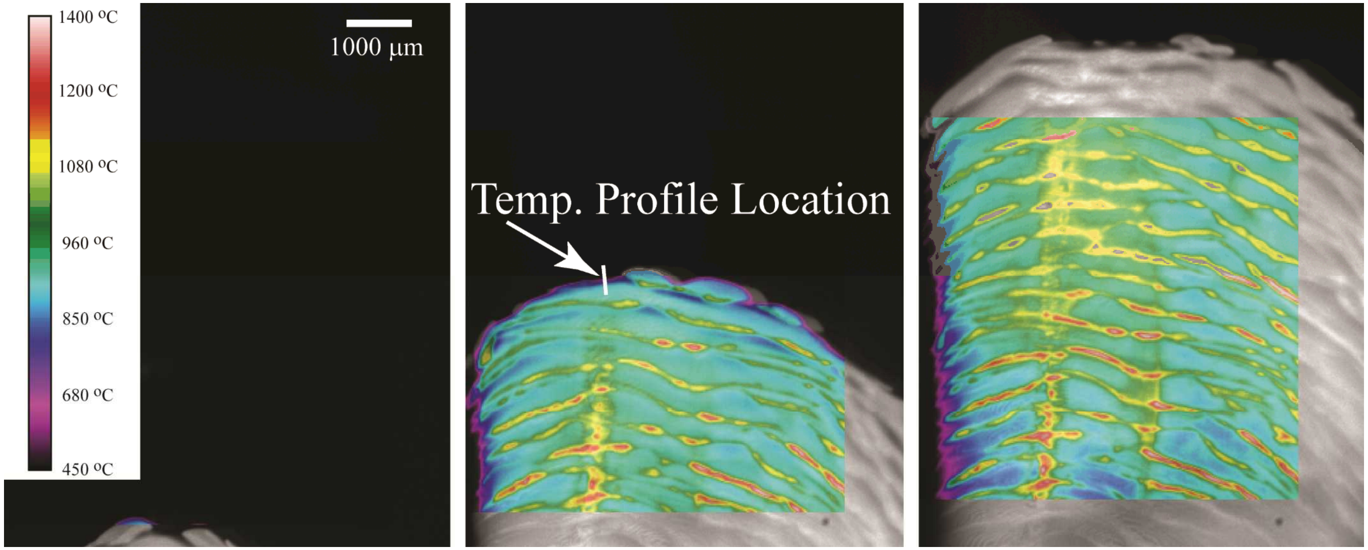

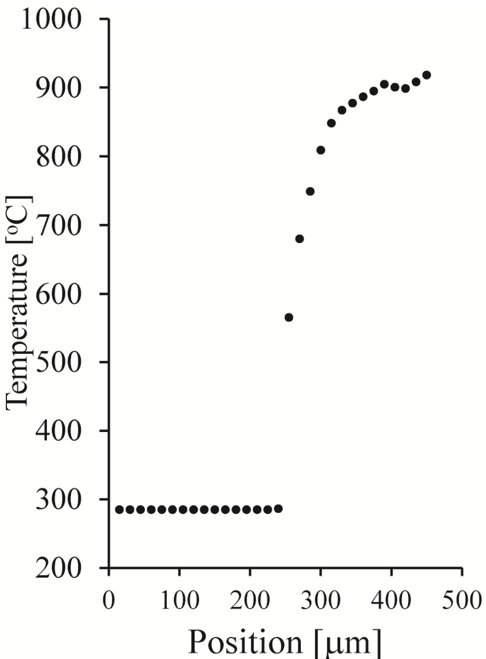

- Front can remain still for up to 1 ms
- Steep, unmoving temperature gradient at edge of transverse band
- Heat transfers from reacted material to unreacted material, but no significant self-heating occurs

Le^{-1} at Transition to Stability

- Using Armstrong's relationship,

$$Le^{-1} = \frac{D}{\lambda} = \frac{u^2 \delta^2 E_a (T_f - T_0)}{3\lambda^2 {T_f}^2 R} = \mathcal{A}\ exp\left(\frac{-E_a}{RT_f}\right)$$

[R. Armstrong, Combust. Sci. Technol. **71,** 155 (1990)]

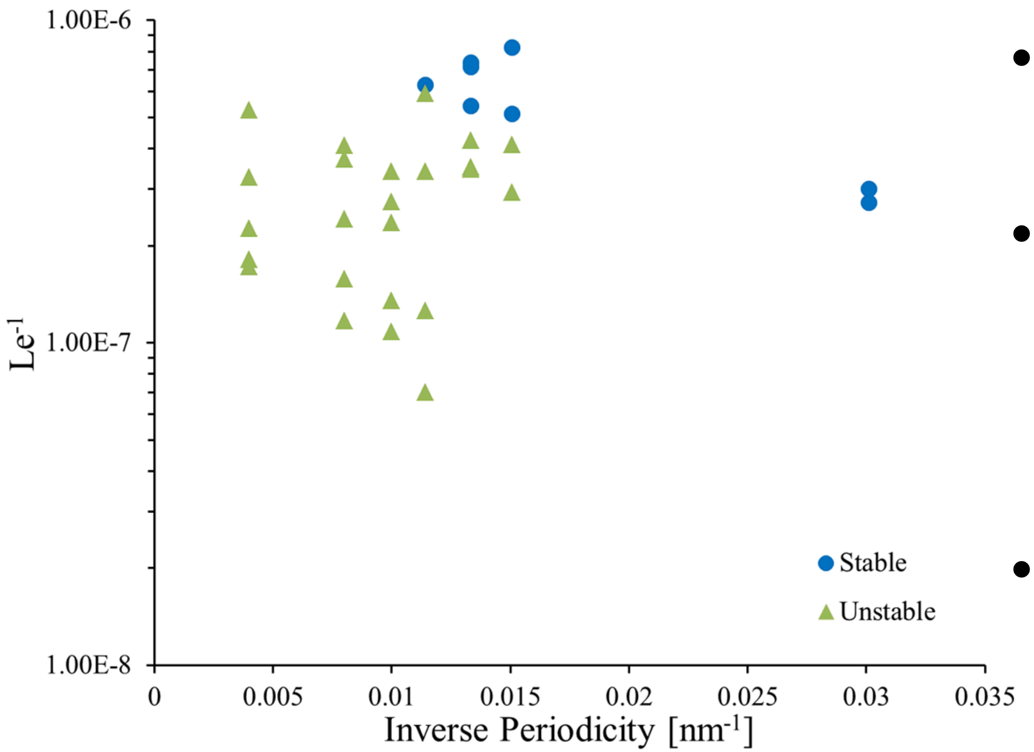

- Thinner BLs exhibit stable front at lower Le^{-1}
- Assuming constant λ, thicker BLs require higher mass diffusivity (reaction rates) for stability
- Fits with idea of critical heat transfer rate

Propagation Rates Dependences on T_0

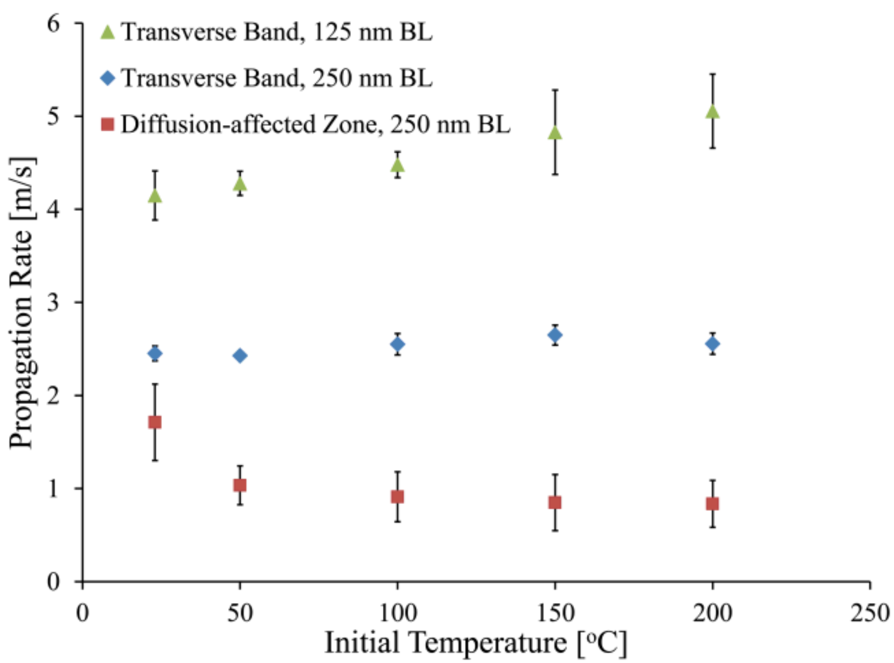

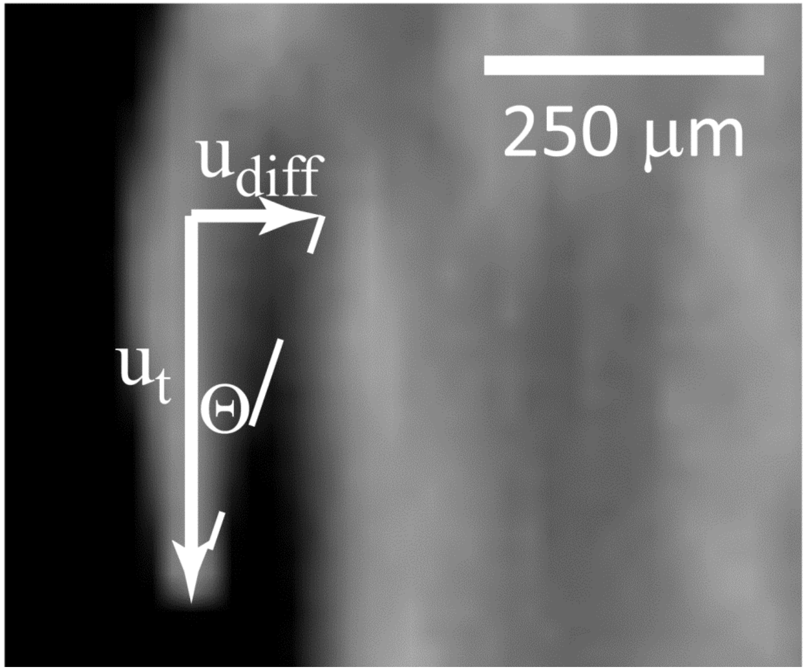

- U_t slightly increases with T_0 for 125 nm BL foils
- U_t has little dependence on T_o for 250 nm BL foils
- U_{diff} has a slight negative dependence on T_0 for 250 nm BL foils

Simultaneous IR/Visible Light Imaging

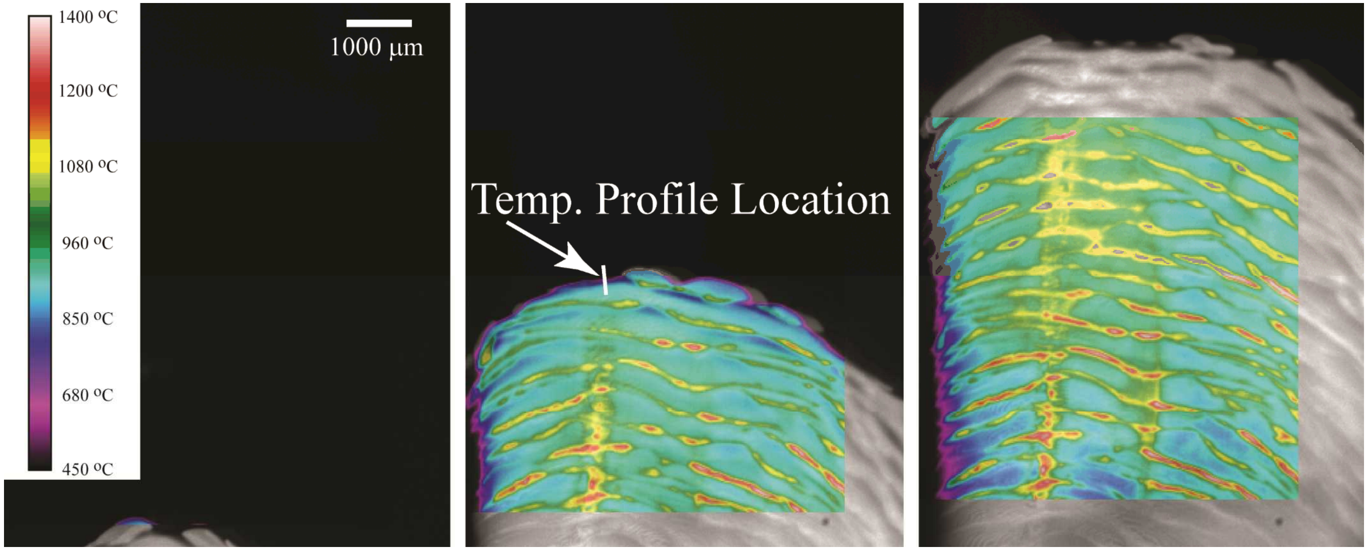

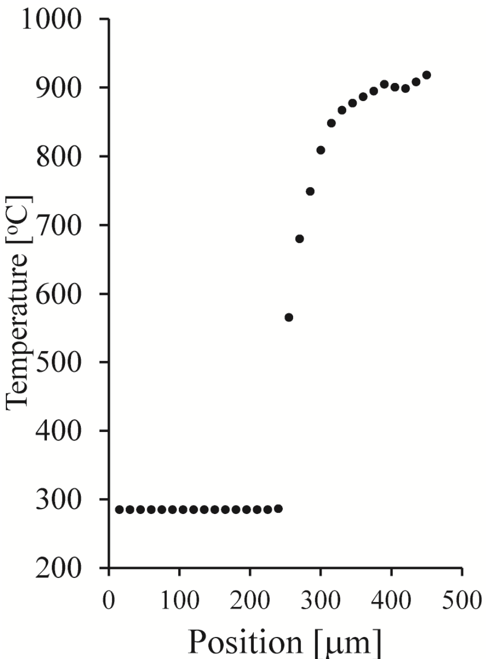

- Forward heat transfer w/o self-heating will be at conductive rates (<10^3)
- This might cause stationary reactions similar to initial DSC exotherm
- Solid state products could inhibit local reactions

Proposed Mechanism

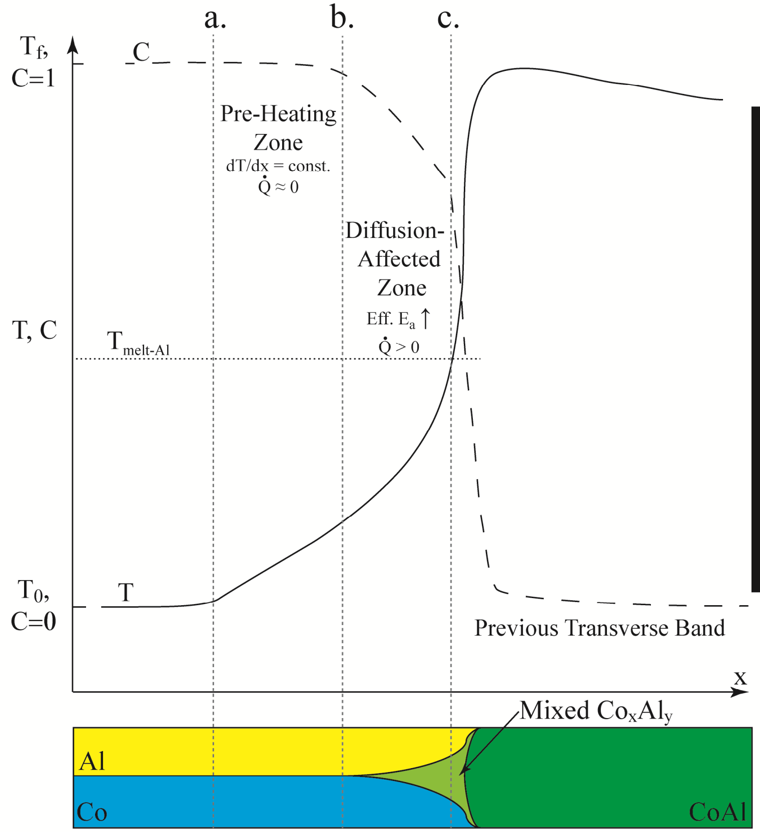

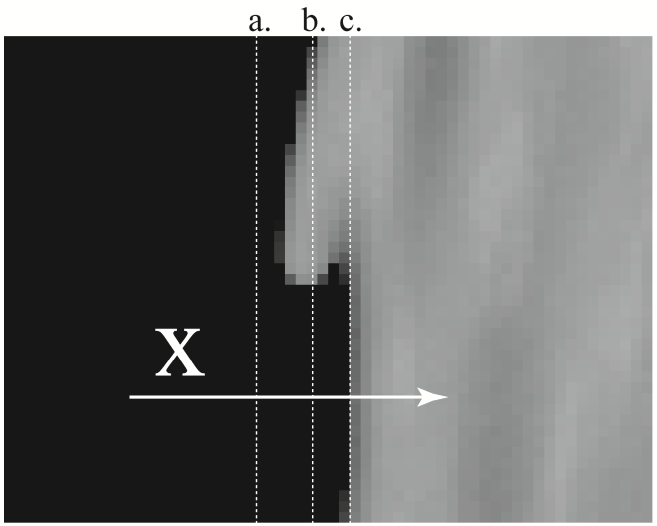

- At front edge of previous transverse band, heat is conducted into unreacted material
- Near transverse band, limited reaction occurs at Al/Co interface
- Farther ahead the local temperature rises, but remains below reaction onset threshold

Proposed Mechanism

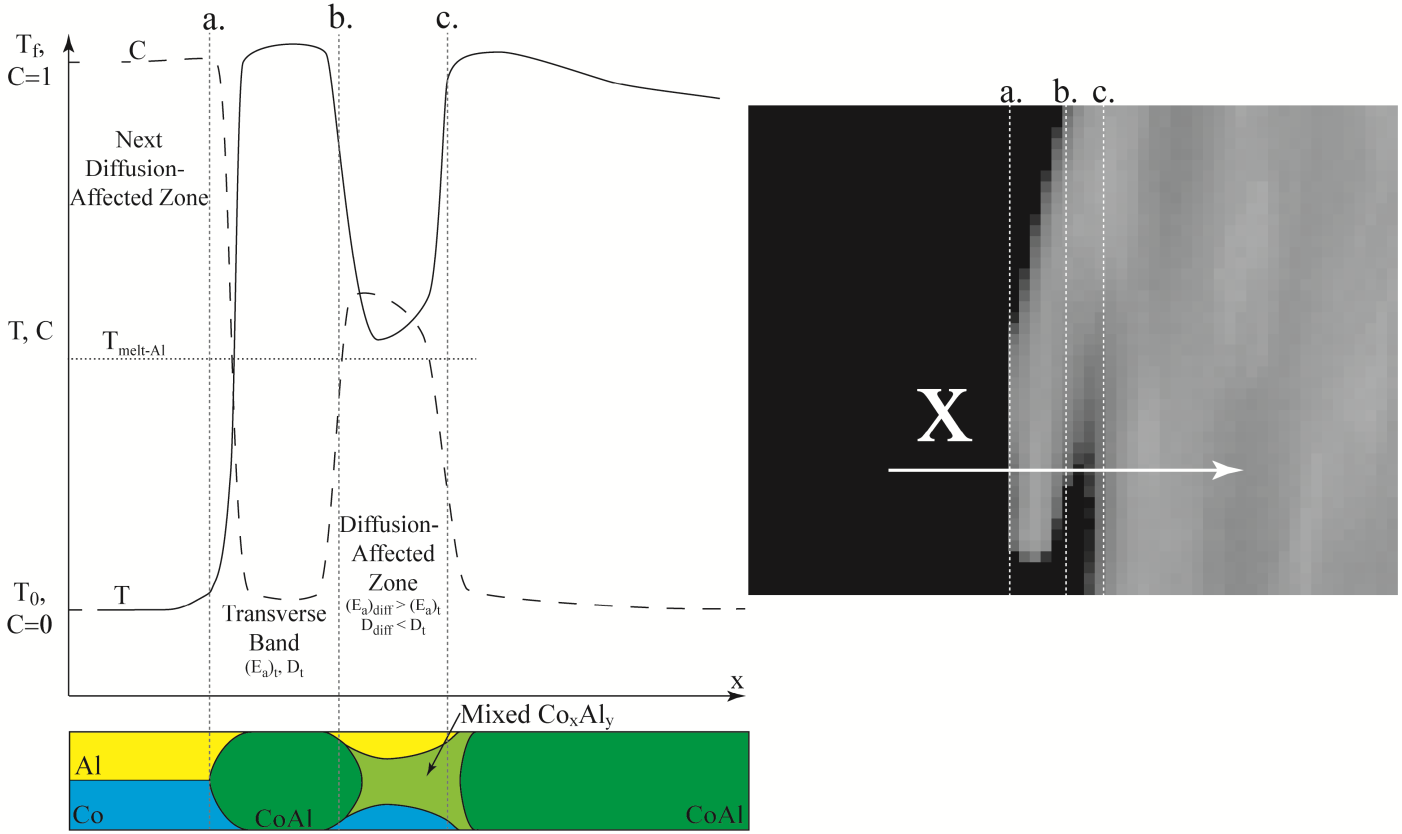

- Preheated, unreacted region hosts next transverse band
- Diffusion affected zone reacts more slowly, after transverse band passage
- Reaction behavior dependent on system kinetics and temperature history

Proposed Mechanism

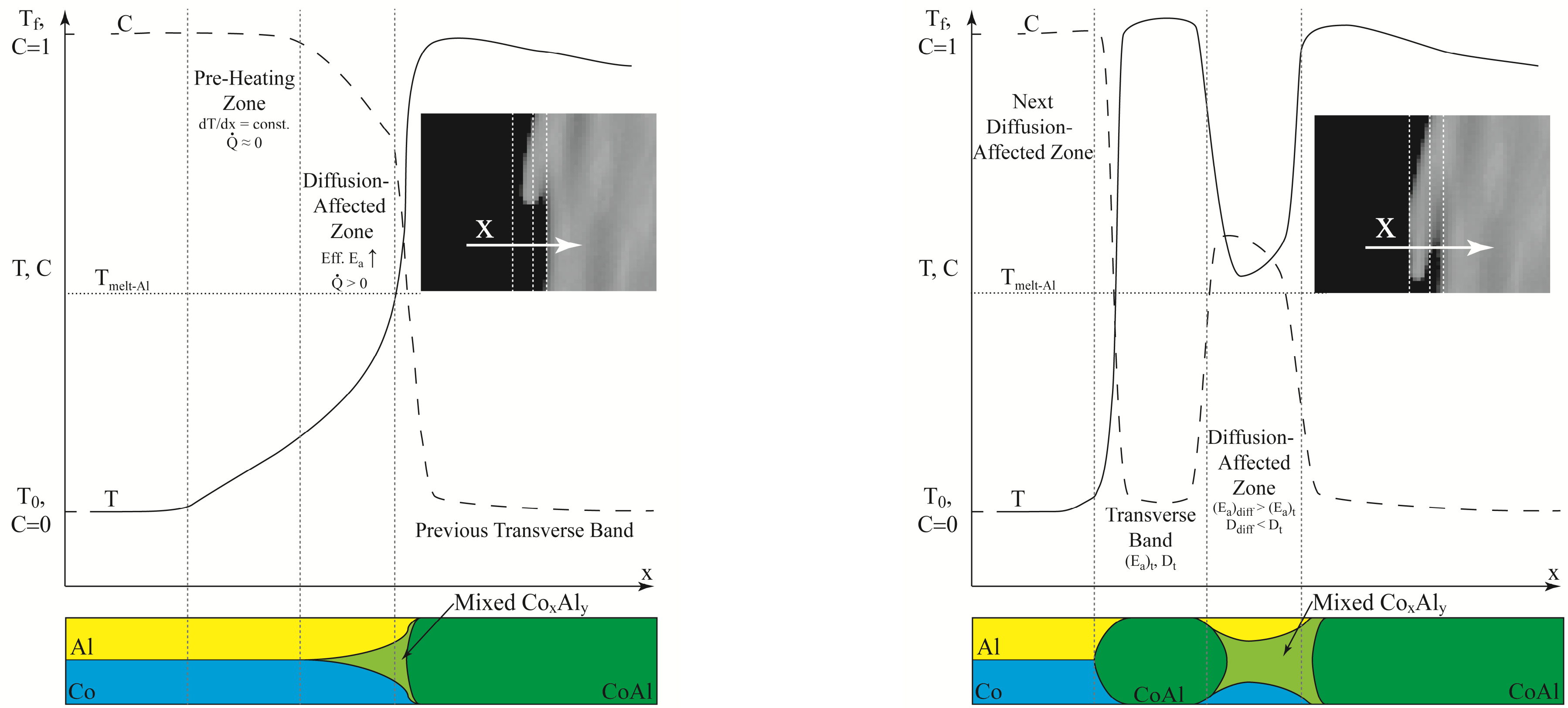

- Preheated, unreacted region hosts next transverse band
- Diffusion affected zone reacts more slowly, after transverse band passage
- Reaction behavior dependent on system kinetics and temperature history

Environmental Coupling for Stability

- Instabilities form when forward heat transfer is insufficient
- $Ti + Ni \rightarrow NiTi; \Delta H = -68 \frac{kJ}{mol_{Ti}}$
- $Ti + O_2 \rightarrow TiO_2; \Delta H = -945 \frac{kJ}{mol_{Ti}}$
- Even minor coupling to gas could aid stability

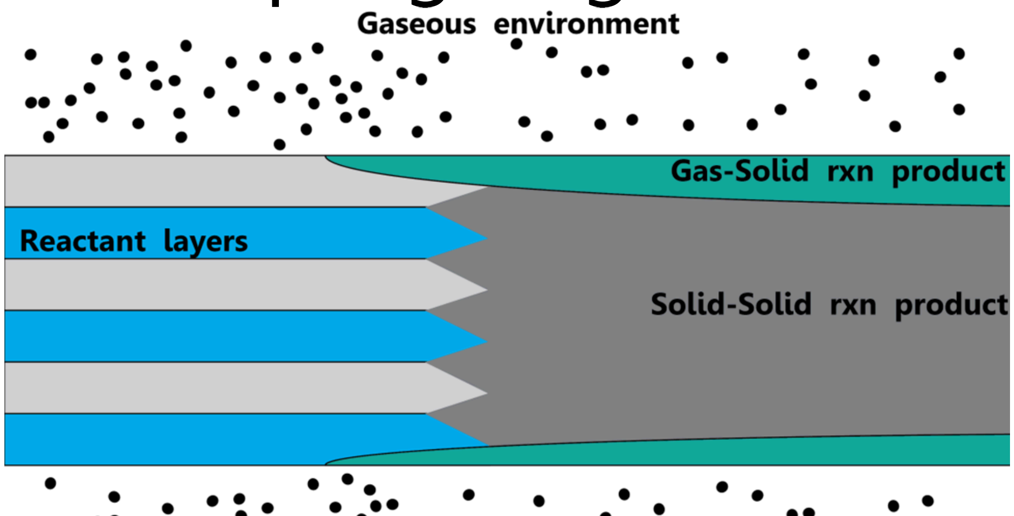

Ni/Ti: High-Speed Imaging
62.5 nm BL, 5 mm Total Thickness

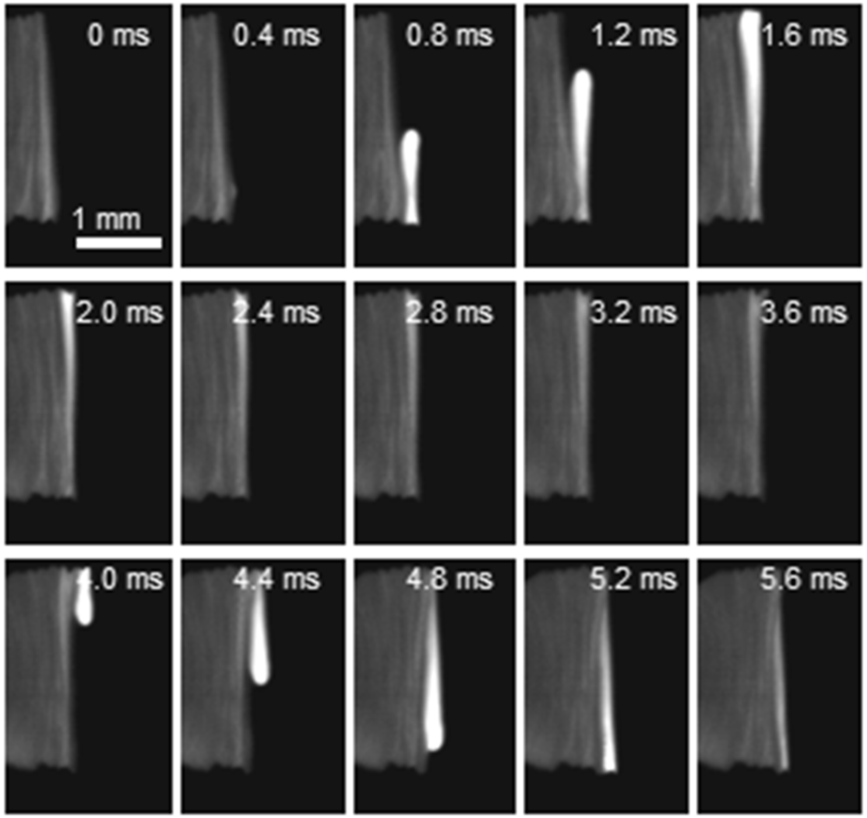

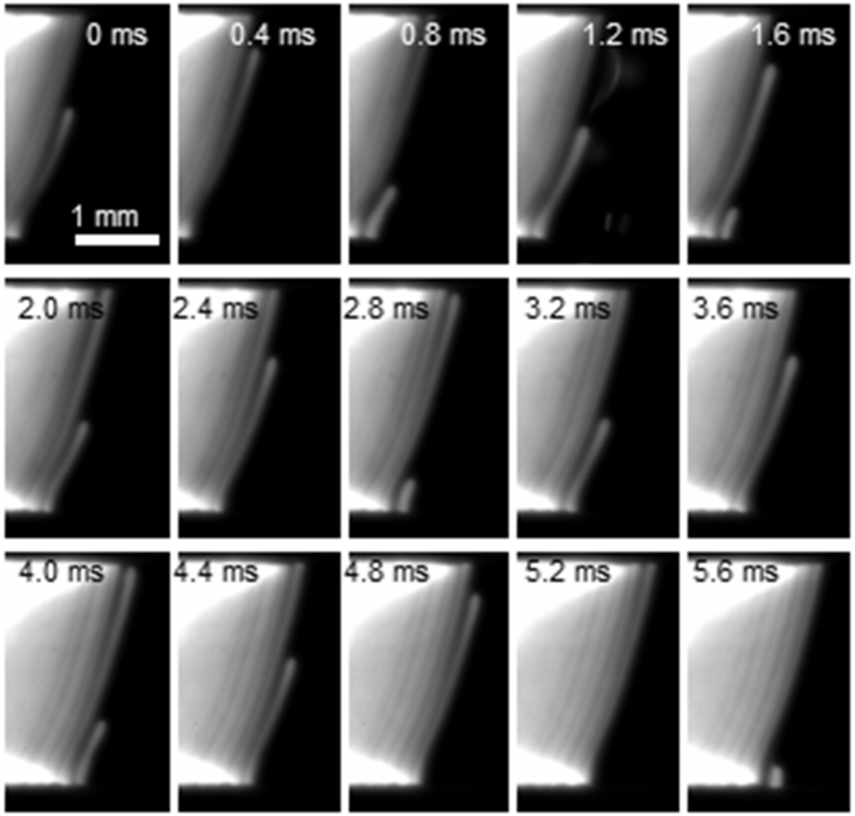

- Reaction at 300 mTorr
- Spin wave of intermetallic reaction only mode present

- Reaction at atm. pressure
- Spin wave followed by bright combustion wave

Ni/Ti: Phase/elemental ID

Auger Electron Spectroscopy

- 1 mTorr: little O penetration (A)
- Atmosphere: Thick O-penetrated, Ti rich layer (B)
  - Excess Ni in interior

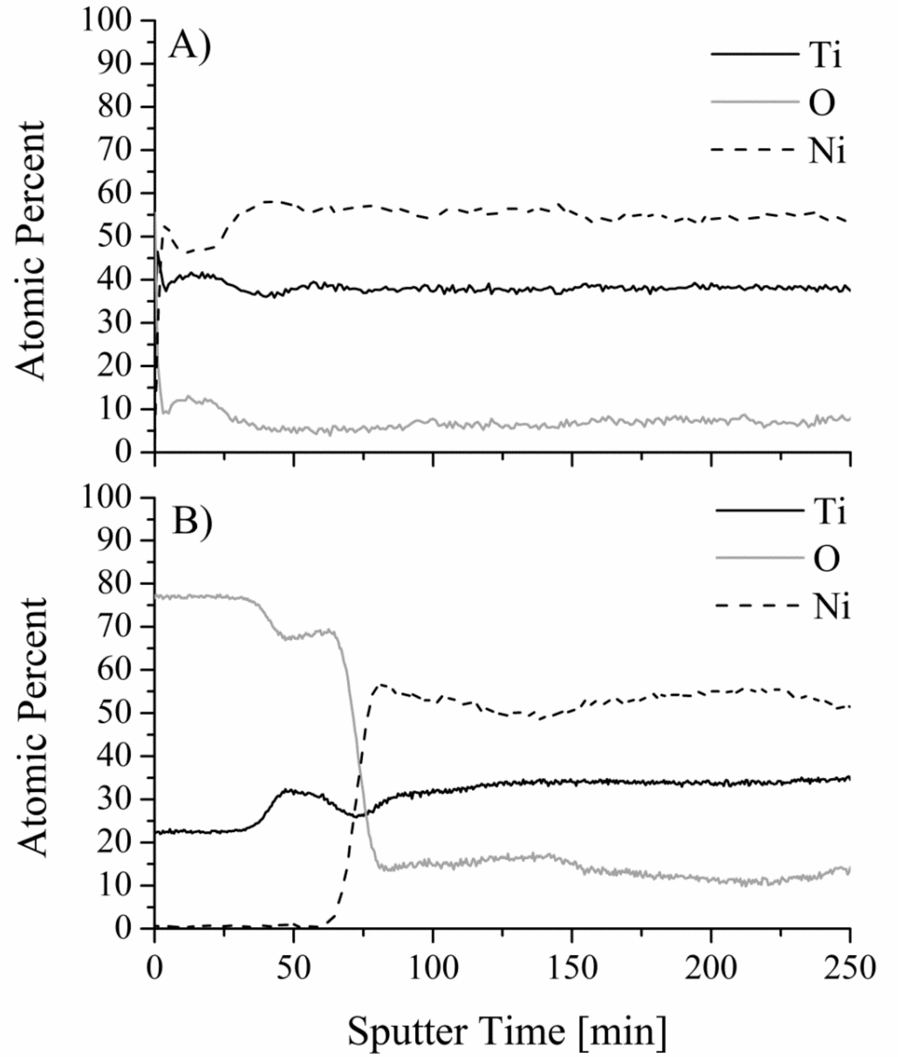

X-ray Diffraction

- 1mTorr: only Ni+Ti phases
- Atmosphere: Ni+Ti phases, elemental Ni, and Ti oxides

Reaction Speed vs. Pressure:
Ni/Ti 473 nm bilayer, 5 mm thick

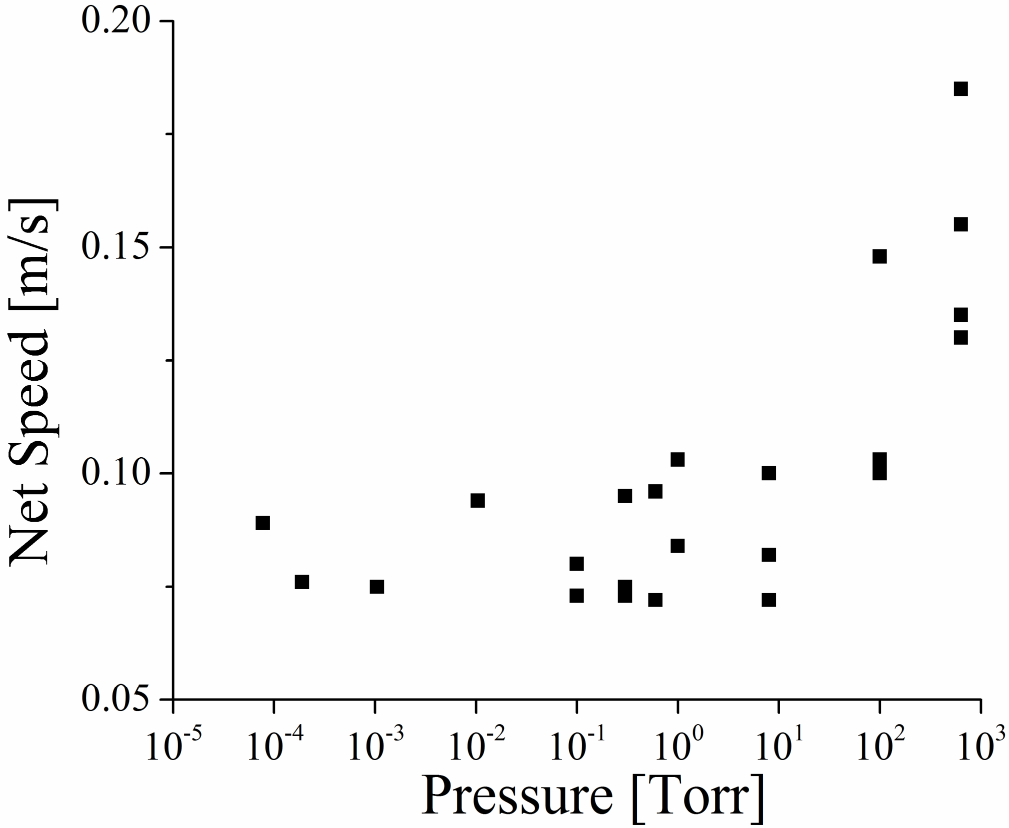

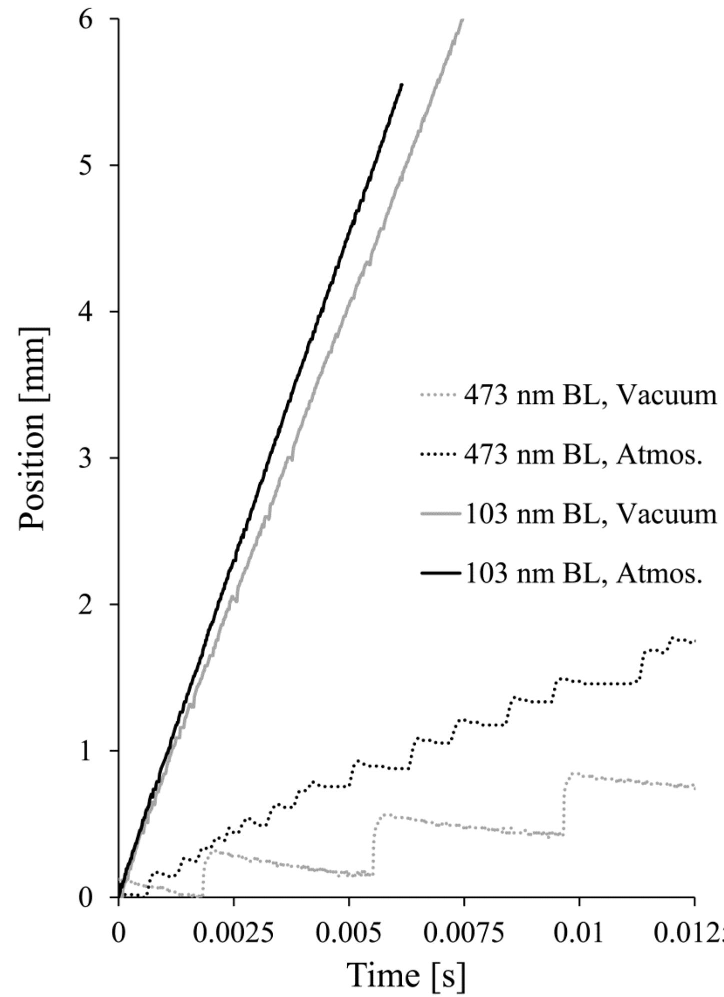

- Reaction velocity increases with air pressure
- Nucleation rate is increased in atmosphere

Gas Coupling in Ni/Ti Thin Films

- Ni/Ti films propagate with unstable, spinning reaction fronts
- Air pressure causes increase in reaction band frequency
  - Adds stability to reaction front
  - Begins to approximate steady reaction front
- Heat release from Ti oxidation increases forward heat transfer, increasing reaction stability

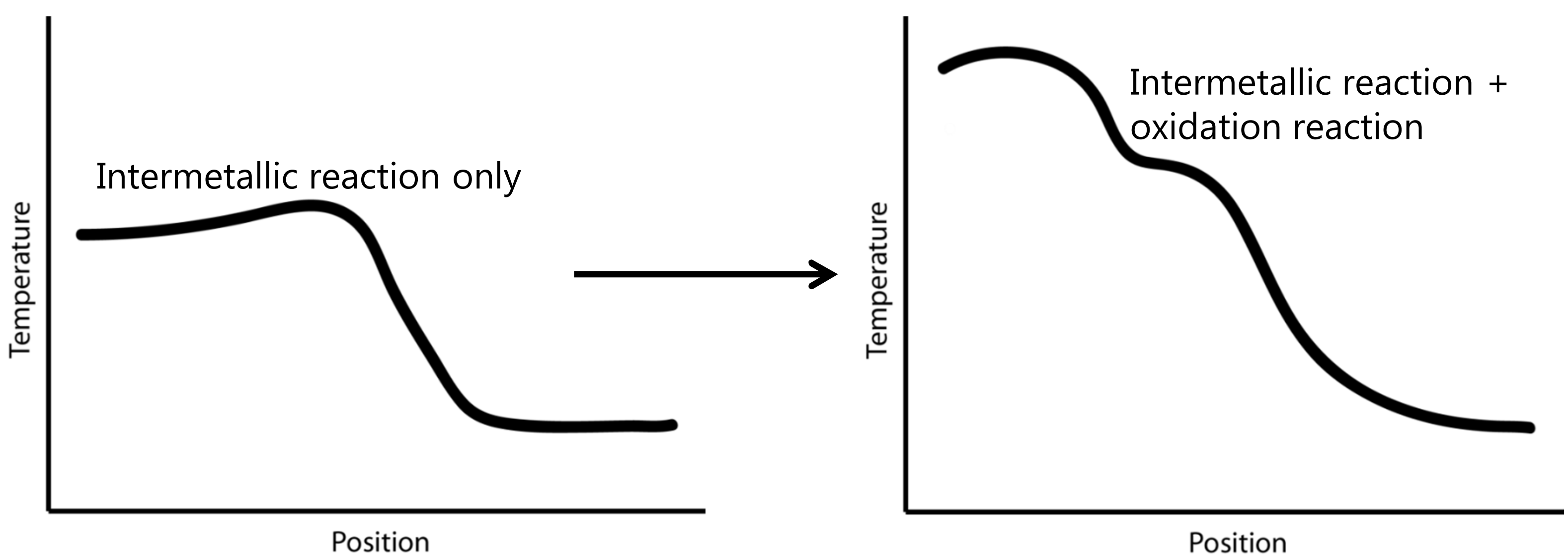

Gas Coupling to Stable Reactions – Ti/2B
50 nm bilayer vs 3000 nm bilayer

1 s real time = 500 μs elapsed reaction time (total elapsed time is 13 ms)

Pressure dependence by bilayer

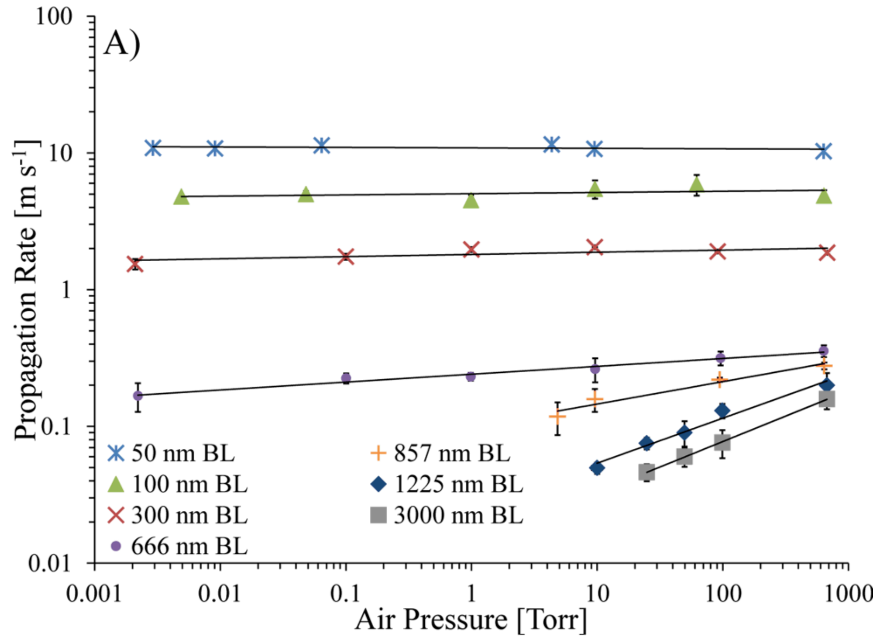

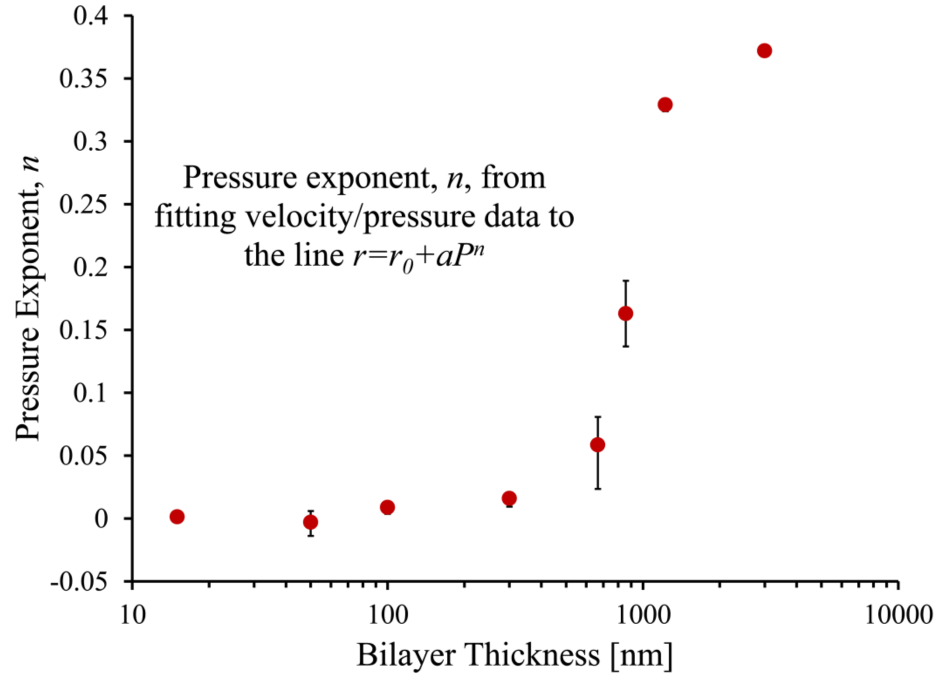

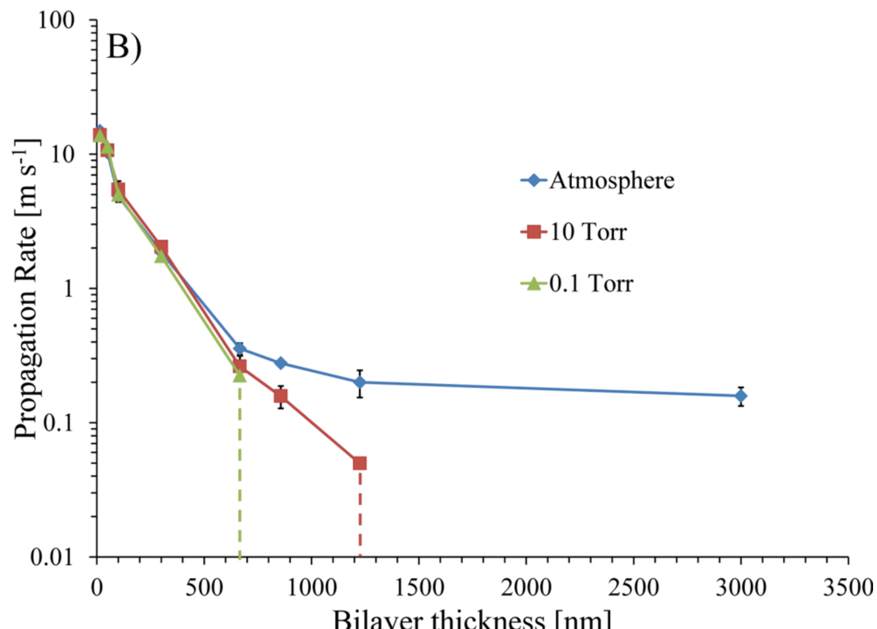

- Thick bilayers: strong pressure dependence
- Thin bilayers: little pressure dependence
- Transitional BL thickness lies between 667 and 857 nm
- Atmosphere extends range of BL thicknesses that propagate

Reaction Wave Stability

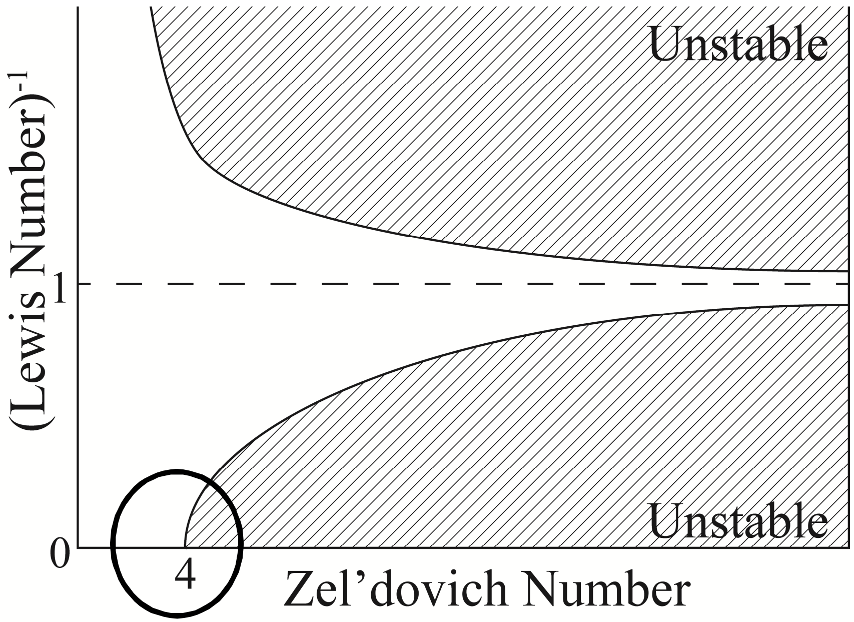

- Above chart from Aldushin and Kasparyan [1,2], discussed by Merzhanov and Rumanov[3]

- Lewis Number, $\frac{\alpha}{D} = \frac{\kappa}{D\rho c}$
  - Compares Mass Diffusion and Thermal Diffusion rates
  - Typical $L_e \approx \frac{10^{-1}}{10^{-3}\ to\ 10^{-7}}$ for gasless systems
- Zel'dovich Number,

$$\beta = \frac{E_a}{R{T_{ad}}^2}(T_{ad} - T_0)$$

  - Compares temperature dependence of reaction to adiabatic flame temp.

[1] *Sov. Phys. Dokl*, **24**, 29, 1979
[2] *Akad. Nauk SSSR*, **247**, 1112, 1979)
[3] *Reviews of Modern Physics*, **71**, 4, 1999

Experimental Plan

Vary *Le* and *b* to determine stability boundary

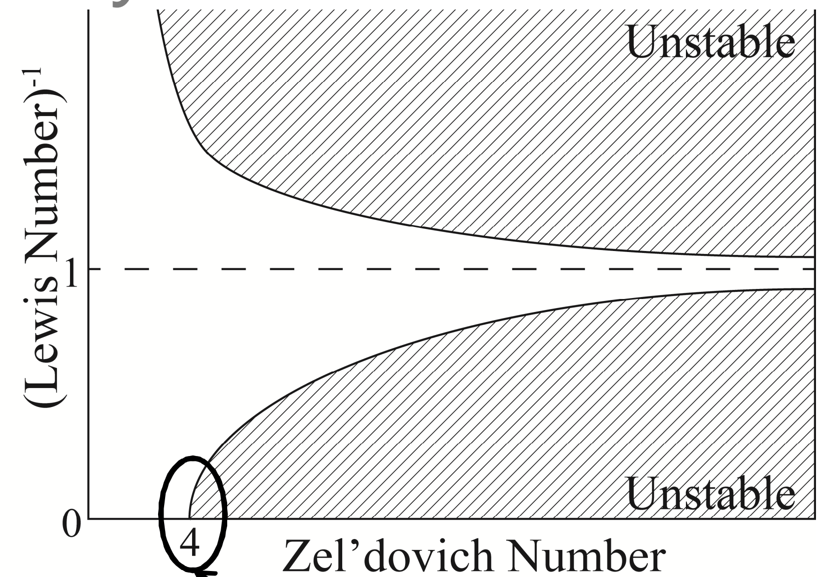

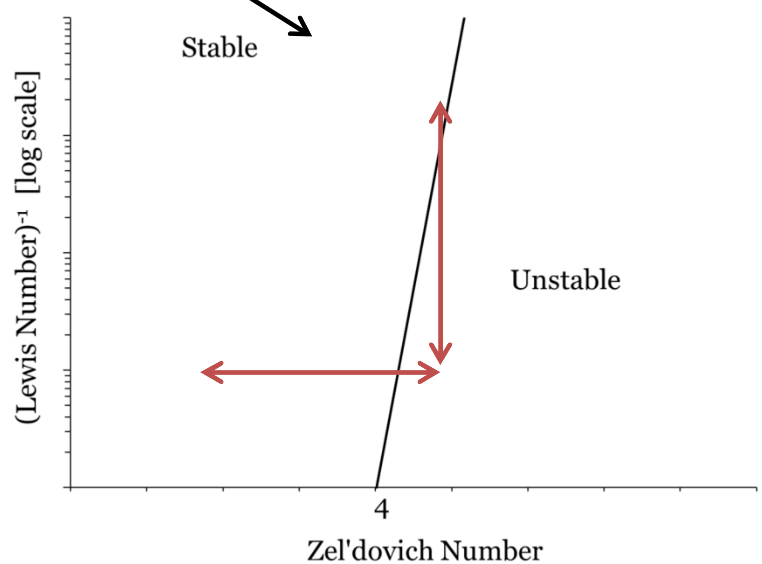

- Lewis Number
  - $Le^{-1} = \frac{D}{\lambda} = \frac{u^2 \delta^2 E_a (T_f - T_0)}{3\lambda^2 {T_f}^2 R} = \frac{u^2 \delta^2 \beta}{3\lambda^2}$
- Zel'dovich Number, $\beta = \frac{E_a}{R{T_f}^2}(T_f - T_0)$
  - Reduce adiabatic flame temperature through dilution

Multilayer Design

Dilution Designs to vary β

- Design for variation of β
  - Layers of CoAl product are deposited *within* each reactant layer
  - Reactive interfaces and diffusion distances are unchanged from the baseline multilayer design
  - Total volumetric dilution from 0% to 30%

- $\beta = \frac{E_a}{RT_{ad}^2}(T_{ad} - T_0)$

so increasing CoAl dilution decreases T_{ad}, increasing *b*

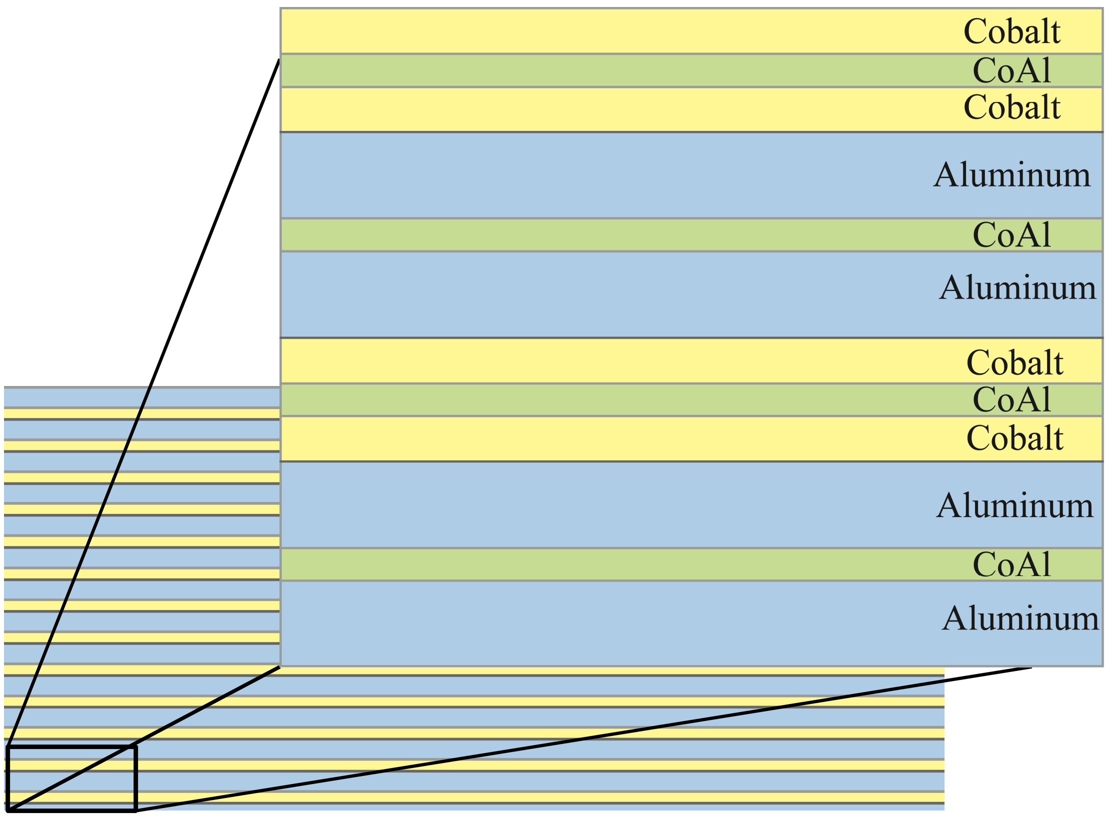

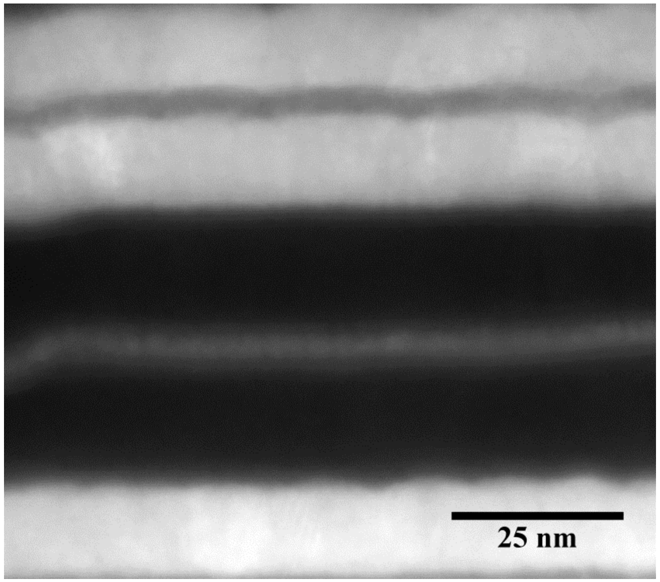

Calorimetry

Determination of ΔH and apparent E_a

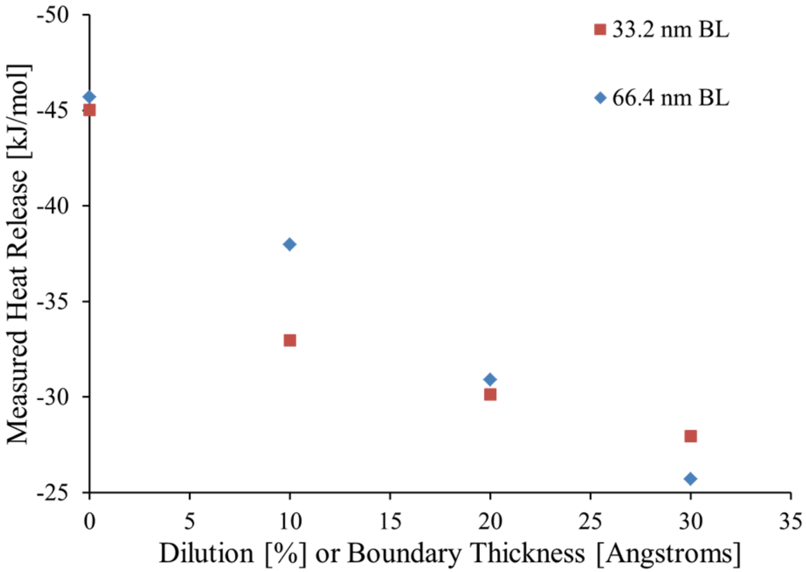

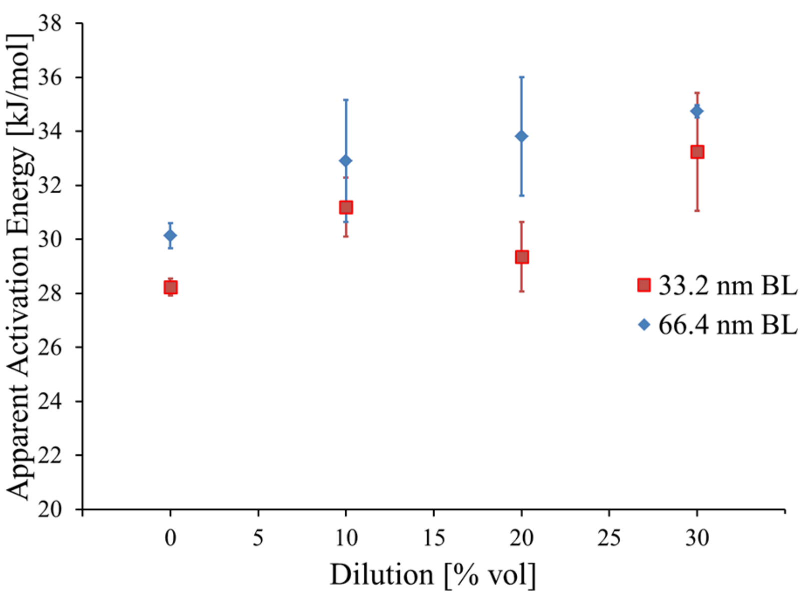

33.2 nm BL

Dilution [Volume Percentage]	Activation Energy [kJ/mol atoms]	Heat Release [kJ/mol atoms]	Heat Release [% max]
0	28.2 ± 0.3	-45 ± 1.5	100
10	31.2 ± 1	-33 ± 1.5	73.2
20	29.4 ± 0.9	-30.1 ± 0.9	66.9
30	33.2 ± 1.3	-27.9 ± 2.4	62.1

66.4 nm BL

Dilution [Volume Percentage]	Activation Energy [kJ/mol atoms]	Heat Release [kJ/mol atoms]	Heat Release [% max]
0	30.1 ± 0.5	-45.7 ± 1.4	100
10	32.9 ± 3.3	-38 ± 2.3	83.1
20	33.8 ± 1.7	-30.9 ± 2.2	67.6
30	34.7 ± 0.8	-25.7 ± 1.3	56.2

- Heat release directly measured from DSC
- Apparent E_a determined by Kissinger method

Propagation Rates

Co/Al Nanolaminates
33.2 nm BL Th.
Diluted with CoAl Alloy
Volumetric Percent CoAl Noted
Air Pressure = 10.0 mTorr

1 s Real Time = 1 ms Reaction Time

Co/Al Nanolaminates
66.4 nm BL Th.
Diluted with CoAl Alloy
Volumetric Percent CoAl Noted
Air Pressure = 10.0 mTorr

1 s Real Time = 1 ms Reaction Time

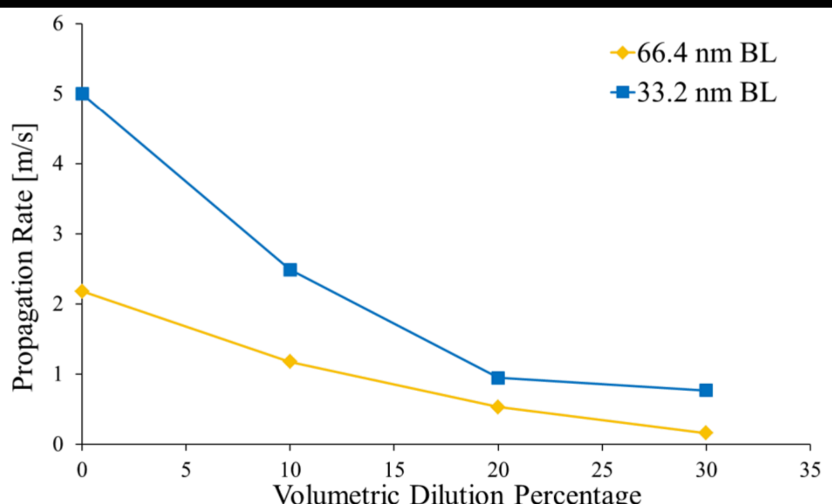

Dilution– Reaction Front Stability

33.2 nm BL

10% Dilution –
Stable front, *u* = 2.49 m/s
20% Dilution –
Spin instability appears, *u* = 0.95 m/s
30% Dilution –
Spin instability is more apparent, *u* = 0.77 m/s

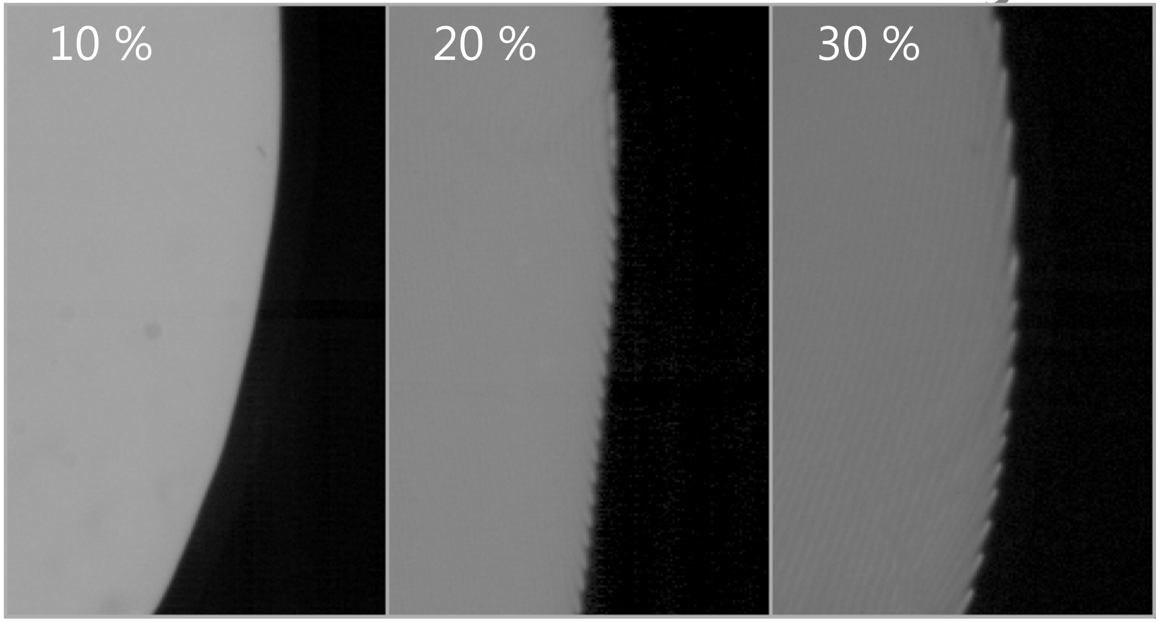

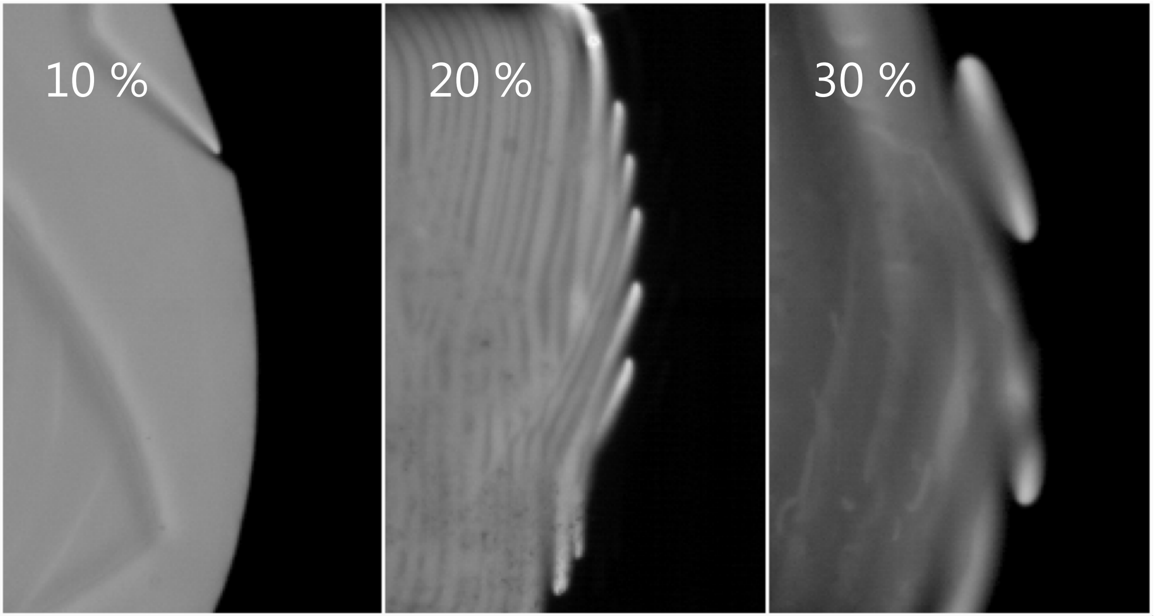

66.4 nm BL

10% Dilution –
Spin instability appears, *u* = 1.18 m/s

20% Dilution –
Spin instability appears, *u* = 0.53 m/s

30% Dilution –
Spin instability becomes very large and irregular, *u* = 0.16 m/s

Stability Criteria
Experimental vs. Analytical

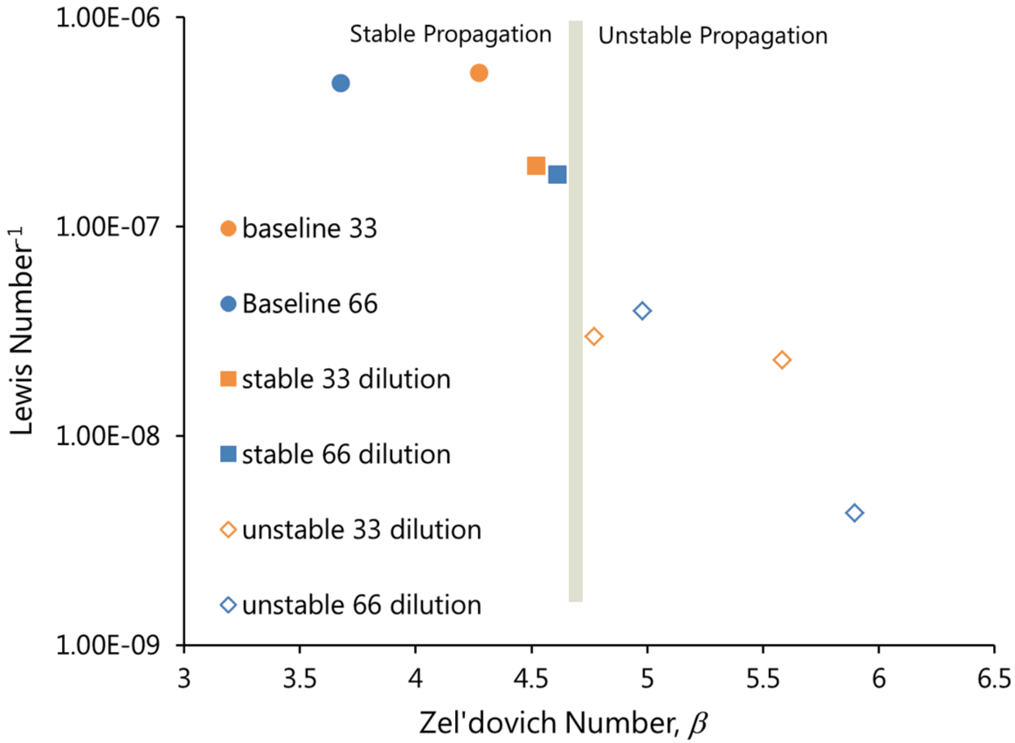

- Plotting on Le^{-1}-β axes, get approximate regions of stability
- Stability boundary similar between BL designs
- Verification across more designs needed

Nanolaminates
Typical Reaction Progression

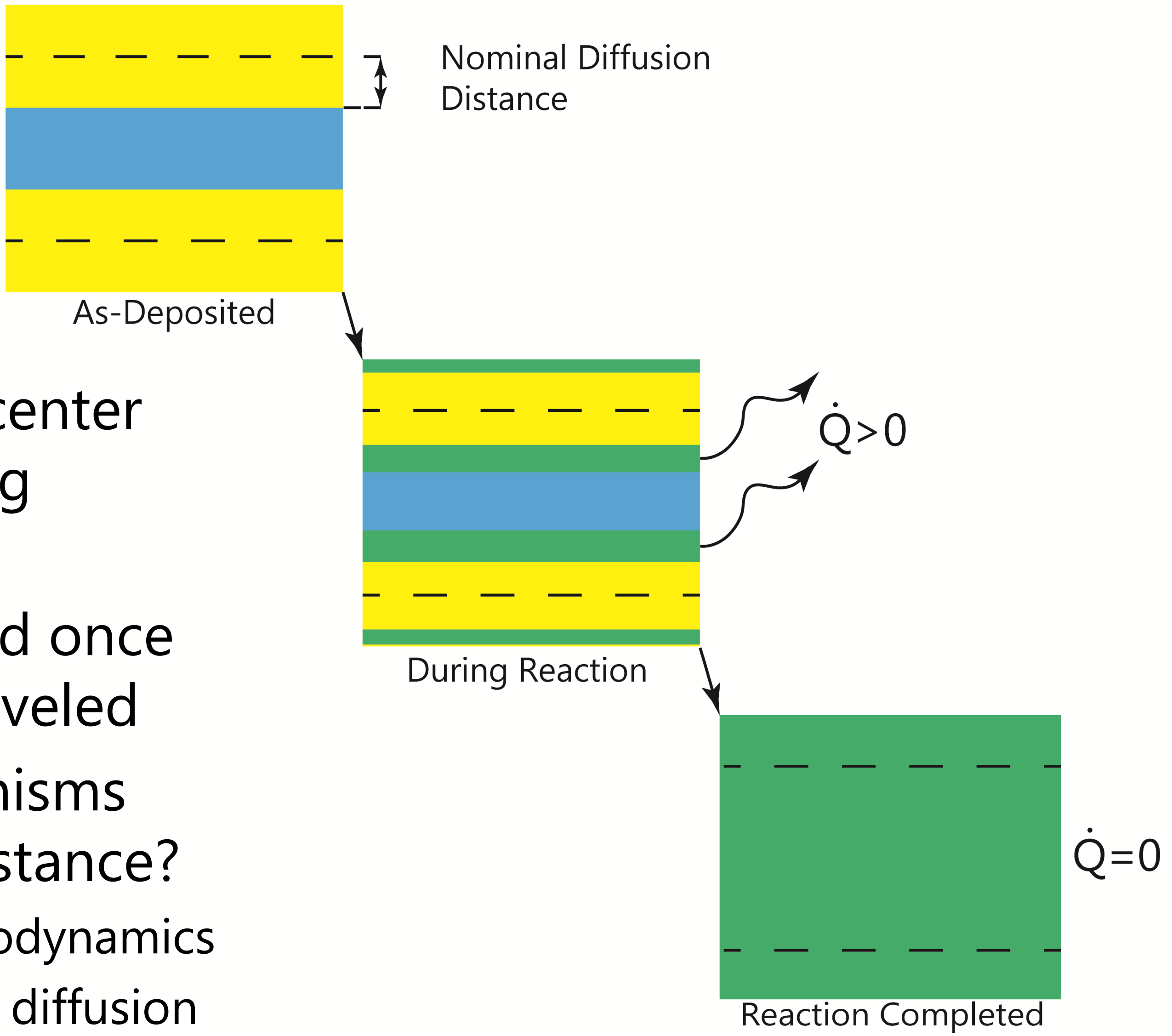

- Atoms diffuse to center line of neighboring reactant layer
- Final phase formed once this distance is traveled
- Can other mechanisms affect diffusion distance?
  - Dissipative thermodynamics
  - High temperature diffusion

Marker Layer Design
Zr+(Hf)/2Al Nanolaminates

- Hf replaces Zr at a single layer
- Hf and Zr:
  - are miscible with no distinct intermetallic phases
  - have similar chemical behavior and product phases with Al

	Atomic Radius	Pauling Electronegativity
Zr	159 pm	1.33
Hf	156 pm	1.3

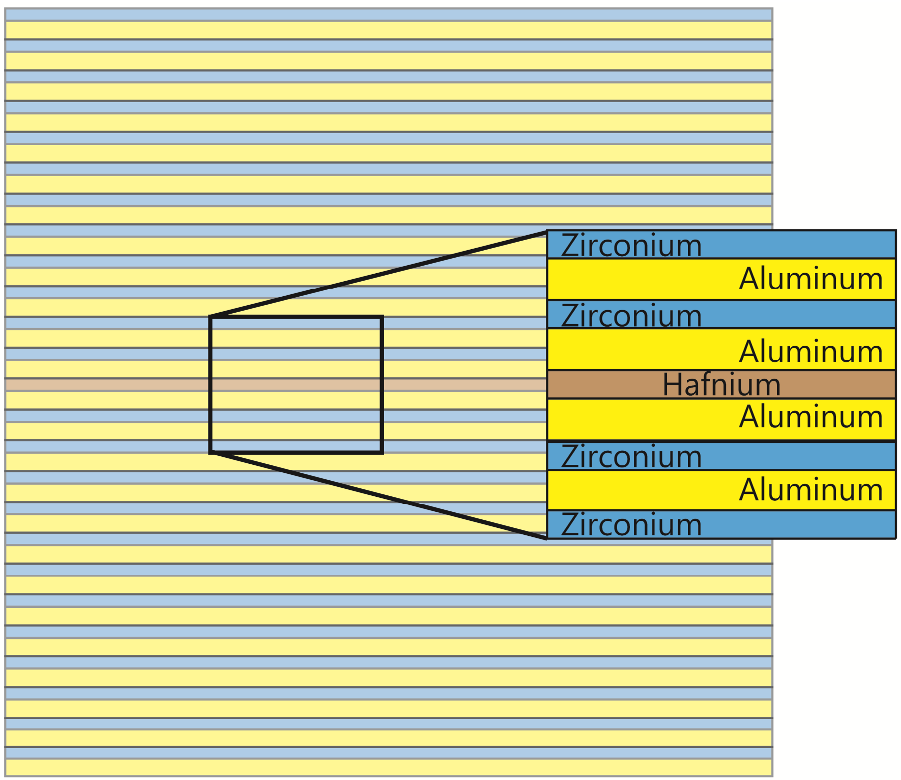

$ZrAl_2$	T_m = 1660 °C	$HfAl_2$	T_m = 1650 °C
	ΔH = -46 kJ/mol		ΔH = -48 kJ/mol
hP12	a = 0.52824	hP12	a = 0.525
	b = 0.52824		b = 0.525
	c = 0.87482		c = 0.868
Zr_2Al_3	T_m ≈ 1590 °C	Hf_2Al_3	T_m = 1660 °C
	ΔH = -47 kJ/mol		ΔH = -48 kJ/mol
oF40	a = 0.9601	oF40	a = 0.9529
	b = 1.3906		b = 1.3763
	c = 0.5574		c = 0.5525

*(de Boer, Boom, Mattens, Miedema, Niessen, *Cohesion in Metals*, 1988)

Marker Layer Analysis

(Zr+Hf)/2Al Nanolaminates

- Marker clearly resolvable with z-contrast and EDS in TEM
- 25 nm BL thickness
- Highly planar interfaces

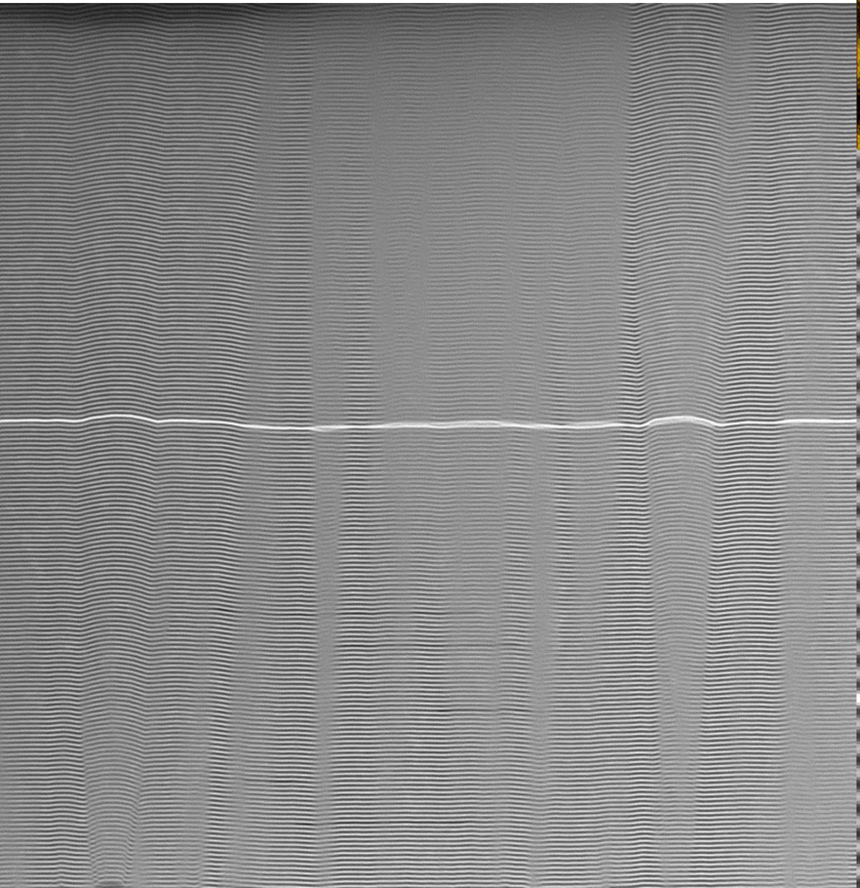

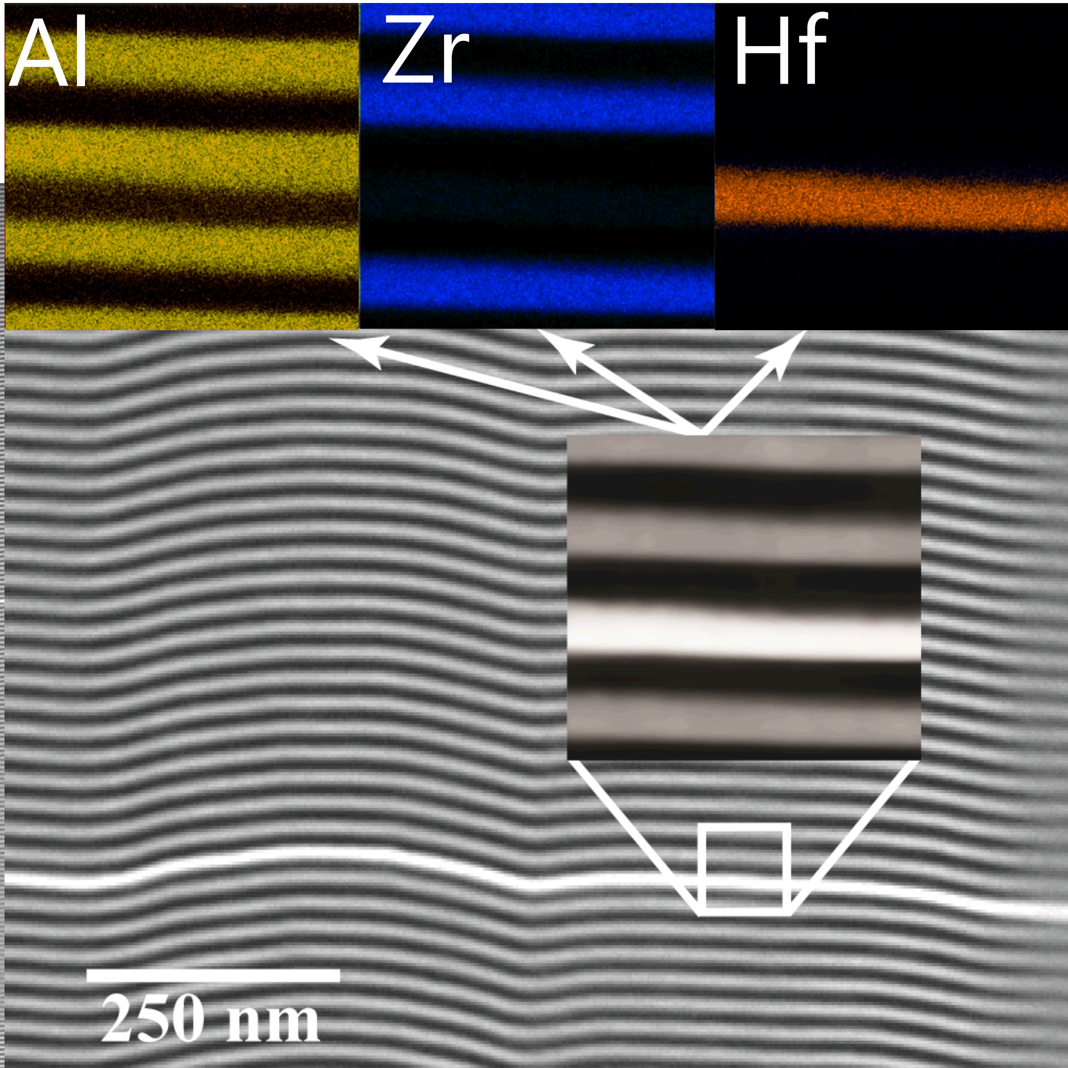

Marker Layer Design

(Zr+Hf)/2Al Nanolaminates

- Reaction disperses Hf marker material

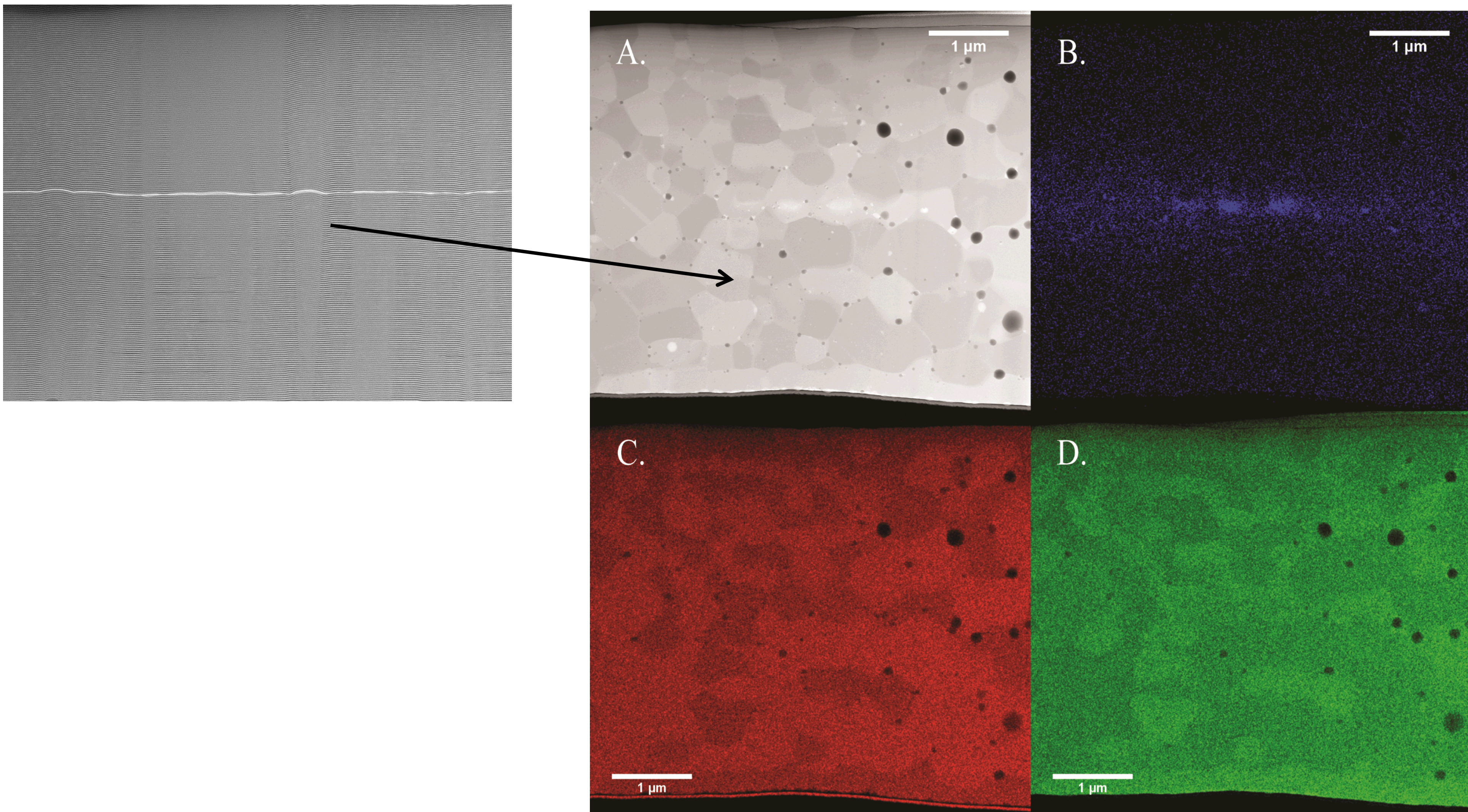

Marker Layer Design

(Zr+Hf)/2Al Nanolaminates

- Reaction disperses Hf marker material

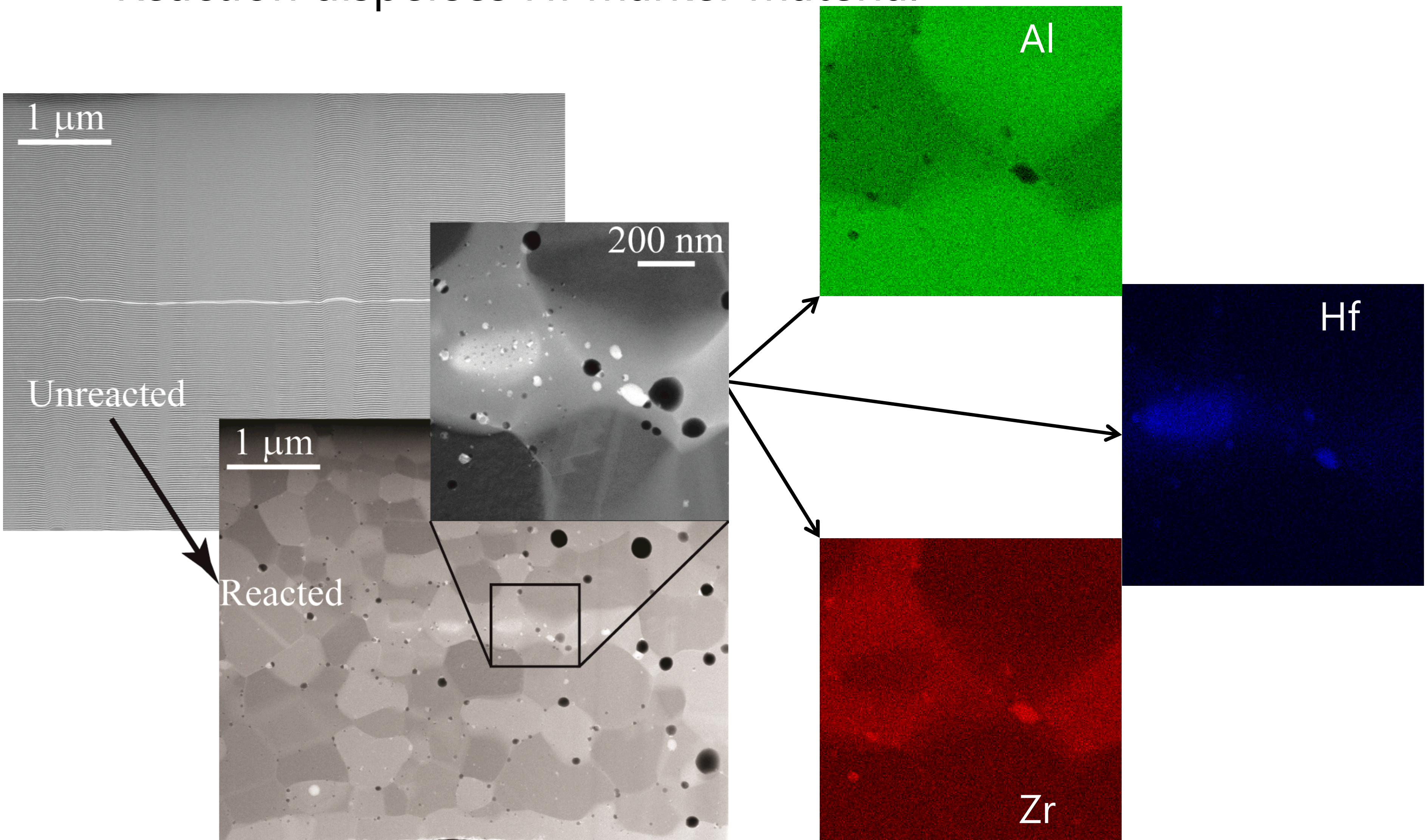

Phase Identification
Zr/2Al and Hf/2Al Standards for Semi-Quant

- Zr/2Al films reacted in vacuum (10 mTorr)
- $ZrAl_2$ (~60% wt%) and Zr_2Al_3 (~40% wt%) phases identified by XRD

- Hf/2Al films reacted in vacuum (10 mTorr)
- Phase pure $HfAl_2$

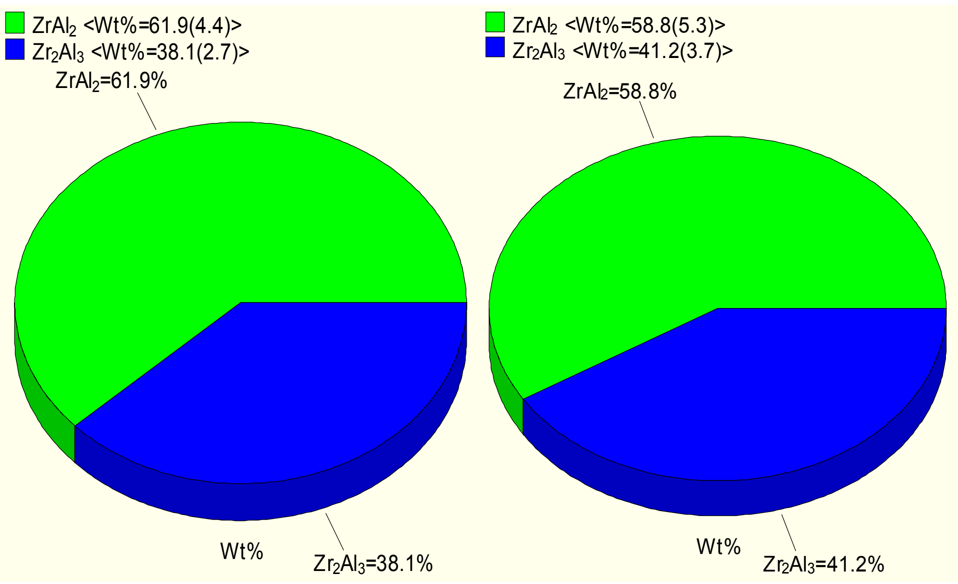

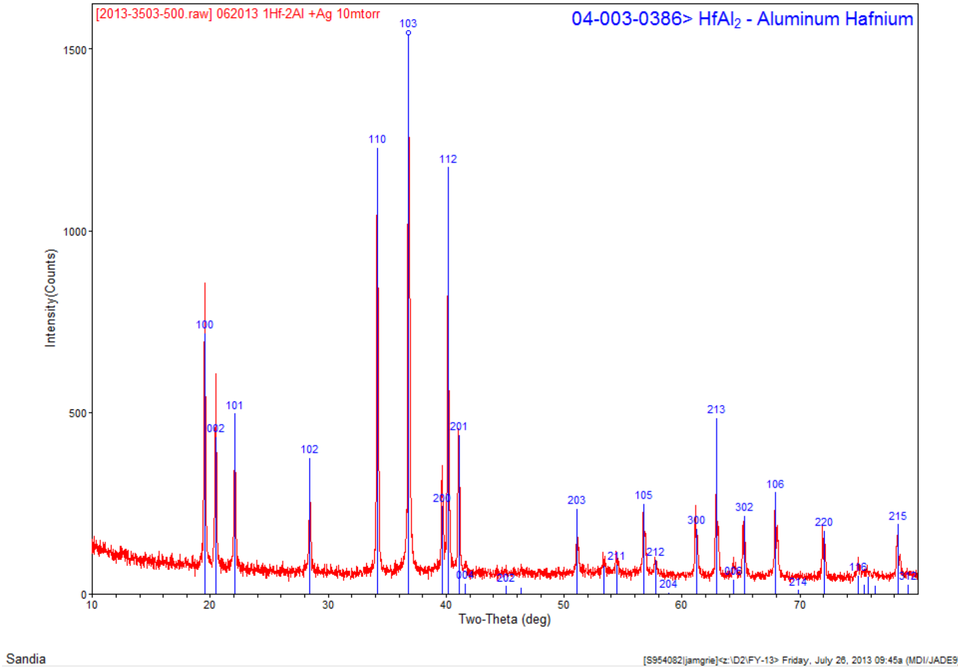

EDS/TEM Imaging of Reacted Samples

(Zr+Hf)/2Al Nanolaminates

- Aberration-corrected TEM (FEI Titan G2)
- Beam: 200kV electrons
- Signals sampled: Al-K (1.486 keV), Hf-M (1.644 keV), Zr-L (2.042 keV)
- Advantage: Spatial resolution (0.08 nm)
- Disadvantage: Composition (~ part per 1000)

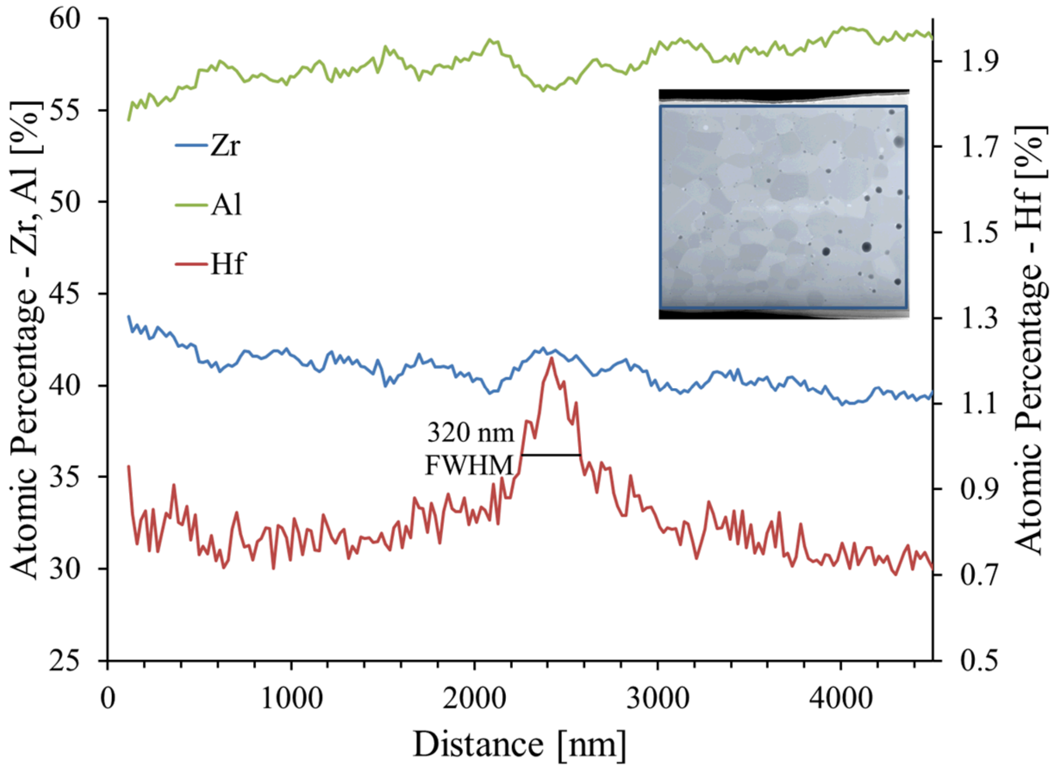

Variation at smaller length scales

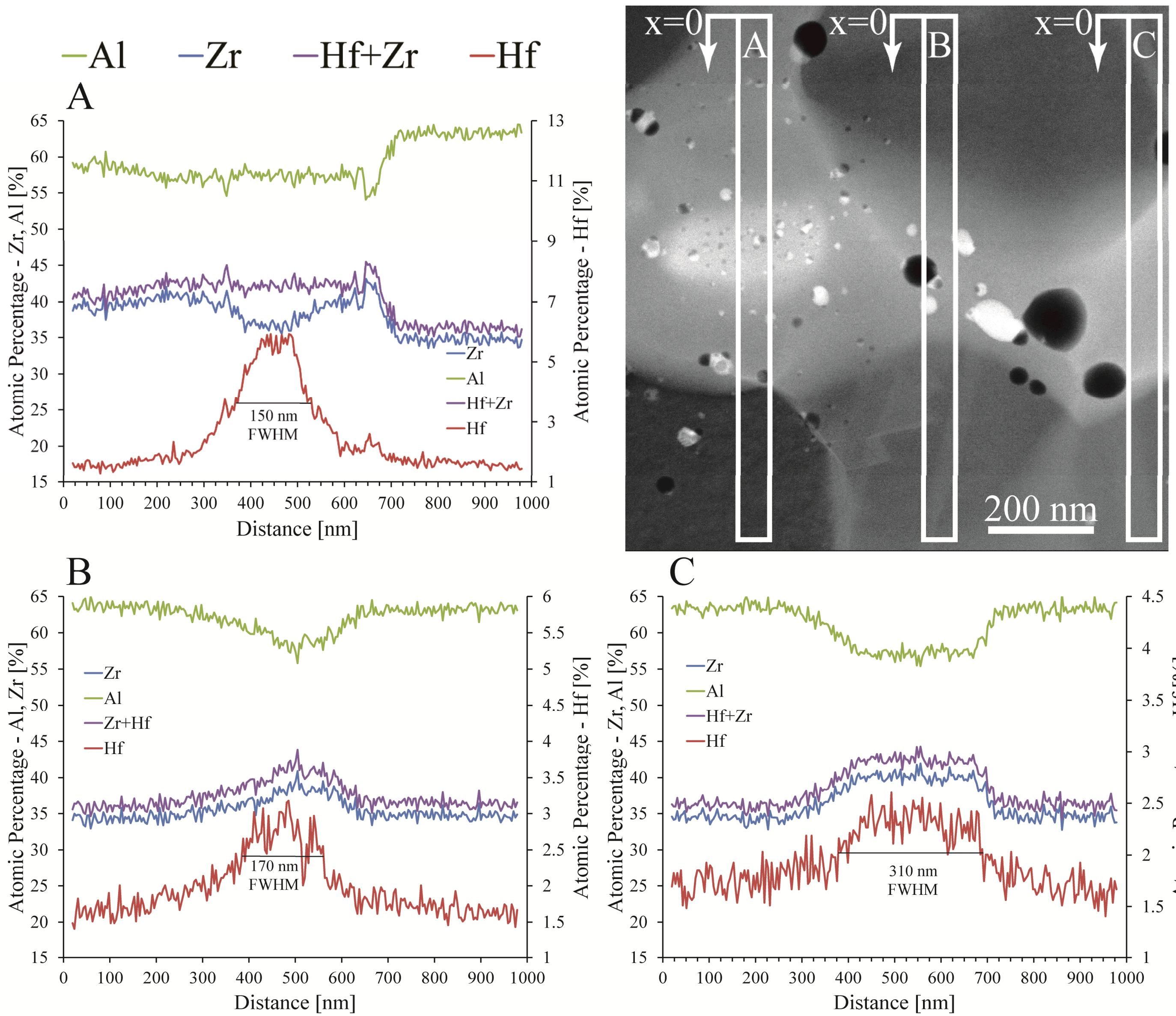

Marker Analysis by SIMS
(Zr+Hf)/2Al Nanolaminates

- Time of flight SIMS (Ion-TOF)
- Sputter: 2kV O_2^+, 250 nA, 200x200 μm^2
- Analysis: 25kV Bi^+, 50x50 μm^2
- Species sampled: ^{27}Al, ^{90}Zr, $^{177-180}$HfO

- Advantage: Composition (ppm)
- Disadvantage: Roughness/thickness
- Hf-baseline subtracted from signal
- Requires accurate detailing of sputter rate effects to determine position

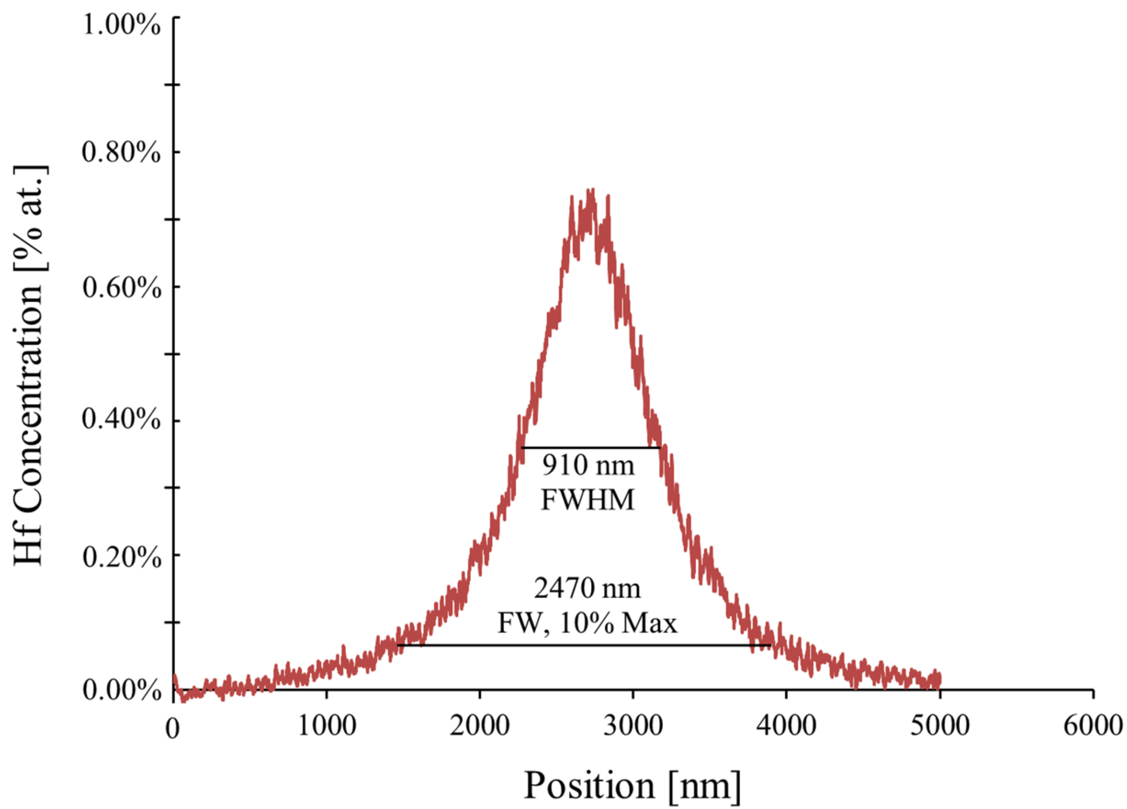

Diffusion model – Assumed progression

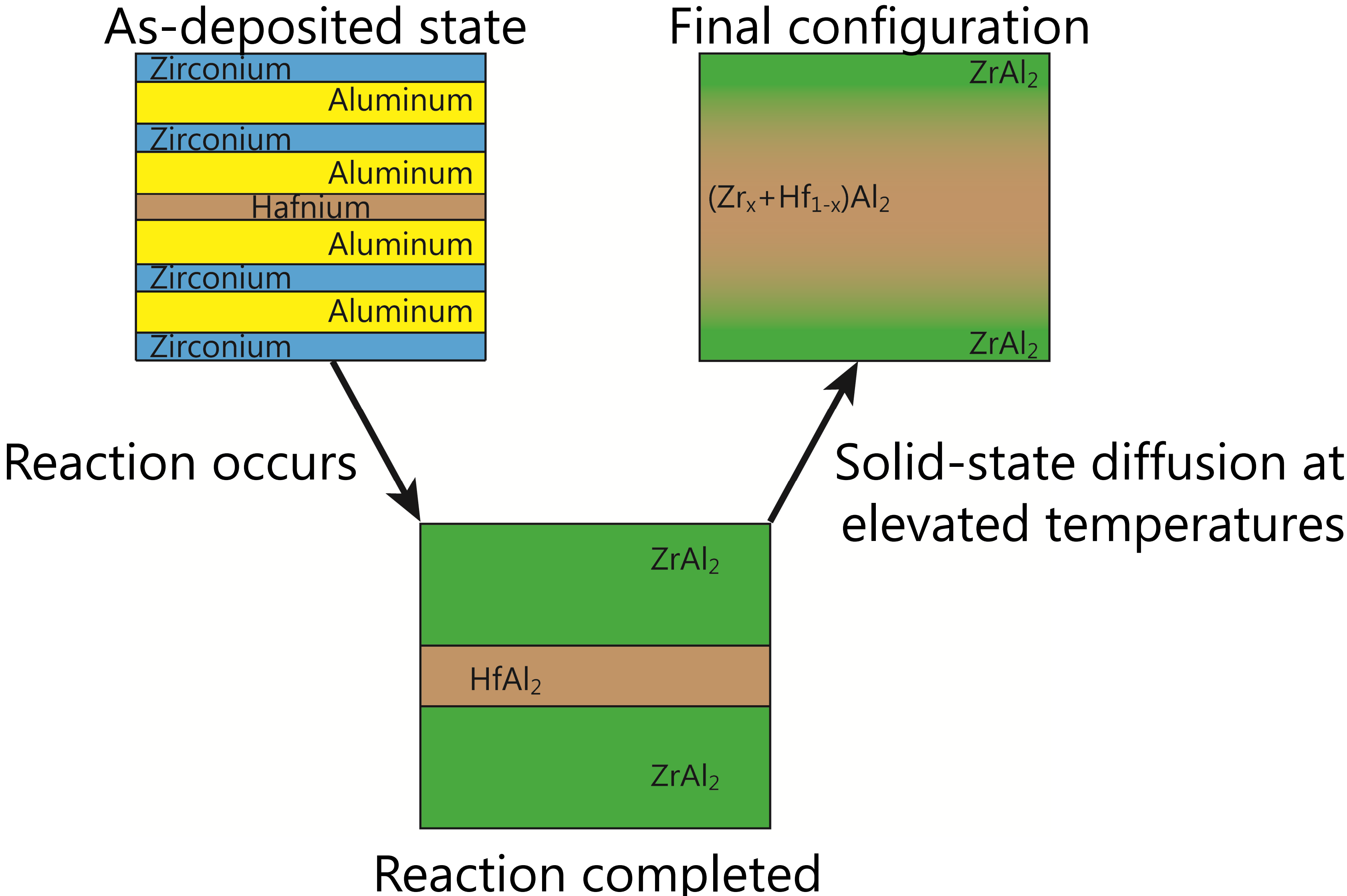

IR imaging of temperature history

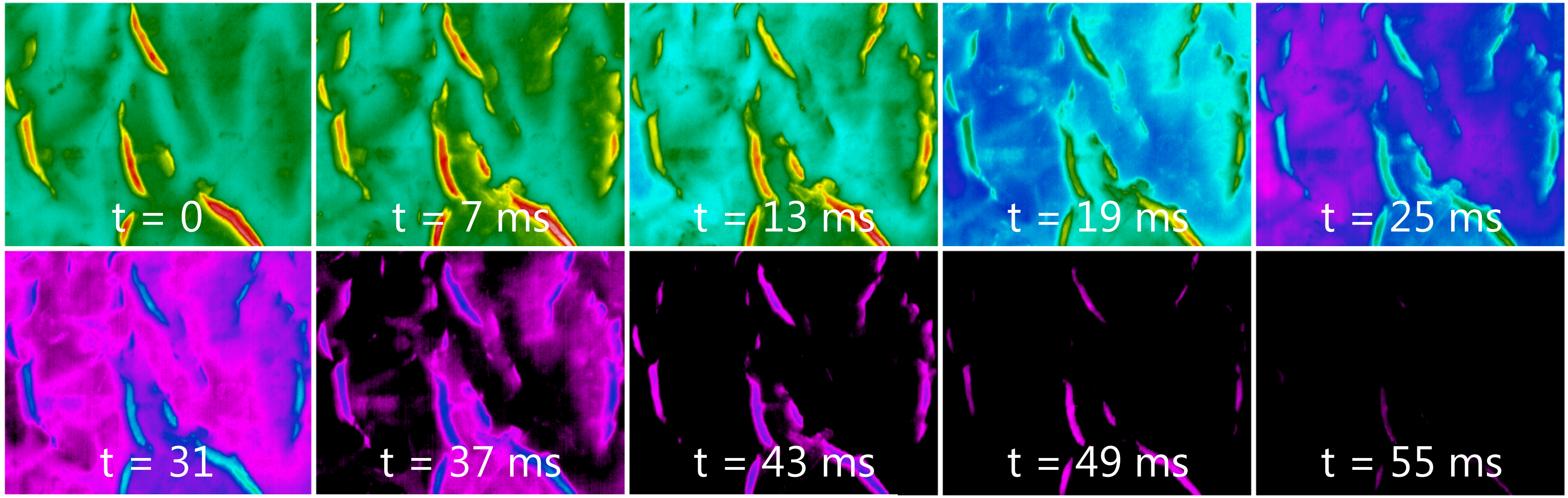

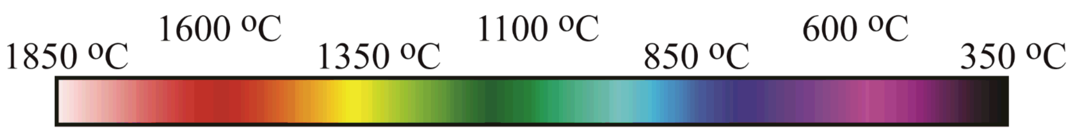

- Plot is average meas. temp of surface in image (4.8 x 3.8 mm)
- Time average over 46 ms is 690 ºC (963 K)
- Information for comparison to best fit results from diffusion model

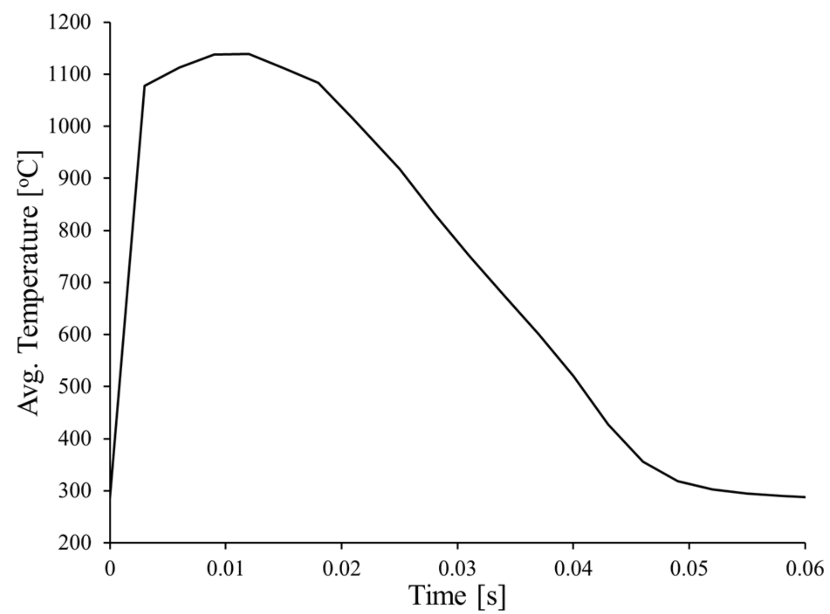

EDS Data
Compare to Simple Fickian Diffusion

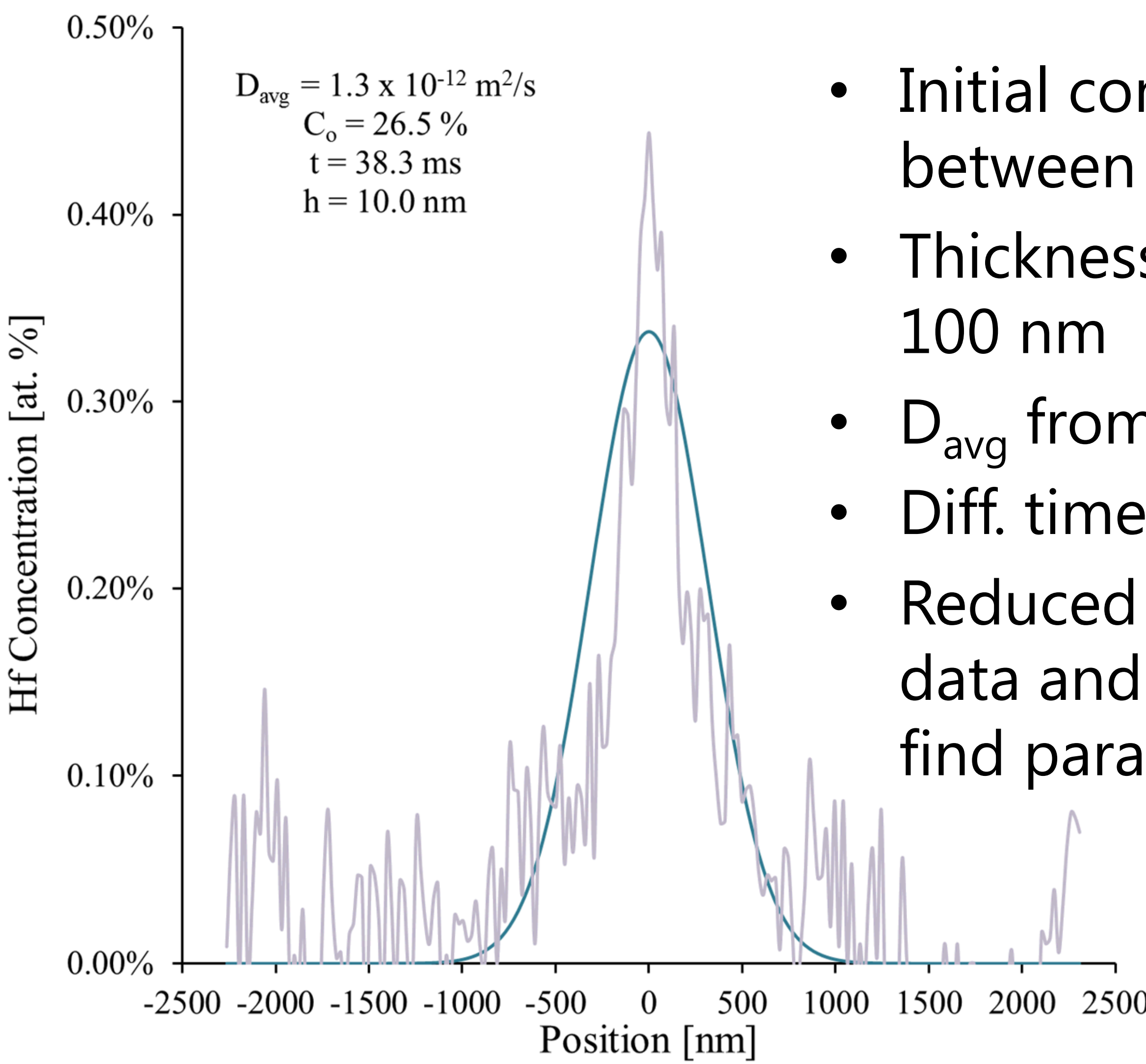

- Initial concentration varied between 25% and 40%
- Thickness of Hf_xAl_y layer up to 100 nm
- D_{avg} from 10^{-10} to 10^{-16} m^2/s
- Diff. time from 20 ms to 60 ms
- Reduced squared error between data and model to minimum to find parameters

EDS Data
Compare to Diffusion Model

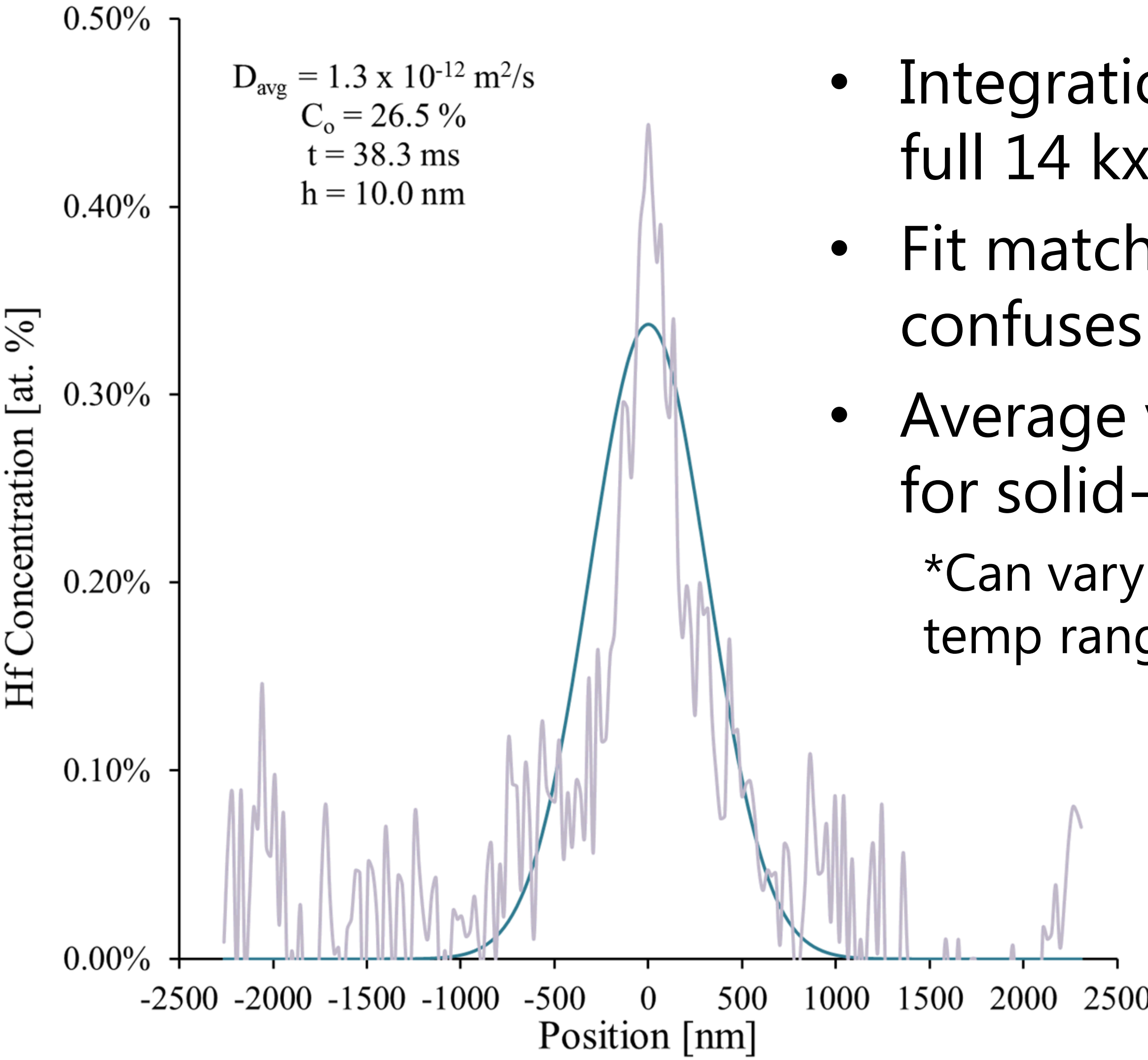

- Integration of EDS Hf signal over full 14 kx image (5x5 μm)
- Fit matches well but high noise confuses results
- Average value for D reasonable* for solid-state diffusion

*Can vary significantly ($\pm 10^3$) over temp range

EDS Data
Compare to Diffusion Model

- Integrated profile across 40 nm x 1000 nm path (shown)
- Best fit D = 1.5×10^{-15} m^2/s

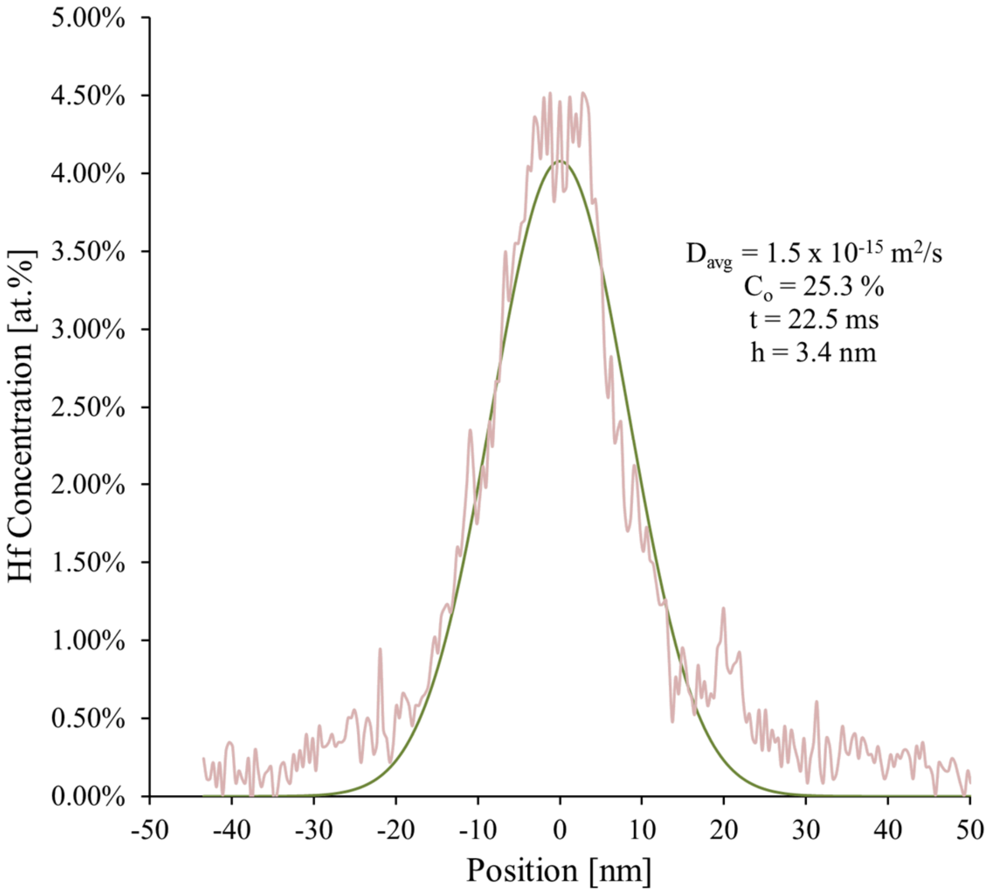

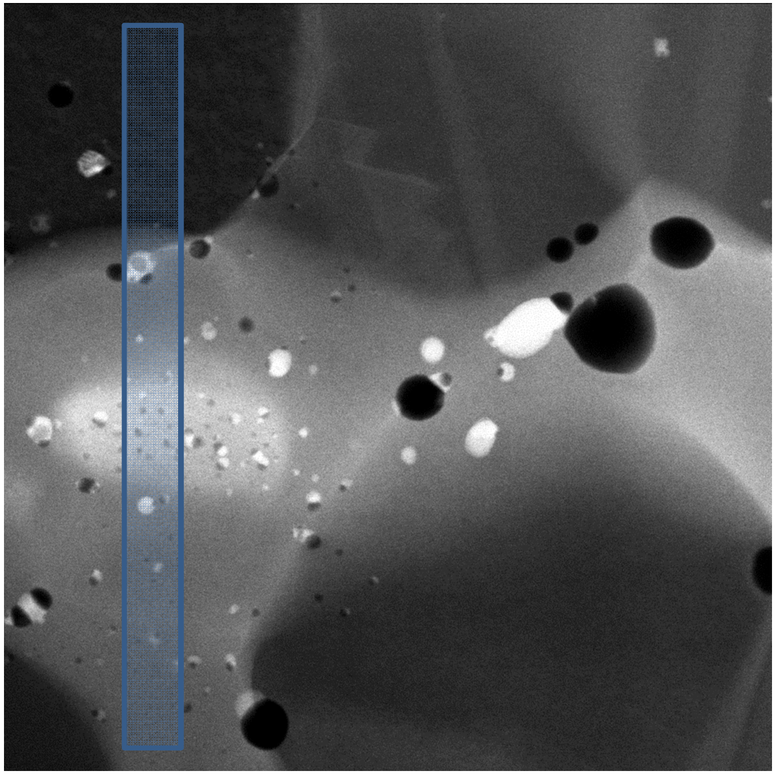

EDS Data
Compare to Diffusion Model

- Integrated profile across 40 nm x 1000 nm path (shown)
- Best fit D = 2.1 x 10^{-13} m^2/s

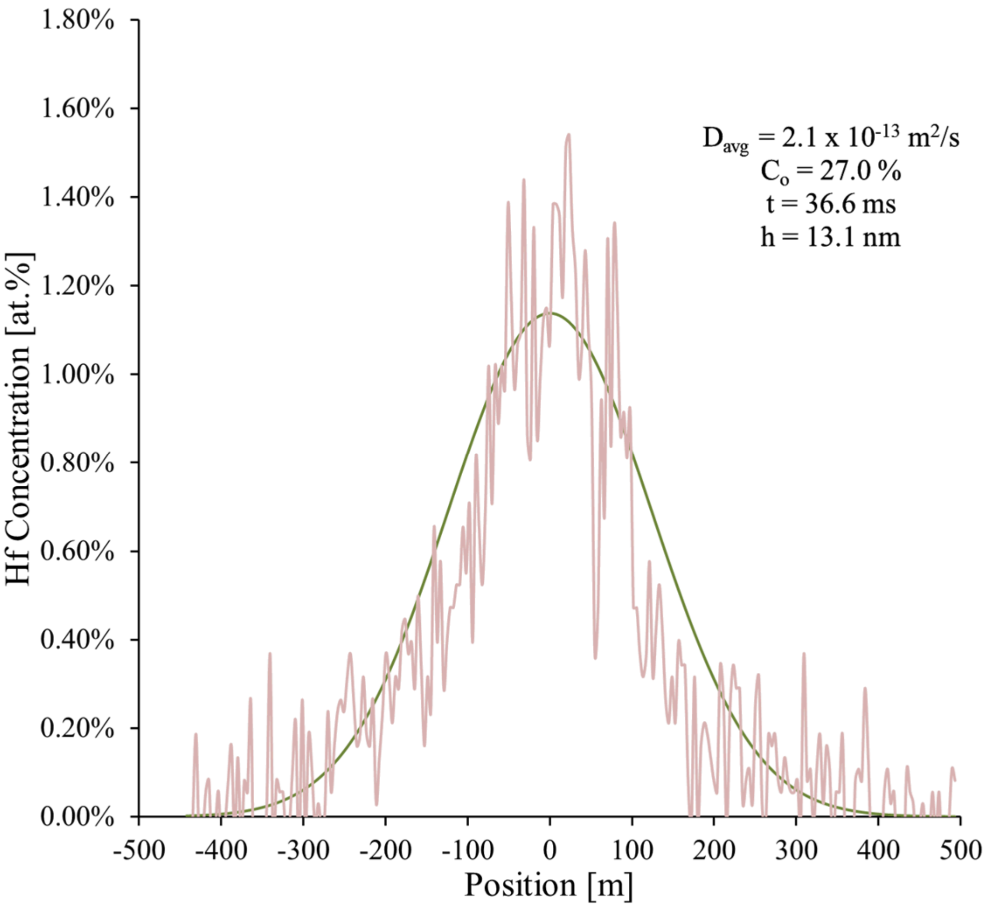

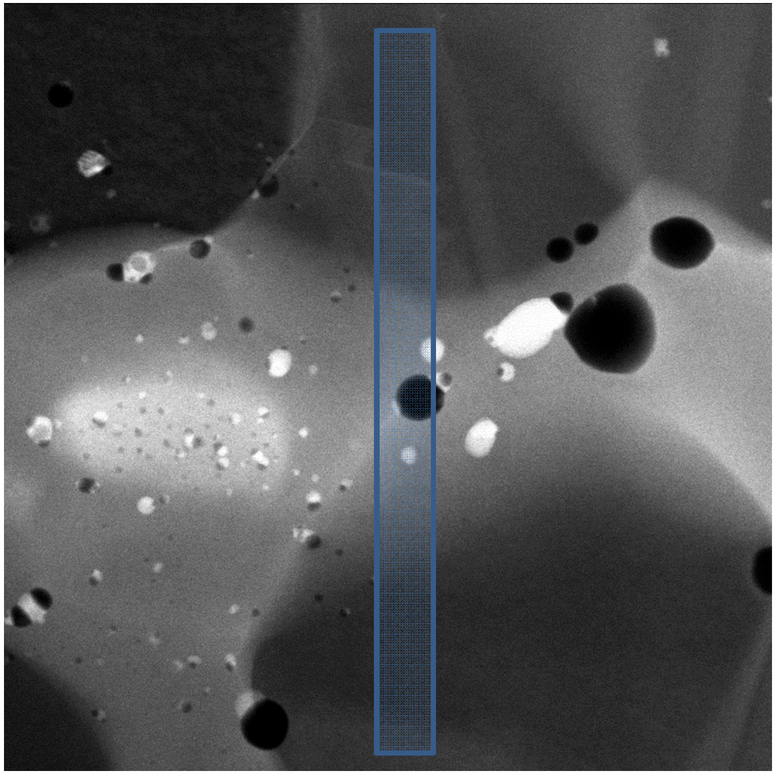

SIMS Data
Compare to Diffusion Model

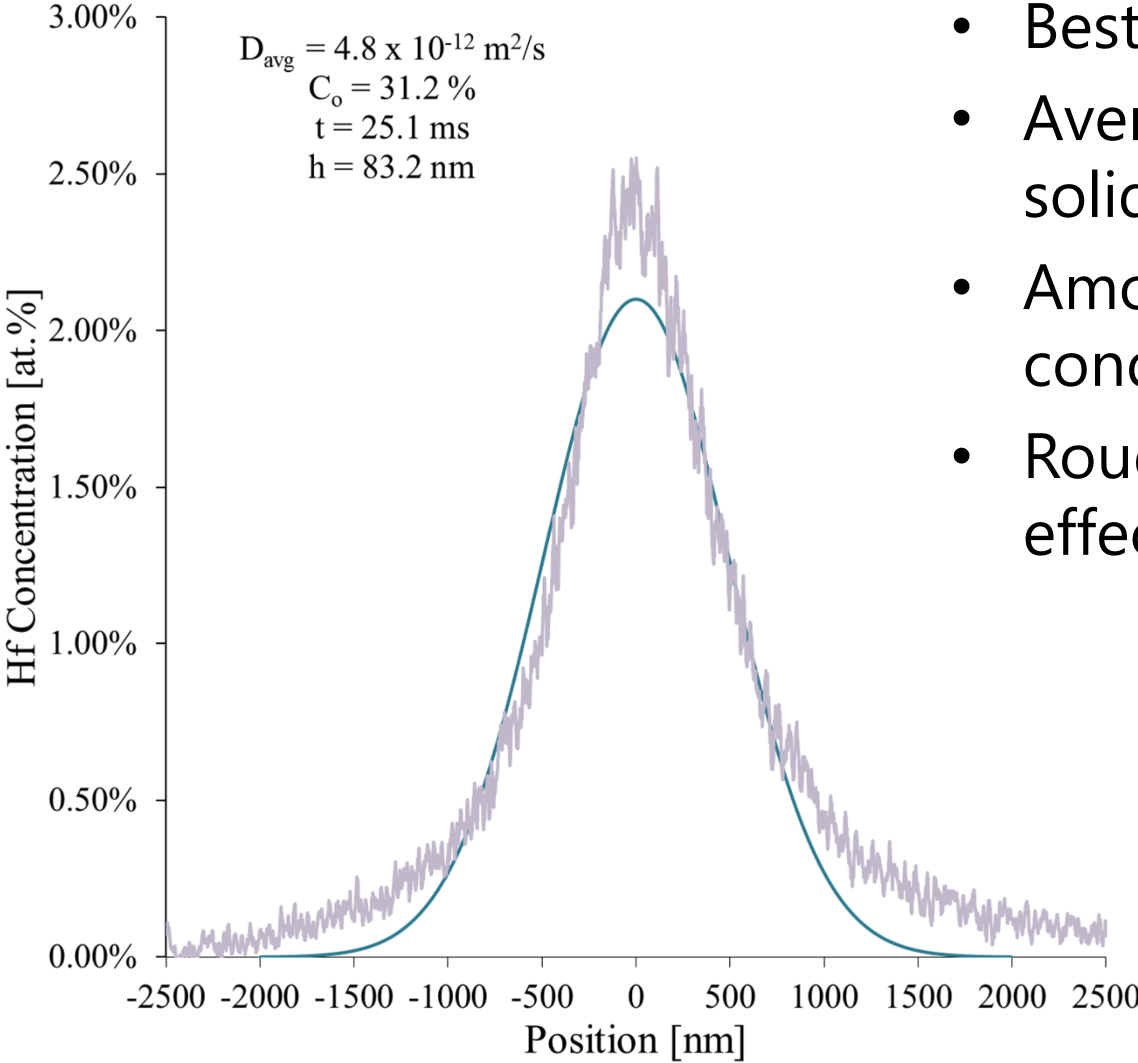

- Best fit D = 4.8×10^{-12} m^2/s
- Average D is reasonable for solid-state diffusion at 960 K
- Amount of Hf in initial condition not appropriate
- Roughness/sputter rate effects need correction

Conclusions

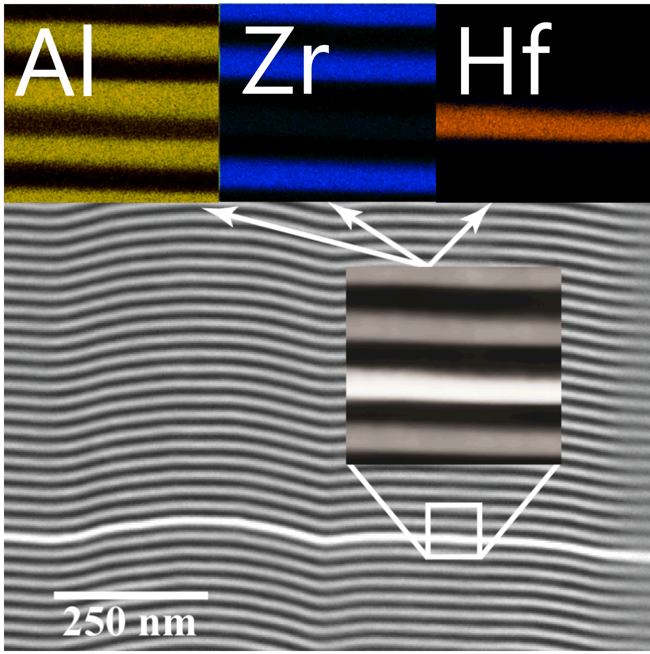

- TEM-EDS and SIMS methodologies allow spatial tracking of marker layers in reactive multilayers
- Hf marker layers showed atomic diffusion much greater than expected
  - 100's of nm vs. 1's of nm
  - Most likely occurred during elevated temperatures, post-reaction
  - No evidence of preferred diffusion along grain boundaries
  - No clear evidence for preferred phase for diffusion ($ZrAl_2$ vs Zr_2Al_3)
- Reduction in uncertainty due to analysis methods needed
- Will investigate rapidly quenched materials and unstable fronts

100 nm BL (Zr+Hf*)/2Al

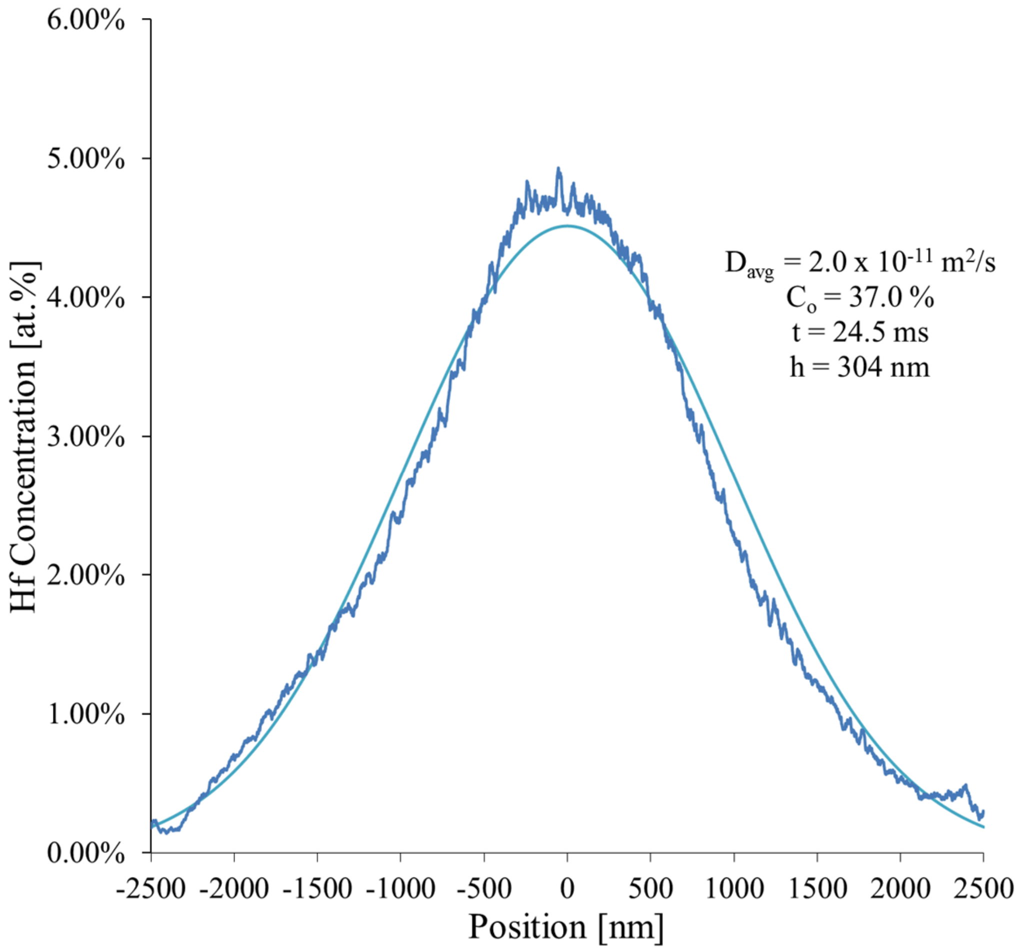

Reaction Initiation

- Despite all positive attributes, thermally ignited materials can suffer from instabilities
  - Reaction behavior dependent on forward heat transfer
- Mechanical loading can input energy faster than thermal diffusivity

Gas Gun Testing

- Asay shear impact test
- Creates compressive and shear stresses
- Samples tested at 65-67%TMD
  - Nanopowder mixtures
  - HEBM mixture

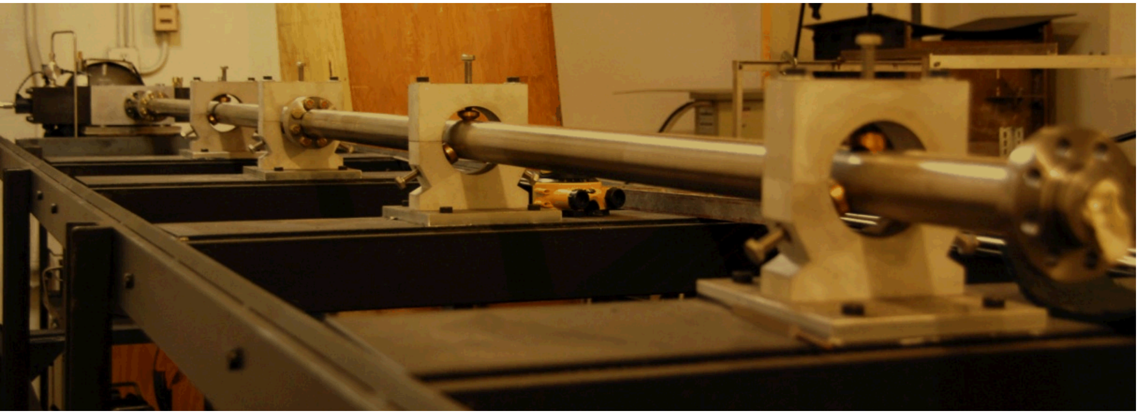

B. W. Asay *et al.*, in Shock Compresssion of Condensed Matter, (1997), pp. 567

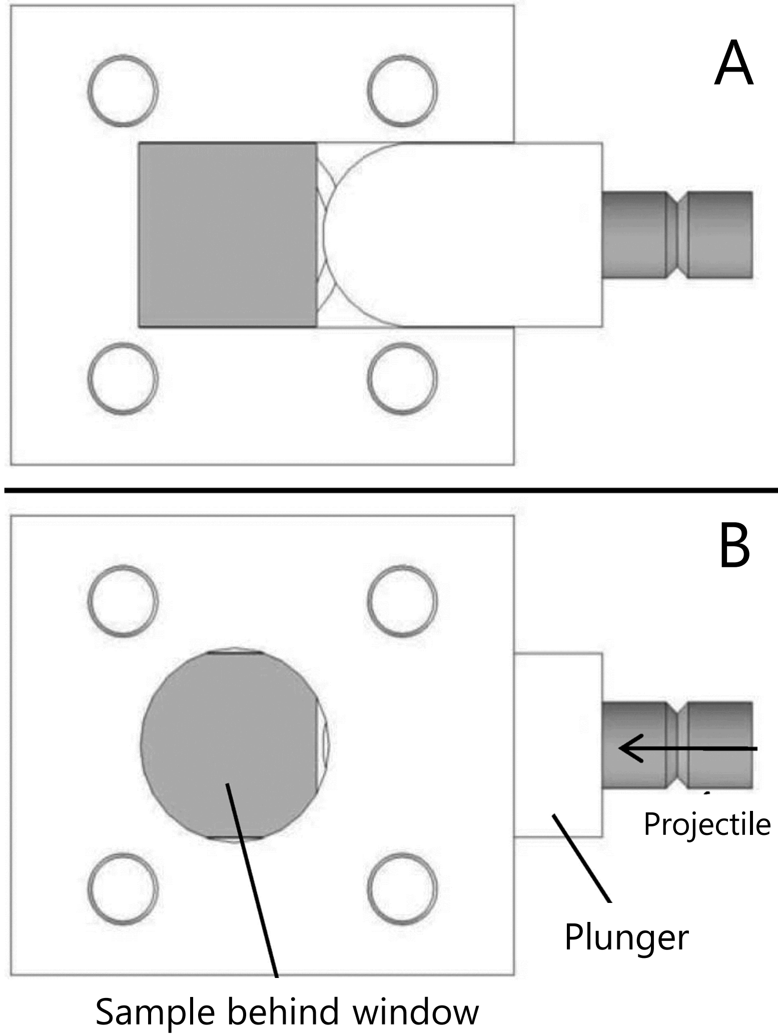

Gas Gun Testing

- Impact followed by delay, thermal reaction onset
  - Low energy impacts in nanopowders, all milled powder experiments
  - Propagation rate of 1-10 cm/s

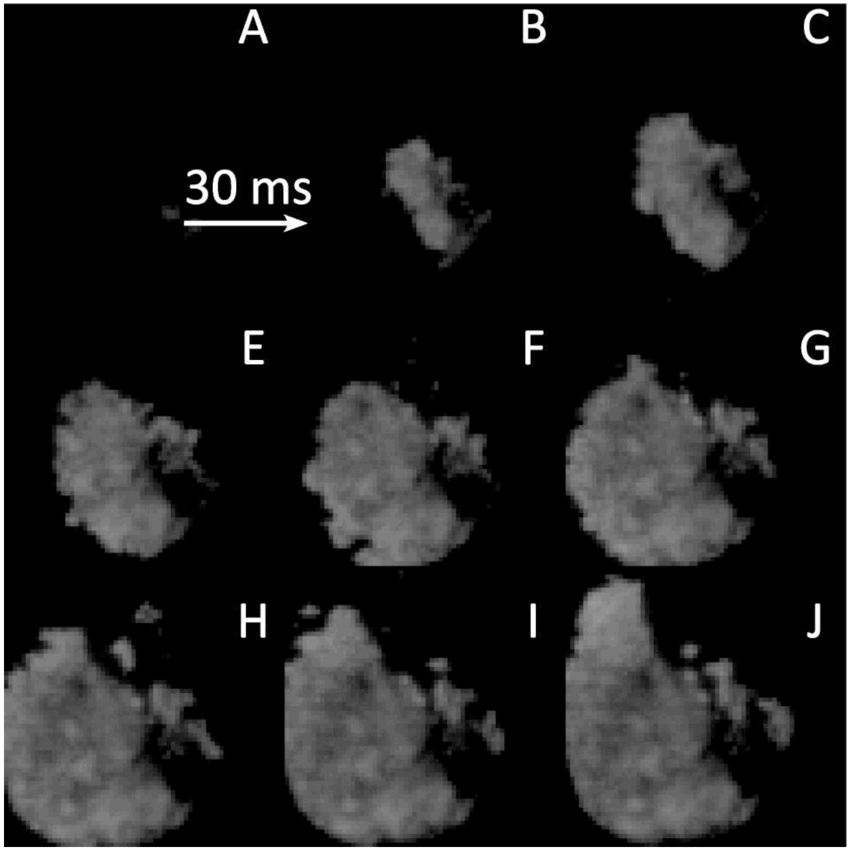

Gas Gun Testing

- Prompt reaction on impact
  - Tied to stress wave passage
    - Only in nanopowders
- Fast mode slows, like overdriven shock
- Interpreted to be a mechanically-induced thermal explosion, rather than “solid-state detonation”

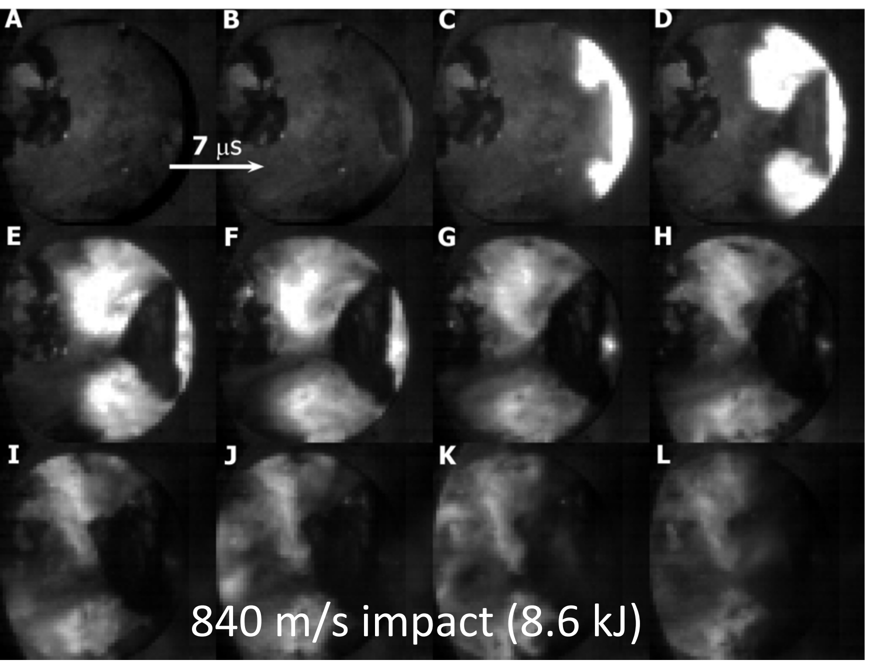

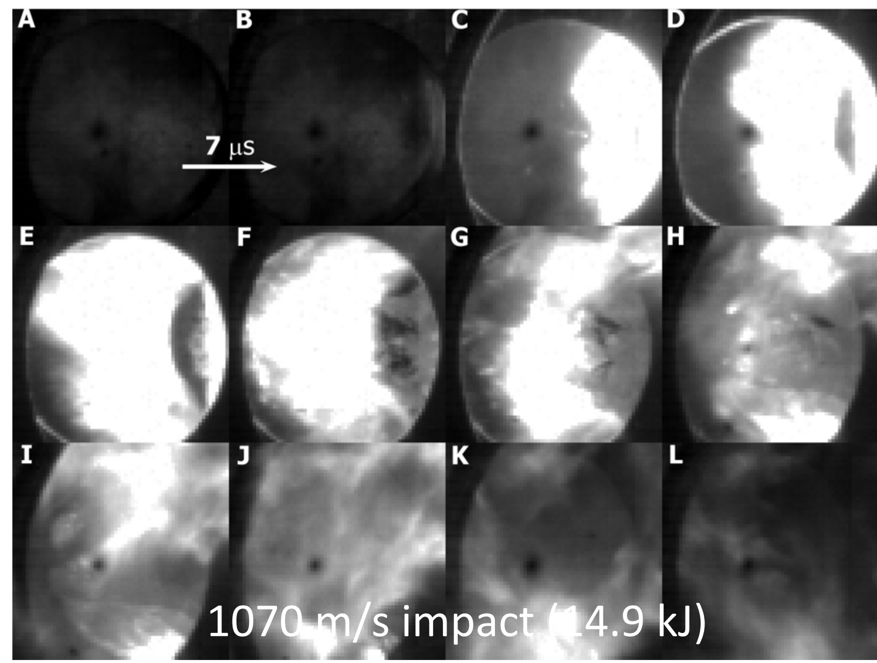

Gas Gun Testing

HEBM Material –Impact Vel. 794 m/s (7.50 kJ)

- Shear Bands appear during impact
- Local, non-propagating reactions appear in shear bands with short residence times (~14 μs)
- Slow reaction mode occurs after induction period

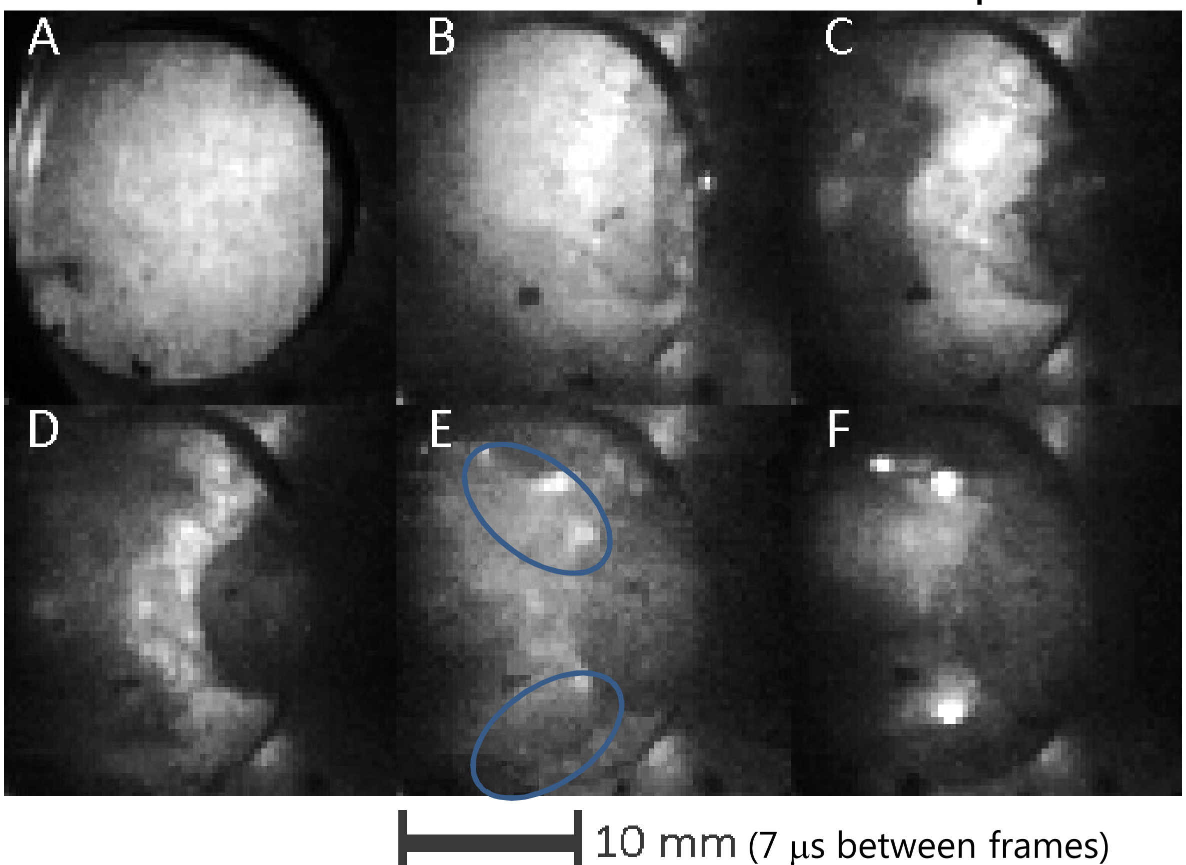

- Shear bands form during impact, circled in frame E
- Local ignition initiate in shear bands in frame E. in frame F, reaction zones are clearly apparent.

Prompt Ignition Requires Understanding Kinetic Energy Storage

- For nanopowder mixtures, porosity is intimate with interfacial areas
- For milled materials, porosity is distant from most interfaces
  - Time is necessary to transfer heat from pore collapse to reactive areas
  - Reaction can be activated by shear

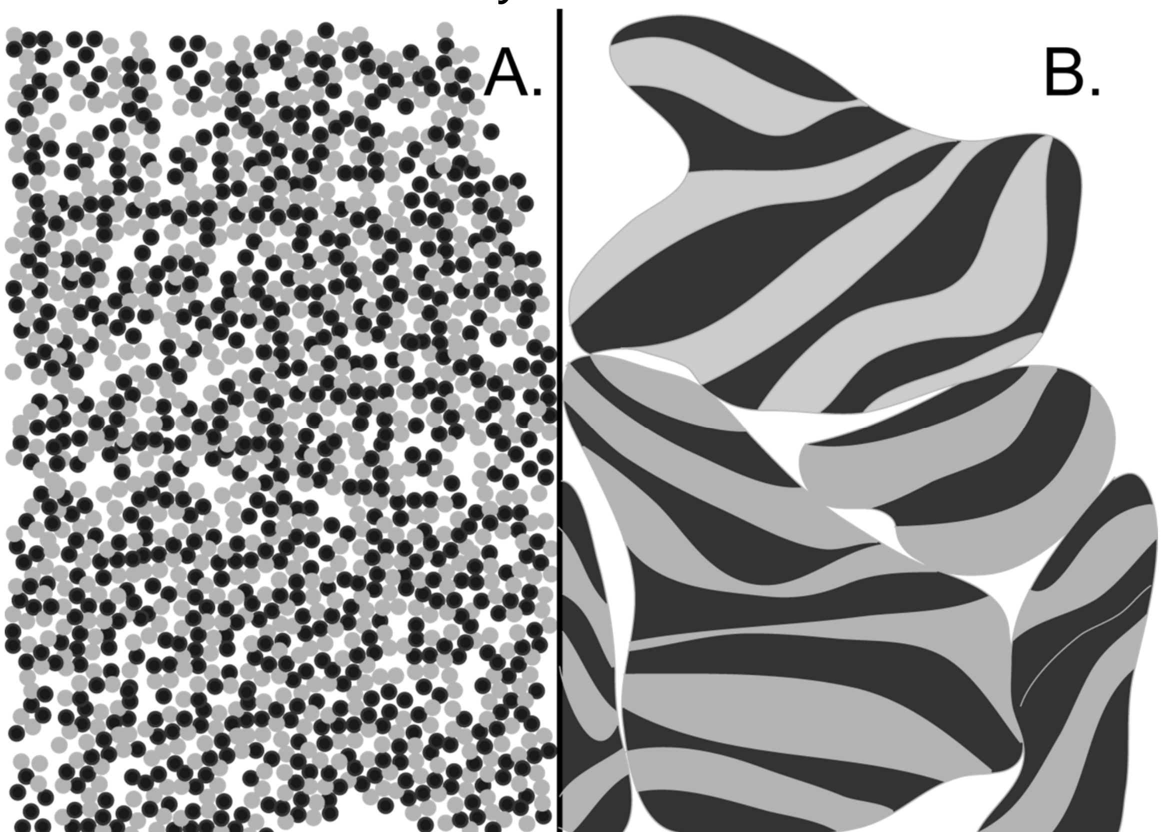

Mechanical Ignition of Thin Films

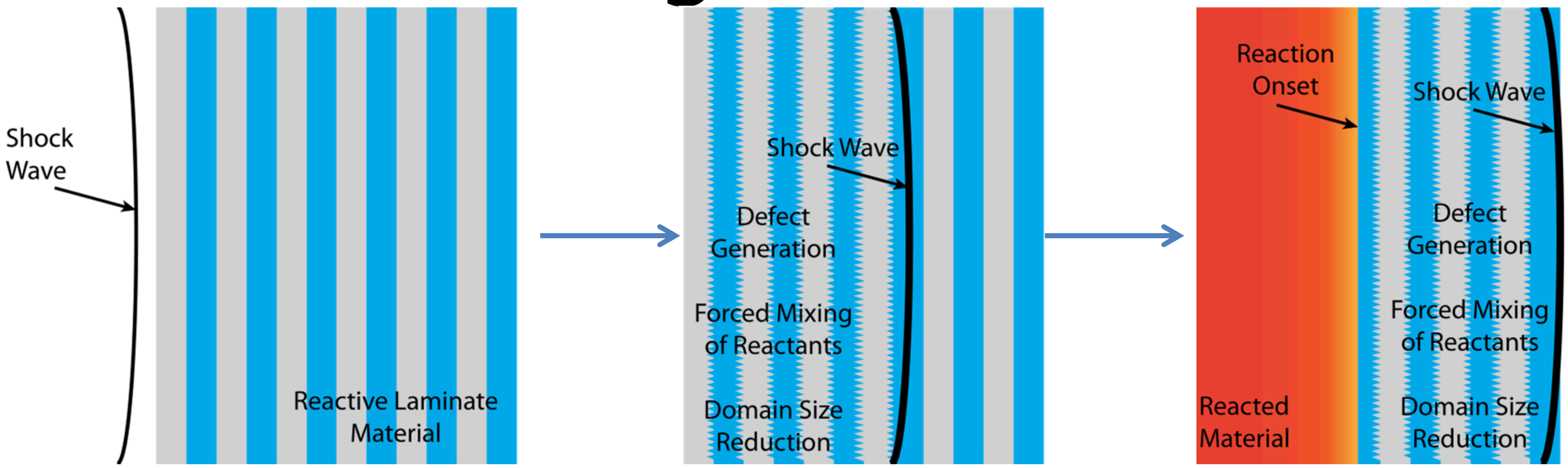

1. Planar shock compression
2. Combined shear/compression loading
3. Micro-ballistic impact
4. Shockless compression

Pure Compression ↕ Regions of Pure Shear

- Quantify input conditions and material changes
- Tabletop Laser to perform flyer plate experiments:
  - Greater throughput– 10's of shots per day vs. 1 shot per day (gas gun)
  - Wide variation in test conditions by simple schematic changes
  - Input pressure range to 10^{10} Pa

Ex-situ Diagnostics and Analysis

- Sub-critical impacts provide history of changes leading to ignition
- Quantification of domain size, defect generation, metastable phase formation
- Coupling to modeling allows prediction for material and design selection

J.-H. Lee, J. P. Singer, and E. L. Thomas, Advanced Materials **24,** 4782 (2012)

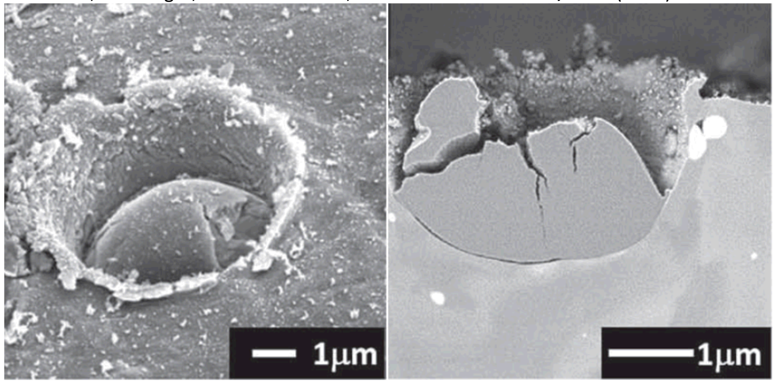

Electron microscopy provides description of deformation and microstructural changes

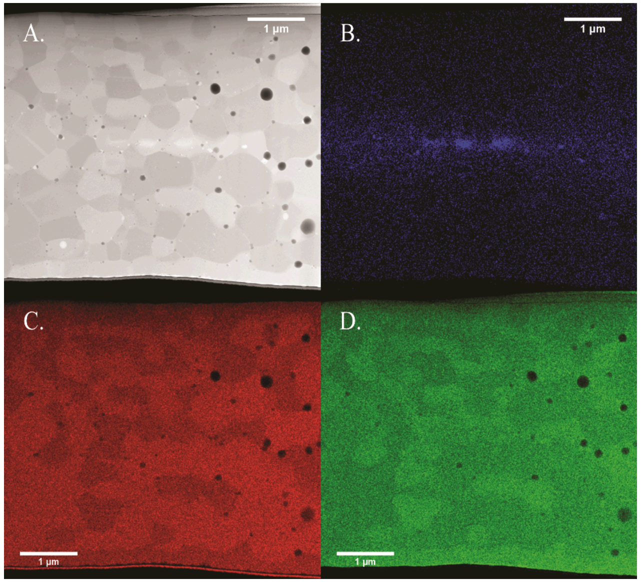

Spectroscopy on AC-TEM provides unprecedented capability to map diffusion after reaction or impacts

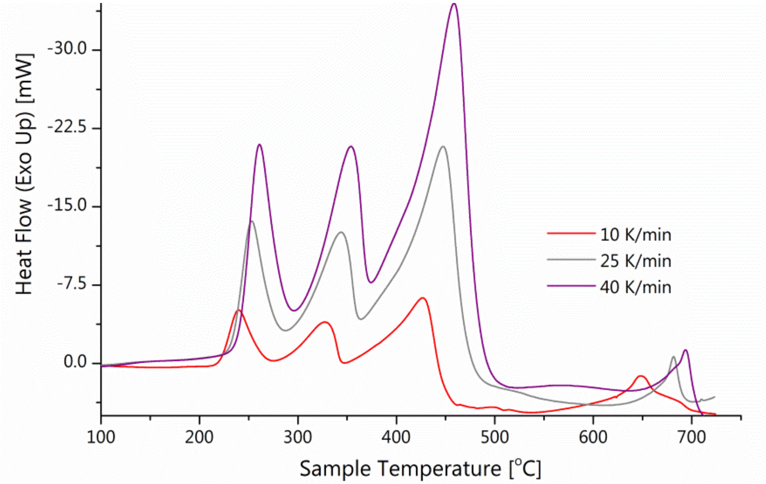

Calorimetry allows quantification of reaction progress and material sensitization

Gasless reactive systems…

- Have high stored chemical energy
  - Reduced pyrotechnic volume
- But can be used as more than a heat source
  - Functional devices – optical, magnetic, electronic switches

The different forms of reactive systems allow for…

- Controllable heat release rates and stability
  - Tunable for faster or slower heat release
- Flexible ignition types and thresholds
  - Thermal
  - Mechanical – requires more study, but significant benefits

Acknowledgements

- Sandia National Laboratories – Thin Film Characterization
  - Dr. David Adams
  - Dr. Mark Rodriguez
  - Dr. Ron Goeke
  - Eric D. Jones, Jr.
  - Tony Ohlhausen
  - Dr. Paul Kotula
- Lawrence Livermore National Laboratories
  - Dr. Thomas LaGrange
- Purdue University – Ball-milling and Gas Gun Experiments
  - Prof. Steven Son
- University of Notre Dame
  - Prof. Alex Mukasyan
  - Dr. Jeremiah White
- Funding Agencies while at Purdue University
  - Office of Naval Research
  - Defense Threat Reduction Agency

- This work was supported by the Laboratory Directed Research and Development program at Sandia National Laboratories.
- Sandia National Laboratories is a multi-program laboratory managed and operated by Sandia Corporation, a wholly owned subsidiary of Lockheed Martin Corporation, for the U.S. Department of Energy's National Nuclear Security Administration under contract DE-AC04-94AL85000.

Additional slides

Conclusions

- Experiments show some BL designs can switch from unstable to stable reaction fronts by increasing T_0
- All foils transitioned to stability at a common bulk propagation rate
- Calculations show greater diffusion rates required for stability in thicker BL foils
- Dark regions between transverse band ("diffusion-affected zones") exhibit high-E_a behavior
  - Conduction heats material causing limited reaction
  - Product layer forms at interface, inhibiting reaction
- Disparate reaction kinetics likely occurring in diffusion-affected zones and transverse bands

Quenched Samples – Phase ID

- 21 nm BL Foil – All Al disrupted in 1st exotherm

$$Co + Al \xrightarrow[250\ ^oC]{} Co + Co_2Al_9 + Co_xAl_y \xrightarrow[400\ ^oC]{} CoAl$$

- 66.4 nm Foil – Elemental Al ID'd after 1st exotherm

$$Co + Al \xrightarrow[260\ ^oC]{} Co + Al + Co_2Al_9 + Co_xAl_y \xrightarrow[400\ ^oC]{} Co + Co_xAl_y \xrightarrow[480\ ^oC]{} CoAl$$

- Co_2Al_9, Co_4Al_{13}, Co_2Al_5 are possibilities for Co_xAl_y

- Initial exotherm results in ~10 nm Co diffusion

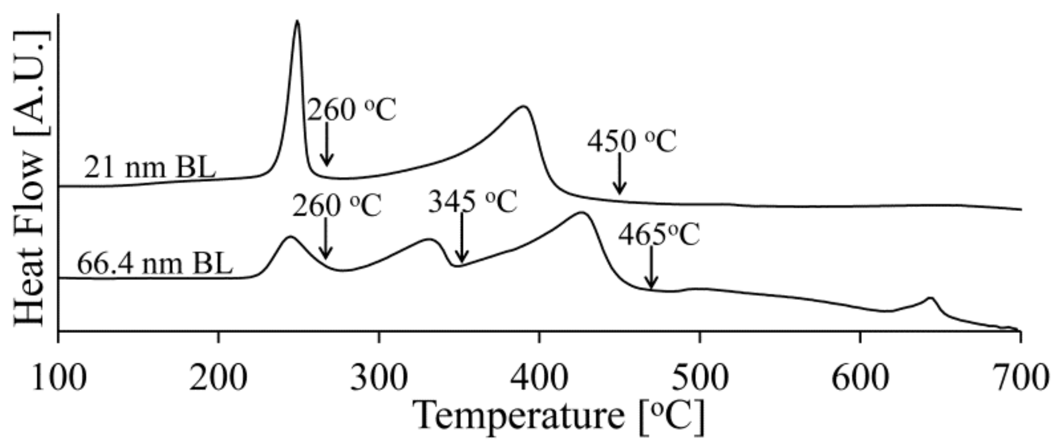

Local Variation in Effective Activation Energy

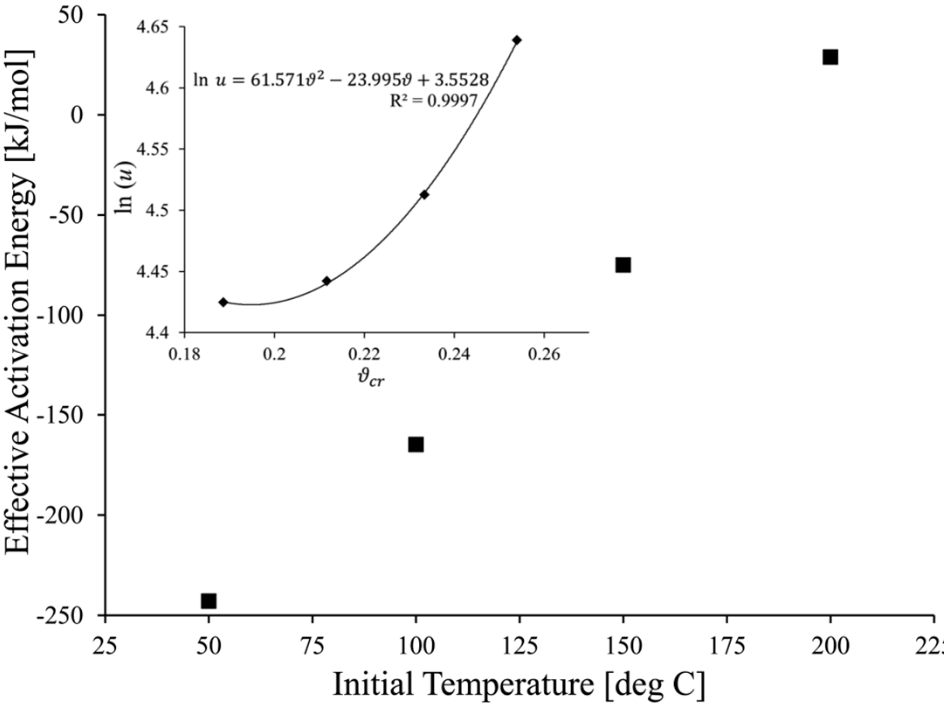

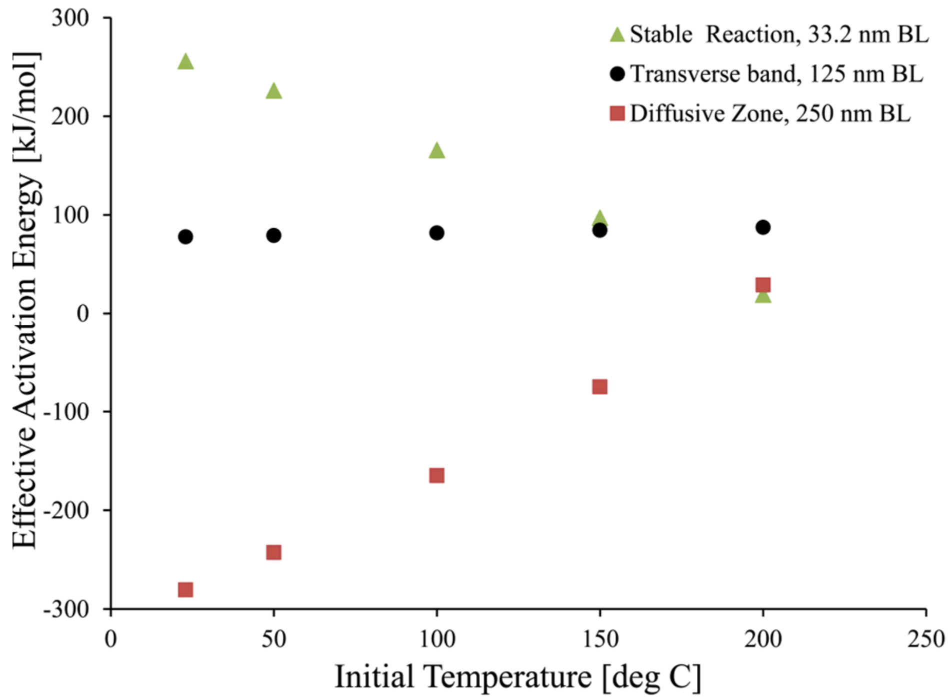

- E_a decreases with T_0 for stable bulk reaction
  - Increased local kinetics
- E_a is unaffected by T_0 for transverse reaction bands
  - Region is dominated by heat transfer
- E_a increases with T_0 for reactions in the diffusion-affected zones
  - Higher initial temp possibly producing more robust product films

Conclusions

- Can grow thin films that can well isolate effects of diffusion and mass dilution
- Variation in *Le* and *b* can introduce reaction instabilities, as predicted by theory
- Induced instabilities in Co/Al laminates limited to 2-D spinning instability
- Similar but not identical stability limits between BL designs
- Need dimensionally dependent heat release and mass transfer terms in the basic transport equations for analytical criteria and predictive models